

MASTERS DISSERTATION

**VOLTAGE, CURRENT, IMPEDANCE,
POWER AND LINEAR TRANSFORMATIONS
BY MEANS OF QUATERNIONS**

Victor do Prado Brasil

Brasília, February 2019

UNIVERSIDADE DE BRASÍLIA

FACULDADE DE TECNOLOGIA

UNIVERSIDADE DE BRASÍLIA
FACULDADE DE TECNOLOGIA
DEPARTAMENTO DE ENGENHARIA ELÉTRICA

Tensão, Corrente, Impedância,
Potência e Transformações Lineares
via Quatérnios

VICTOR DO PRADO BRASIL

ORIENTADOR: ANÉSIO DE LELES FERREIRA FILHO
CO-ORIENTADOR: JOÃO YOSHIYUKI ISHIHARA

DISSERTAÇÃO DE MESTRADO EM
ENGENHARIA ELÉTRICA

PUBLICAÇÃO: PPGEE.DM - 139/2019
BRASÍLIA/DF: Fevereiro - 2019.

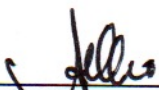
UNIVERSIDADE DE BRASÍLIA
FACULDADE DE TECNOLOGIA
DEPARTAMENTO DE ENGENHARIA ELÉTRICA

VOLTAGE, CURRENT, IMPEDANCE, POWER AND LINEAR
TRANSFORMATIONS BY MEANS OF QUATERNIONS

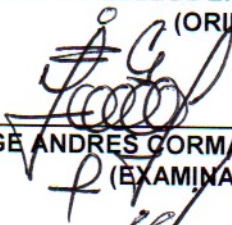
VICTOR DO PRADO BRASIL

DISSERTAÇÃO DE MESTRADO SUBMETIDA AO DEPARTAMENTO DE ENGENHARIA ELÉTRICA DA FACULDADE DE TECNOLOGIA DA UNIVERSIDADE DE BRASÍLIA, COMO PARTE DOS REQUISITOS NECESSÁRIOS PARA A OBTENÇÃO DO GRAU DE MESTRE.

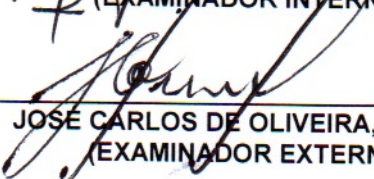
APROVADA POR:



ANESIO DE LELES FERREIRA FILHO, Dr., ENE/UNB
(ORIENTADOR)



JORGE ANDRES CORMANE ANGARITA, Dr., ENE/UNB
(EXAMINADOR INTERNO)



JOSÉ CARLOS DE OLIVEIRA, Dr., UFU
(EXAMINADOR EXTERNO)

Brasília, 15 de fevereiro de 2019.

FICHA CATALOGRÁFICA

BRASIL, VICTOR DO PRADO
VOLTAGE, CURRENT, IMPEDANCE,
POWER AND LINEAR TRANSFORMATIONS
BY MEANS OF QUATERNIONS. [Distrito Federal] 2019.
xiv, 77p., 297 mm (ENE/FT/UnB, Mestre, Electrical Engineering)
Master Dissertation - Universidade de Brasília.
Faculdade de Tecnologia.
Departamento de Engenharia Elétrica.
1. Power Quality 2. Quaternions
3. Circuit Theory 4. Linear Transformations
I. ENE/FT/UnB II. Título

BIBLIOGRAPHY

BRASIL, V. P. (2019). VOLTAGE, CURRENT, IMPEDANCE, POWER AND LINEAR TRANSFORMATIONS BY MEANS OF QUATERNIONS. Dissertação de Mestrado em Engenharia Elétrica, Publicação PPGENE.DM-139/2019 Departamento de Engenharia Elétrica, Universidade de Brasília, Brasília, DF, 77p.

CESSÃO DE DIREITOS

AUTOR: Victor do Prado Brasil.

TÍTULO: VOLTAGE, CURRENT, IMPEDANCE, POWER AND LINEAR TRANSFORMATIONS BY MEANS OF QUATERNIONS.

GRAU: Mestre ANO: 2019

É concedida à Universidade de Brasília permissão para reproduzir cópias deste trabalho de dissertação de mestrado e para emprestar ou vender tais cópias somente para propósitos acadêmicos e científicos. O autor reserva outros direitos de publicação e nenhuma parte deste trabalho pode ser reproduzida sem a autorização por escrito do autor.

Victor do Prado Brasil
SQN 212 bloco J, asa norte, Brasília.
70.864-100 Brasília - DF - Brasil.

Dedication

To Jesus Christ, my saviour, to my beloved wife Julyana and to my parents Ana and Joaquim for sharing with me this adventure called life.

Victor do Prado Brasil

Acknowledgments

My deepest gratitude to all of those who made this work easier. Writing a dissertation can be quite challenging and lonely sometimes. Getting through this moments with joy and motivation to work can only be accomplished with friends. Therefore, this page is dedicated to them.

First, I would like to thank my forever best friend and saviour Jesus Christ. I also acknowledge my beloved wife for her endless support and all the nights she stayed up late while I was working. I am grateful for my parents encouraging and for all the faith they have put in me. I would like to thank Professor Dr. Anésio de Leles Ferreira Filho for his guidance and attention. Always cordial in manner, he put much effort in providing me with the best working conditions. He was always open to discussion of both technical and philosophical aspects. Professor Dr. João Yoshiyuki Ishihara also deserves a special note of gratitude for his co-supervision and for his dedication to my work. I would like to thank “Coordenação de Aperfeiçoamento de Pessoal de Nível Superior” (CAPES) for the financial support provided along my research.

Last, but not least, I thank my colleagues at Universidade de Brasília. In special, I thank all of the REILab group. The discussions and ideas exchanged made my academic journal very pleasant. I will forever remember ours seminars and the coffee breaks we shared during the long and cold afternoons (specially when the computer cluster air conditioning was not functioning well).

Victor do Prado Brasil

RESUMO

Nome: Victor do Prado Brasil

Título: Tensão, Corrente, Impedância, Potência e Transformações Lineares via Quatérnios

Nome do Curso: Programa de Pós-Graduação em Engenharia Elétrica - Sistemas de Potência

Data da Defesa: Brasília, 15 de fevereiro de 2019

Orientador: Anésio de Leles Ferreira Filho

Co-orientador: João Yoshiyuki Ishihara

Palavras-Chave: Qualidade da Energia, Quatérnios, Teoria de Circuitos, Transformações Lineares.

Keywords: Power Quality, Quaternions, Circuit Theory, Linear Transformations.

Atualmente, o fasor é a ferramenta matemática mais conhecida e aplicada em sistemas elétricos de potência. Não obstante, ele apresenta desvantagens em condições de operação não-ideais (sistemas desequilibrados e/ou não lineares). Dessa forma, outras representações têm sido propostas e investigadas, tais como vetorial, tensorial, quaterniônica e as que empregam álgebra geométrica. Esta dissertação apresenta as vantagens e desvantagens da aplicação dos quatérnios em sistemas trifásicos. Para tanto, as bases teóricas e matemáticas são primeiramente estabelecidas. Em seguida, tensão e corrente, em condições equilibradas e desequilibradas, são analisadas geometricamente. Adicionalmente, uma versão quaterniônica das componentes simétricas no domínio do tempo é proposta, provendo um espaço de estados linear para a estimação delas a partir das amostras temporais. Ressalta-se que não existe, consoante o conhecimento atual dos autores, abordagem similar no domínio fasorial. Uma impedância/admitância trifásica quaterniônica também é definida para condições equilibradas e desequilibradas. A potência resultante dessa representação é discutida e comparada com outras teorias de potência. A componente reativa proposta é superior à resultante das vetoriais, devido ao fato de haver um significado claro atribuído à sua direção. Ademais, devido à sua natureza algébrica, as potências i) ativa, ii) reativa e iii) desequilibrada são representadas em eixos ortogonais. Assim, essa teoria pode ser empregada para o desenvolvimento de compensadores ativos de potência. Por fim, implementações quaterniônica das transformadas de Clarke e Park são estabelecidas. Em ambos os casos, são necessários menos elementos numéricos em comparação com a respectiva versão matricial tradicional. No caso de Park, o método proposto foi aproximadamente quatro vezes mais rápido. Em suma, esta dissertação provê os fundamentos para o desenvolvimento dos quatérnios dentro do contexto de sistemas de potência, assim como ressalta as suas possíveis aplicações.

ABSTRACT

Name: Victor do Prado Brasil

Title: Voltage, Current, Impedance, Power And Linear Transformations By Means Of Quaternions

Name of Program: Programa de Pós-Graduação em Engenharia Elétrica - Power Systems

Date of Defense: Brasília, February 15th, 2019

Supervisor: Anésio de Leles Ferreira Filho

Co-supervisor: João Yoshiyuki Ishihara

Palavras-Chave: Qualidade da Energia, Quatérnios, Teoria de Circuitos, Transformações Lineares.

Keywords: Power Quality, Quaternions, Circuit Theory, Linear Transformations.

Despite being the most widely known tool for power systems engineers, phasors have some disadvantages under non-ideal operating conditions. As a result, several researchers have been investigating other mathematical tools, for example, vectors, tensors, quaternions and geometric algebra. This dissertation focus on quaternions, and it presents their advantages in three-phase systems. Although, definitions for voltage and current quaternion already exists in literature, this dissertation provides a geometrical analysis of them. It is found that three phase voltage and current can be described as rotational elements, and their derivatives and integrals can be mapped to products, due to \mathbb{H} calculus. Based on this property, an innovative concept of three-phase impedance by means of quaternions is obtained. In order to cover the basic topics of an electrical system analysis, a power theory built on the hamiltonian algebra is briefly discussed. It is noteworthy that the power quaternion is redefined, yielding a direct relationship with the application of phasors in a single phase system. The proposed instantaneous reactive power definition is proved to be superior to those existing on literature, because an explanation for its direction can be provided. This dissertation also suggests a novel quaternion time-domain symmetrical components theory, which provides a linear state-space model for estimation of these components based on instantaneous samples of voltage and/or current. A similar approach in the phasorial domain is yet to be found. At last, a quaternion version of Clarke and Park transformation is proposed. In both cases, the number of values needed are smaller than in the traditional matrix implementation. For the Park transform, this novel method performed approximately four times faster. In summary, this dissertation lay out the fundamentals for quaternion research in the field of power system as well as highlights promising applications.

Contents

1	Introduction.....	1
1.1	OVERVIEW	1
1.2	STATE OF THE ART	3
1.3	OBJECTIVES	6
1.4	CONTRIBUTIONS	6
1.5	DISSERTATION ORGANIZATION	7
2	Theoretical Background	9
2.1	QUATERNION DEFINITIONS	9
2.1.1	THE STANDARD <i>Quadrnomial</i> FORM	9
2.1.2	SUM AND SUBTRACTION	10
2.1.3	PRODUCT	11
2.1.4	NORM	12
2.1.5	CONJUGATE	12
2.1.6	INVERSE.....	13
2.1.7	THE POLAR FORM	14
2.1.8	ROTATION QUATERNION.....	14
2.1.9	DERIVATIVES AND INTEGRALS	14
2.2	MATRICES AND QUATERNIONS.....	15
3	Voltage and Current: A Geometrical Analysis	19
3.1	BALANCED CONDITIONS	19
3.2	UNBALANCED CONDITIONS.....	27
4	Symmetrical Components, Passive Elements and Power	41
4.1	SYMMETRICAL COMPONENTS	41
4.2	LOADS	49
4.2.1	WITHOUT MUTUAL COUPLING	49
4.2.2	WITH MUTUAL COUPLING	52
4.2.3	UNBALANCED IMPEDANCE	53
4.3	TRANSMISSION LINES.....	54
4.4	ACTIVE, REACTIVE AND APPARENT POWER.....	55
5	Signal Transformation.....	59

6	Conclusions	67
	Bibliography.....	69
	Appendix	75
I	Matlab Code for Comparison of the QVL Plane Computation Method.....	77
II	Matlab Code for Comparison of Matrix and Quaternion Implementation of Clarke Transform.....	81
III	Matlab Code for Comparison of Matrix and Quaternion Implementation of Park Transform.....	85

List of Tables

2.1	Quaternion Product Rules. First column denotes the left multiplier and the first row the right multiplier.	11
3.1	Comparison of the computation time needed for the null space and the cross product methods for determining the QVL plane, <i>i.e.</i> \mathbf{n}	24
3.2	QVL parameters for different conditions.....	40
5.1	Comparison of vector and reference rotation around \mathbf{y} by 90°	63

List of Figures

2.1	Example of the purely vectorial quaternion \mathbf{a} representation.	10
2.2	Cross product cyclic rule.....	12
3.1	General concept of a balanced quaternion voltage and its locus.....	21
3.2	Animated balanced quaternion voltage and its locus.	21
3.3	Cumulative average for the demanded computational time of the QVL plane via the cross product method.....	25
3.4	QVL for balanced, amplitude unbalanced and phase unbalanced conditions.....	28
3.5	Arbitrary ellipse in the plane $\mathbf{q}_1\mathbf{q}_2$ with major and minor semi-axes denoted by V_α and v_β , respectively	31
3.6	Geometric representation for the oscillatory voltage norm component in terms of its magnitude and angle.....	33
3.7	QVL for the magnitude unbalanced condition of Example 2. Balanced QVL is presented for comparison. Major and minor semi-axes denoted α and β are in blue and red colors.....	35
3.8	QVL for the phase unbalanced condition of Example 3. Balanced QVL is presented for comparison. Major and minor semi-axes are denoted α and β in blue and red colors.....	37
4.1	Unbalanced set of three phasors being represent by three sets of three balanced phasors. The first set is the positive sequence, the second is the negative and the third is the zero.	42
4.2	Animated unbalanced quaternion voltage and its locus in terms of its symmetrical quaternion components.....	46
4.3	QVL Analyser app designed in <i>Matlab</i>	47
4.4	System consisting of an ideal power supply connected via three wires to a balanced load consisting of three RLC impedances connected in wye.	49
4.5	Three-phase system consisting of a source, a transmission line and a load.	55
5.1	Initial reference frame before Clarke Transformation.....	60
5.2	Reference frame after a clockwise rotation of C around A by 45°	61
5.3	Resulting reference frame after Clarke transformation.	61
5.4	Comparison of the Clarke transformation implemented via matrix and via quaternions.	64

5.5	Cumulative average for the demanded computational time of the Clarke quaternion implementation. The red dashed line indicates the final average value obtained.....	64
5.6	Comparison of the Park transformation implemented via matrix and via quaternions.	66
5.7	Cumulative average for the demanded computational time of the Park quaternion implementation. The red dashed line indicates the final average value obtained.....	66

LIST OF SYMBOLS

\mathbb{H}	Hamiltonian space	
\mathbb{R}	Real space	
t	Time variable	[s]
ω	Angular electrical frequency	[rad/s]
T_S	Sampling interval	[s]
$p(t)$	Single phase instantaneous active power	[W]
$v_x(t)$	Instantaneous voltage of phase/sequence “X”	[V]
$i_x(t)$	Instantaneous current of phase/sequence “X”	[A]
S	Apparent power	[VA]
P	Active power	[W]
Q	Reactive power	[VAr]
R	Resistive element	[Ω]
X	Reactive element	[Ω]
\hat{Z}	Impedance	[Ω]
\hat{Y}	Admittance	[\mathcal{U}]
$\mathbf{V}(t)$	Quaternion voltage	[V]
$\mathbf{I}(t)$	Quaternion current	[A]
$\mathbf{S}(t)$	Quaternion power	[VA]
\mathbf{Z}	Quaternion impedance	[Ω]
\mathbf{Y}	Quaternion admittance	[\mathcal{U}]
α	Quaternion voltage locus major semi-axis direction	
β	Quaternion voltage locus minor semi-axis direction	
$ \mathbf{X} $	Quaternion norm of quantity “X”	
$X \cdot Y$	Inner product between X and Y vectors	
$X \times Y$	Cross product between X and Y vectors	
$vec()$	Operation of mapping a quaternion into a four dimensional column vector	

Subscripts

abc	three-phase quantity
CBA	inverse phase sequence
$[k]$	k-th variable sample

Superscript

$\hat{}$	Complex number (represents a phasor if applied to voltage or current)
$*$	Conjugate
-1	Inverse
$\vec{}$	Vectorial part of a quaternion
T	Vector transposition
H	hermitian operation (transposition followed by conjugation)

Abbreviations

KVL	Kirchhoff Voltage Law
RLC	Circuit containing a resistor, an inductor and a capacitor
RMS	Root Mean Square
QVL	Quaternion voltage locus
QCL	Quaternion current locus

Chapter 1

Introduction

1.1 Overview

According to Fourier's law, any function can be described sine and cosine series. So, in electrical systems, voltages and currents can be expressed, without loss of generality, as a linear combination of sinusoidal functions. Power is defined as the amount of energy per time consumed or provided. In a single phase circuit, instantaneous power is given by the product of instantaneous voltage and current. This product yields, for sinusoidal systems, one unidirectional and one alternating term, as shown in (1.1).

$$p(t) = P [1 + \cos (2wt)] + Q \sin (2wt) \quad (1.1)$$

The unidirectional term (P) is the active power, and it is equal to the load energy consumption, or source energy supplied. The alternating term (Q) represents an exchange between source and load, and it is named reactive power [1].

Working with voltages and currents in the time domain requires dealing with sinusoidal functions. This aspect increases the complexity of calculations. For this reason, phasors were introduced for steady-state studies. With this tool, derivatives and integrals are computed as a complex number times a phasor. Additionally, trigonometric products are mapped into algebraic ones between real numbers (*i.e.* the magnitudes of each phasor) followed by their angles sum. These properties simplifies mathematical operations. As a result, phasors advent shaped the development of the actual power system scenario. Nowadays, they are applied to almost every problem and have become the most widely known tool for electrical engineers. However, it has some drawbacks.

Although they represent adequately balanced systems under sinusoidal conditions, Steinmetz noticed, in 1892, that phasorial power theory is not applicable to an arc bulb, which is a type of lamp based on electrical discharges. The apparent power (S) squared was not equal to the sum of the squares of active (P) and reactive (Q) powers. Mathematically, what Steinmetz found out was that in the mentioned case $S^2 \neq P^2 + Q^2$ [2]. In this case specifically, harmonics originated by the arc bulb were responsible for the inequality [3].

In a three phase circuit, phasor limitations are also present under ideal conditions. Accordingly to [3], the usual comprehension of reactive power, as an alternating flux of energy between load and source, is not applicable for three phase systems. In fact, the physical meaning of three phase reactive power is not yet well established.

Under unbalanced situations, power is also not yet fully comprehended and definitions are still in discussion [3–7]. In a three phase unbalanced load consisting purely of resistors connected in wye, instantaneous power is not constant. Actually, it has an oscillating nature [6, 7]. Moreover, phasorial power in this case can be equal to the one resulting from a balanced case [3]. Phasorial components, hence, fail to i) represent alternating power originated by unbalanced loads, and ii) provide a physical meaning for the reactive quantity. If harmonics are considered simultaneously with unbalance, then the effects of both phenomena are combined. Furthermore, since harmonics are not linear, the superposition principle does not apply. Therefore, the resulting effects are not the sum of the individual ones. So, phasors drawbacks becomes even more tangible.

These facts drew the attention of several researchers. As a result, power phenomenon has been investigated considering ideal (linear time invariant systems with balanced and sinusoidal voltages) and non ideal conditions [2–4, 8–28]. Notwithstanding, a consensus of the most adequate theory has not yet been reached. However, it is possible to observe that many works dedicated to this issue have been proposed in the time domain [8, 9, 17–28]. This is a setback, because phasors were introduced in order to simplify mathematical operations by working in the frequency. So, a mathematical tool that operates in the time domain and that preserves the phasors advantages previously discussed might be the most adequate choice for power systems analysis.

It is worth emphasising that besides poorly representing power, phasors are also limited to a per phase approach. In other words, they are capable of representing only one phase at a time. In a three-phase system, phases are mutually coupled [3]. Decoupling techniques such as Fortescue, Clarke, Park or Karrenbauer transformations may be employed. Some phenomena, for example harmonics, may still affect all of the decoupled voltages and currents. As a result, signal processing needs to be repeated for each phase, and it may become unfeasible due to its computational burden. A solution found was to make use of Clarke transformation to come up with a complex valued signal to represent the system. Signal's real part is equal to the alpha component and its imaginary to the beta component. With this complex signal, frequency estimation algorithms such as the minimum variance distortionless response (MVDR), the multiple signal classification (MUSIC) and the complex Kalman Filter might be applied [29–32]. These approaches, nevertheless, have been proved non-optimal in unbalanced conditions because the zero sequence is not considered, even though it may be hazardous for transformers [33]. This highlights i) another phasor limitation, and ii) the need for alternative approaches that are capable to deal with all phases simultaneously.

In the search for alternative representations, several mathematical tools - *e.g.* vectors, tensors, geometric algebra and quaternions - have been applied to electric power system analysis and modelling in order to better represent and solve power quality (PQ) problems that were traditionally addressed via phasors [8, 9, 13, 16–28, 33–41]. Among these, quaternions (also called hypercomplex elements) are slowly regaining attention due to i) the related mathematical advents (\mathbb{H} calculus,

for instance), and ii) their intensified use in several other signal processing contexts [33, 42–45]. They are capable of both representing quantities in the time domain and preserving phasors advantages [41]. Hence, they may be an adequate framework for power theories. Although they have been applied in the power systems context, there is a literature lack regarding a complete quaternion electrical theory.

1.2 State of the Art

Literature related to the applications of quaternions in electrical power system is still flourishing. In this section, quaternion development will be briefly presented and discussed, followed by its applications on the specified context.

Quaternions were discovered by William Rowan Hamilton in 1843. His objective was to rotate elements in the three dimensional (\mathbb{R}^3) space via products in a similar way complex numbers do in \mathbb{R}^2 [46]. A first approach was to use a set of three real numbers, but dividing two sets was not well defined. A solution found was to employ four elements, in which three would act as complex numbers representing the \mathbb{R}^3 space and one auxiliary real number. As a consequence the non-commutative algebra of quaternions was established forming a closed mathematical group, *i.e.* with operations well defined. With these definitions, he was able to execute any rotation and scaling with products, as it was his primary objective.

According to [35], the pioneer in applying quaternions to electrical engineering was James Clerk Maxwell, in 1865, in his electricity and magnetism treatise [47]. He wrote the equations for the electric and magnetic fields in each axis separately and did likewise for the forces involved, obtaining a total of 20 equations. With quaternion operators, he managed to group the sets of three equations - one for each axis - into sets of single ones. As a result, he was able to write general expressions that correctly represents the effects of such phenomena on all of the three axes. However, due to the advent of vectorial calculus, his electromagnetic theory was rewritten by J. Willard Gibbs [48] and Oliver Heaviside [49] into the known form, thereupon burying quaternion usage in this context.

Although they remained little explored for a while, their usage has recently been rescued in several knowledge areas. For example, in the study of rigid bodies, they are being employed for rotations instead of matrices for the following reasons [50]: i) their representation is more compact, using the only four necessary elements (two for the axis of rotation, one for the scaling factor and one for the angle), instead of nine; ii) normalization is computationally less expensive; and iii) mathematical singularities (such as the gimbal lock problem) are avoided. If rotations matrices are used in another field, then these same arguments applies.

Nowadays, quaternions are regaining attention in the field of power systems. First, its mathematical structure allows to operate the three phases simultaneously [6, 41]. Phasors applies a single complex number for representing one phase. With quaternions, three complex numbers are used, one for each phase. Second, the advent of \mathbb{H} calculus is causing the development of quaternion-based algorithms that have been proved to be computationally efficient and accurate [42–45].

Third, several theories are being developed in the time domain, so a tool that operates in this domain is also desirable. Thus, the possibility of applying these algorithms and dealing with all phases of the system simultaneously and in the time domain has been motivating quaternion usage.

In 1996, [51] proposed the representation of instantaneous power via an algebraic framework that is related to “Hamilton operators” (as stated by the authors)¹. With some mathematical manipulations, they were able to decompose current into “real” and “imaginary” components². The “real” current was defined as the responsible only for the active instantaneous power. The “imaginary” part was found to be related to non active power. Authors showed that the decomposition generates the same currents as those resulting of Willems’ power theory presented in [25]. The authors also proposed a three-phase time varying impedance and admittance. This last definition, nevertheless, was not explored in their study.

In 2012, [34] presented how linear transformations applied to an induction motor can be achieved in the quaternion domain. For this purpose, he presented the equations that are common in electrical machine analysis. Then, using the quaternion representation via Pauli spin matrices, he proposed a quaternion transformation in terms of four coefficients, which he was able to compute after some algebraic effort. According to the author, the proposed method has the advantage of using only 4 parameters instead of the 9 required in the traditional way.

In 2013 and 2016, [35] and [40] proposed a quaternion single phase representation in the references. Voltage and current were defined as hypercomplex elements. The author applied the Kirchhoff voltage law (KVL) to a RLC series circuit and the resulting time domain equation was rewritten in the form of quaternions. For this purpose, current was defined on one axis and its derivative and integral on another. Afterwards, he computed the root mean square (RMS) value of the equation. Therefore, a relation between voltage and current was obtained, and a quaternion impedance was defined as the quaternion voltage RMS divided by the scalar current RMS value. A power quaternion equation, similar to phasors, was also proposed. The article showed how quaternions can be used for representing and analysing a single phase circuit. However, the math involved is more complex and the computational effort is bigger. So, the method did not present any advantage when compared to phasors.

In 2014, [37] and [36] employed quaternions for the control of power factor and harmonics in the project of an active power filter (APF). In order to do so, the authors proposed rewriting instantaneous three phase voltages and currents in the quaternion basis. Power was defined as voltage times current. Consequently, it was possible to identify, compute and compensate inactive power. The designed APF was tested for an unbalanced non-linear load. It reduced the total harmonic distortion (THD) from 37.45% to 8.24%. According to the authors, the implemented strategy did not require high performance hardware and was approximately ten times faster than those strategies based on the Akagi-Nabae pq-theory, proposed in [8].

¹Although the authors did not employ the word quaternion in their work, the mathematical definitions and operations employed are equivalent to the quaternion algebra.

²The nomenclature “real” and “imaginary” used here is the same employed by the authors. Hence they are used with quotations marks. These expressions are not to be confused with complex numbers components.

In [39], it is presented some more theoretical details related to the articles [36,37]. Additional properties of the compensating current, which when added to the original ones results in balanced and sinusoidal waveforms, were provided. More practical examples of the implemented filter were also presented, corroborating the former conclusions.

In 2015, [38] proposed a quaternion frequency estimator for three-phase systems with the objective of estimating the fundamental frequency considering noisy, unbalanced and distorted situations. Applying \mathbb{H} calculus, a discrete state space model was developed and applied in the quaternion extended Kalman filter (QEKF) proposed in [44]. Using voltage samples, the estimator presented a stable behaviour and was able to correctly track the fundamental frequency. The authors employed synthetic and real-world data in order to evaluate the estimator. Voltage unbalance, and frequency rise and decay conditions were investigated. The estimator presented lower steady-state errors and a better dynamic performance than the conventional complex linear ones based on Clarke transformation. Its overshoot and settling time were smaller. The authors did not consider, however, harmonics effects, nor did they model the zero sequence component.

In 2017, [6] compared phasorial, tensorial and quaternion representation for power systems. The author concluded that phasors are limited to a steady-state representation and to a per phase analysis. On the other hand, tensors were able to represent instantaneous voltage, current and power. Quaternions were shown to have the advantages of both of the previous tools, and to have a more compact representation than tensors. Additionally, a quaternion theory for balanced three-phase circuits was developed. Results were later augmented in [41].

Although voltage, current and power had been defined as hyper elements in [37], the resulting properties from these definitions were not yet explored. In this sense, [41] presented a quaternion three phase circuit analysis as an extension of [6]. Voltage and current were shown to be rotating elements in the quaternion domain. So, it was proposed to represent them via rotation formula. Thus, derivatives and integrals were rewritten as products, and a three phase quaternion impedance definition was proposed and explored. A novel power quaternion, that is directly related to the load reactance, was also proposed. This provided a physical to the reactive quantity direction which lacks in vectorial theories. A complete analogy between quaternions in three phase circuit and phasors in single phase circuits was achieved. The authors concluded that the proposed method i) preserves the instantaneous, as well as steady-state information, ii) allows to operate three phases simultaneously rather than one at a time, and iii) the formulae are identical to the phasorial ones in a single phase circuit.

In 2018, [33] presented a quaternion valued signal for three phase voltage harmonics estimation. They proposed rewriting the balanced quaternion voltage harmonics in terms of their positive, negative and zero sequences. After noticing that all terms had an exponential associated with a specific axis, they proposed substituting the sweeping vector (which is a complex exponential) by one with the axis found (resulting in a quaternion exponential). With this new sweeping vector, the authors applied the MVDR and the MUSIC algorithms for harmonics estimation. Results were compared to the ones obtained by Clarke-based algorithms. The proposed method outperformed the others in the sense that it was able to detect all harmonics, including zero sequence harmonics.

Although voltage was proposed in terms of symmetrical components, the expressions are simply supposed. There was no proof given, nor their relation to Fortescue’s definitions were shown. The authors also did not consider the possibility of having unbalance simultaneously to harmonics.

In synthesis, quaternions have been used for i) instantaneous power representation [51], ii) perform linear transformations of induction motor models [34], iii) analysis of single phase systems (computation of current and power for a given circuit) [35], iv) design of an active power filter [36, 37], v) estimating electrical frequency [38], vi) computing currents and representing a three-phase system [6, 41], and vii) harmonics estimation [33]. Although [38] decomposed voltage quaternion into positive and negative sequences, there was no approach to the zero component. On the other hand, [33] included the zero sequence for a balanced system with harmonics. However, the development of the decomposition was not presented, nor the authors commented on the relation between their definition and Fortescue’s. So, a thorough study is needed. It is also noteworthy that a three-phase impedance for non-ideal conditions is still lacking. The same applies to an equivalent version of Clarke and Park transformations, which are typical on power systems analysis.

On the basis of the foregoing, quaternion applications in power systems needs further investigation, as evidenced by the literature. Hence, the main motivations for the development of this dissertation are i) the topicality, ii) the lack of systematic studies in this area, and iii) the possibility of laying the mathematical basis for the usage of quaternion-based algorithms in power systems.

1.3 Objectives

The main objective of this dissertation is to provide a novel three phase circuit theory based on Hamilton non commutative algebra. For this purpose, it is expected to i) define quaternion voltage, current, “impedance”³ (passive elements in delta or wye and transmission lines with and without electrical coupling) and power in the time domain; ii) propose a quaternion version for symmetrical components; iii) provide a quaternion implementation of Clarke and Park transformations; and iv) indicate possible applications in up to date researching problems.

This dissertation is expected to lay a theoretical foundation, that will support future development of quaternion-based solutions for power systems. Despite the absence of this foundation in the literature, a few researchers managed to apply this tool. So, with this work, it is expected to boost the development of such solutions and, hopefully, to provide better power quality world-wide.

1.4 Contributions

The contributions of this dissertation are divided into two groups:

³The concept of three phase quaternion impedance is not to be confused with the phasorial one. Although it also represents the load voltage and current relationship, the quaternion impedance is defined in the time domain, rather than the frequency domain, and it represents all phases elements of the load.

1. A novel three-phase circuit theory based on quaternions is proposed and established. Voltage, current and power definitions provided in [21,33,34,36,38,39] are systematically investigated and related to other theories whenever is possible. A quaternion version of Fortescue's theory is proposed in the time domain. Three-phase quaternion impedance and admittance are generalized for both balanced and unbalanced conditions. With exception to the symmetrical components theory developed, these results were published in the 18th International Conference of Harmonics and Quality of Power [41].
2. A quaternion implementation of Clarke and of Park transformations based on rotation formula is provided. Both are proven to be storage efficient, and the Park version is shown to perform better than its classic matricial transformation.

1.5 Dissertation Organization

This dissertation is organised into 6 chapters.

Chapter 1 presents the need for alternative mathematical tools in order to better represent and operate power systems. Phasors main advantages and limitations are discussed. In this context, quaternion is suggested as a feasible option that still needs further investigation. Next, literature regarding its applications in power systems is revisited. Finally, the dissertation objectives and its organization are provided.

Chapter 2 provides the necessary theoretical foundations and the methodology adopted in this work. Quaternion mathematical definitions as well as its properties are presented. The relation between real matrices and quaternions is discussed. Additionally, methods to alternate from one framework to the other are investigated. At last, the methods for the theory development are presented along with those applied for the simulations and for comparing the developed algorithms.

Chapter 3 presents the quaternion definition for time-domain voltage and current. A geometrical approach, based on a three-dimensional hypercomplex space, is evaluated and the advantages and disadvantages of such representation are discussed.

Chapter 4 proposes a novel circuit theory. A novel quaternion symmetrical components equivalent to Fortescue's [52] is developed. A generalized three-phase quaternion impedance and admittance definitions are shown for passive loads and transmission lines with and without electrical coupling for both balanced and unbalanced conditions. Next, the electrical power defined in the \mathbb{H} space is addressed with focus on its interpretation. Its relation to other power theories is discussed. At last, a geometrical interpretation of Clarke and Park transformations based on [53] are presented. Their implementations via quaternions are proposed and compared against their classical version.

In chapter 6, conclusions and guidelines for future research are provided.

Chapter 2

Theoretical Background

In this chapter, the theoretical background necessary for the understanding of this dissertation is provided along with the methods applied. First, quaternion definitions are examined. Then, the existing link between real matrices and quaternions is presented along with a technique to change from one type of representation to the other. At last, the methods employed for developing and validating the theory hereby proposed are presented.

2.1 Quaternion Definitions

Quaternions are a system of numbers that composes the Hamiltonian (or the hypercomplex) space denoted by \mathbb{H} and named after the mathematician William Rowan Hamilton. He discovered quaternions in 1843 in the search to represent three dimensional (\mathbb{R}^3) elements in a similar way \mathbb{R}^2 elements can be represented by complex numbers. In other words, he wanted to rotate elements by means of products [46]. A first approach was to use sets of three real numbers, but division was not well defined. A solution found was to employ three complex units representing the \mathbb{R}^3 space and one auxiliary real number. As a consequence the non-commutative algebra of quaternions was established forming a closed mathematical group. With these definitions, it was possible to execute any rotation and scaling with products.

2.1.1 The Standard *Quadranomial* Form

A quaternion (\mathbf{q}) is defined by a set of four real numbers, *e.g.* $\{a_0, a_1, a_2, a_3\}$. The standard *quadranomial* form for \mathbf{q} is

$$\mathbf{a} = a_0 + a_1\mathbf{x} + a_2\mathbf{y} + a_3\mathbf{z}, \quad (2.1)$$

in which \mathbf{x} , \mathbf{y} and \mathbf{z} are the \mathbb{H} basis and are commonly used to denote individual axes of a three dimensional reference frame.

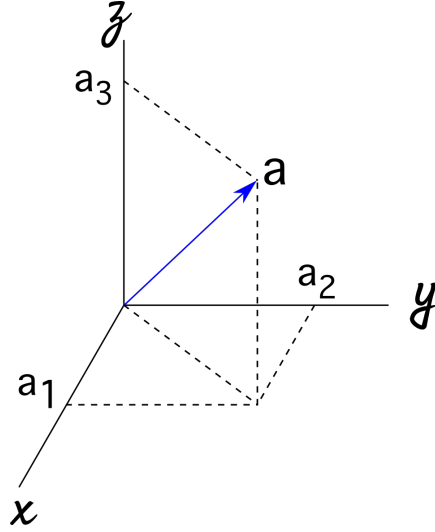


Figure 2.1: Example of the purely vectorial quaternion \mathbf{a} representation.

Similarly to complex numbers, quaternions can be decomposed in their real and vectorial (instead of imaginary) parts as

$$\text{Re}(\mathbf{a}) = a_0 \quad (2.2)$$

$$\vec{\mathbf{a}} = a_1\mathbf{x} + a_2\mathbf{y} + a_3\mathbf{z}. \quad (2.3)$$

If its real part is null, the quaternion is said to be purely vectorial, and it can be geometrically represented. Actually, the real part usually act as an auxiliary element to perform rotations, and purely vectorial quaternions are employed for representing three-dimensional quantities. An example is provided in Figure 2.1. In this dissertation, quaternions are denoted by bold letters. An arrow above them denotes their vectorial part (which is also a quaternion, but a purely vectorial one).

2.1.2 Sum and Subtraction

Considering two arbitrary quaternions \mathbf{a} and \mathbf{b} given by $\mathbf{a} = a_0 + a_1\mathbf{x} + a_2\mathbf{y} + a_3\mathbf{z}$ and $\mathbf{b} = b_0 + b_1\mathbf{x} + b_2\mathbf{y} + b_3\mathbf{z}$, their sum and subtraction are operated term by term,

$$\mathbf{a} + \mathbf{b} = (a_0 + b_0) + (a_1 + b_1)\mathbf{x} + (a_2 + b_2)\mathbf{y} + (a_3 + b_3)\mathbf{z} \quad (2.4)$$

$$\mathbf{a} - \mathbf{b} = (a_0 - b_0) + (a_1 - b_1)\mathbf{x} + (a_2 - b_2)\mathbf{y} + (a_3 - b_3)\mathbf{z}. \quad (2.5)$$

These operations are associative, *i.e.*

$$\mathbf{a} + (\mathbf{b} + \mathbf{c}) = (\mathbf{a} + \mathbf{b}) + \mathbf{c} \quad (2.6)$$

$$\mathbf{a} - (\mathbf{b} - \mathbf{c}) = (\mathbf{a} - \mathbf{b}) + \mathbf{c}. \quad (2.7)$$

Similarly to real numbers, addition is commutative and subtraction is not, hence the following equalities

$$\mathbf{a} + \mathbf{b} = \mathbf{b} + \mathbf{a} \quad (2.8)$$

$$\mathbf{a} - \mathbf{b} = -(\mathbf{b} - \mathbf{a}). \quad (2.9)$$

2.1.3 Product

The main obstacle for the quaternion theory advent was division and product operations. Hamilton solved this problem by using four elements, in which three would act as complex numbers and one as a real number. This idea is present in the governing quaternion equation

$$\mathbf{x}^2 = \mathbf{y}^2 = \mathbf{z}^2 = \mathbf{xyz} = -1 \quad (2.10)$$

Hamilton originally employed the letters \mathbf{i}, \mathbf{j} and \mathbf{k} to represent the orthonormal basis. In this dissertation, in order to avoid nomenclature ambiguity, i will be used for current in the time domain and the quaternion basis will be denoted by \mathbf{x}, \mathbf{y} , and \mathbf{z} .

Hamilton derived all other product rules from (2.10). As a result, 16 rules were established. They are summarized in Table 2.1, in which the first column denotes the left multiplier and the first row the right multiplier since \mathbb{H} is non-commutative.

Table 2.1: Quaternion Product Rules. First column denotes the left multiplier and the first row the right multiplier.

Product	r	\mathbf{x}	\mathbf{y}	\mathbf{z}
r	r^2	$r\mathbf{x}$	$r\mathbf{y}$	$r\mathbf{z}$
\mathbf{x}	$r\mathbf{x}$	-1	\mathbf{z}	$-\mathbf{y}$
\mathbf{y}	$r\mathbf{y}$	$-\mathbf{z}$	-1	\mathbf{x}
\mathbf{z}	$r\mathbf{z}$	\mathbf{y}	$-\mathbf{x}$	-1

An alternative method for multiplying two quaternions is based on the inner and on the cross product. The former is computed as

$$\vec{\mathbf{a}} \cdot \vec{\mathbf{b}} = a_1b_1 + a_2b_2 + a_3b_3 \quad (2.11)$$

and the latter is given by the following determinant

$$\vec{\mathbf{a}} \times \vec{\mathbf{b}} = \begin{vmatrix} \mathbf{x} & \mathbf{y} & \mathbf{z} \\ a_1 & a_2 & a_3 \\ b_1 & b_2 & b_3 \end{vmatrix} \quad (2.12)$$

or equivalently

$$\vec{\mathbf{a}} \times \vec{\mathbf{b}} = (a_2b_3 - a_3b_2)\mathbf{x} + (a_3b_1 - a_1b_3)\mathbf{y} + (a_1b_2 - a_2b_1)\mathbf{z}. \quad (2.13)$$

The cross product can also be computed following the cyclic product rule illustrated in Figure 2.2. Clockwise products (in the same direction of the arrows) are positive and counter-clockwise are negative.

Combining the inner and outer products, quaternion multiplication is computed as

$$\mathbf{ab} = \underbrace{Re(\mathbf{a})Re(\mathbf{b}) - \vec{\mathbf{a}} \cdot \vec{\mathbf{b}}}_{Re(\mathbf{ab})} + \underbrace{Re(\mathbf{a})\vec{\mathbf{b}} + \vec{\mathbf{a}}Re(\mathbf{b}) + \vec{\mathbf{a}} \times \vec{\mathbf{b}}}_{\vec{\mathbf{ab}}}. \quad (2.14)$$

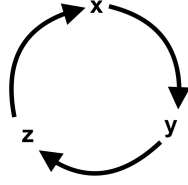


Figure 2.2: Cross product cyclic rule.

Substituting (2.11) and (2.13) into (2.14), yields

$$\begin{aligned}
 \mathbf{ab} = & (a_0b_0 - a_1b_1 - a_2b_2 - a_3b_3) + \\
 & \mathbf{x} (a_0b_1 + a_1b_0 + a_2b_3 - a_3b_2) + \\
 & \mathbf{y} (a_0b_2 - a_1b_3 + a_2b_0 + a_3b_1) + \\
 & \mathbf{z} (a_0b_3 + a_1b_2 - a_2b_1 + a_3b_0)
 \end{aligned} \tag{2.15}$$

It is worth mentioning that quaternion product is non commutative because of the cross product, *i.e.*

$$\vec{\mathbf{a}} \times \vec{\mathbf{b}} = -\vec{\mathbf{b}} \times \vec{\mathbf{a}}. \tag{2.16}$$

But associative properties remains. So, the computation order does not change the result

$$\mathbf{a}(\mathbf{bc}) = (\mathbf{ab})\mathbf{c}. \tag{2.17}$$

2.1.4 Norm

The quaternion norm (length, absolute value or magnitude) is a real number (a scalar) defined according to the Euclidean norm. It is given by

$$|\mathbf{a}| = \sqrt{a_0^2 + a_1^2 + a_2^2 + a_3^2}. \tag{2.18}$$

This definition may differ from author to author, some of them consider the square root employed in this dissertation [?, 35, 38, 40, 43, 44], while others do not [21, 36, 39].

2.1.5 Conjugate

Complex number conjugate changes the signal of the imaginary part. In the case of quaternions, the vectorial part that is changed. It is denoted as

$$\mathbf{a}^* = \text{Re}(\mathbf{a}) - \vec{\mathbf{a}}. \tag{2.19}$$

It is noteworthy that if \mathbf{a} is purely vectorial, then conjugating is equivalent to multiplying it by (-1)

$$\mathbf{a}^* = -\vec{\mathbf{a}} = -\mathbf{a}. \tag{2.20}$$

It is related to the norm by

$$\mathbf{a}\mathbf{a}^* = \mathbf{a}^*\mathbf{a} = |\mathbf{a}|^2. \quad (2.21)$$

Conjugation can be employed for extracting the real and the vectorial part of a quaternion. Its real part is obtained by the average

$$Re(\mathbf{a}) = \frac{\mathbf{a} + \mathbf{a}^*}{2} \quad (2.22)$$

and the vectorial part by the difference

$$\vec{\mathbf{a}} = \frac{\mathbf{a} - \mathbf{a}^*}{2}. \quad (2.23)$$

Taking into account conjugate and product operations, it is possible to prove that conjugation inverts the product order in a similar way that the transposition of matrices invert the order in which they are operated.

$$\text{Quaternion: } (\mathbf{ab})^* = \mathbf{b}^*\mathbf{a}^* \quad (2.24)$$

$$\text{Matrix: } (AB)^T = B^T A^T \quad (2.25)$$

2.1.6 Inverse

Division between any two mathematical elements can be defined as the product between the first and the second's inverse. Thus, defining the quaternion inverse is equivalent to defining its division operation. Any element times its inverse should be equal to one

$$\mathbf{a}\mathbf{a}^{-1} = 1. \quad (2.26)$$

If both sides of (2.26) are left multiplied by \mathbf{a}^* and property (2.21) is applied, then

$$\mathbf{a}^*\mathbf{a}\mathbf{a}^{-1} = \mathbf{a}^* \quad (2.27)$$

$$|\mathbf{a}|^2\mathbf{a}^{-1} = \mathbf{a}^*. \quad (2.28)$$

Since $|\mathbf{a}|^2$ is a real number (a scalar), it is possible to divide the former equation by it. Hence, quaternion inverse is computed as

$$\mathbf{a}^{-1} = \frac{\mathbf{a}^*}{|\mathbf{a}|^2}. \quad (2.29)$$

Similarly to the conjugation, taking the inverse of a quaternion product changes the operating order. In other words,

$$(\mathbf{ab})^{-1} = \frac{(\mathbf{ab})^*}{|\mathbf{ab}|^2} \quad (2.30)$$

$$= \frac{\mathbf{b}^*\mathbf{a}^*}{|\mathbf{a}|^2|\mathbf{b}|^2} \quad (2.31)$$

$$= \frac{\mathbf{b}^*}{|\mathbf{b}|^2} \frac{\mathbf{a}^*}{|\mathbf{a}|^2} \quad (2.32)$$

$$= \mathbf{b}^{-1}\mathbf{a}^{-1}. \quad (2.33)$$

2.1.7 The Polar Form

Like complex numbers, a quaternion (\mathbf{a}) can also be represented in a polar form, given by

$$\mathbf{a} = |\mathbf{a}|e^{\mathbf{d}\theta} = |\mathbf{a}| (\cos(\theta) + \mathbf{d} \sin(\theta)), \quad (2.34)$$

in which \mathbf{d} is a purely vectorial quaternion with unitary norm and θ is the angle between the real axis and \mathbf{d} .

Conjugating in the polar form is achieved by changing the sign of \mathbf{d} or θ .

2.1.8 Rotation Quaternion

As aforementioned, quaternions are employed for representing elements in a three dimensional reference frame. One of Hamilton's objectives was to rotate and scale elements in the \mathbb{R}^3 . If one attempts to use any method based on transformation matrices, he will find that at least nine elements are needed during computation, when actually only four - *i.e.* two for specifying the axis, one for the scale factor and another for the angle - are needed. So, in terms of memory, quaternions are more effective because only the necessary number of information is stored.

In the \mathbb{H} domain, clockwise rotation ¹ of an element around an axis \mathbf{d} by an angle θ_r is computed as

$$\mathbf{a}_{\text{rot}} = \mathbf{R}\mathbf{a}\mathbf{R}^* \quad (2.35)$$

in which \mathbf{a} is the original element, \mathbf{a}_{rot} is the rotated one and \mathbf{R} is the rotation quaternion that is given by

$$\mathbf{R} = \cos\left(\frac{\theta_r}{2}\right) + \mathbf{d} \sin\left(\frac{\theta_r}{2}\right) = e^{\mathbf{d}\frac{\theta_r}{2}}. \quad (2.36)$$

It is noteworthy that if the quaternion is rotated along a perpendicular axis, (2.35) can be simplified into

$$\mathbf{a}_{\text{rot}} = e^{\mathbf{d}\theta_r}\mathbf{a}. \quad (2.37)$$

2.1.9 Derivatives and Integrals

In this dissertation, \mathbb{H} calculus will be applied in relation to a scalar. In other words, only quaternion derivative and integrals with respect to a real number will be discussed. Information regarding these operations with respect to another quaternion can be found in [43]. Derivatives and integrals are applied term by term. If $\mathbf{a}(t) = a_0(t) + a_1(t)\mathbf{x} + a_2(t)\mathbf{y} + a_3(t)\mathbf{z}$, then

$$\frac{d\mathbf{a}(t)}{dt} = \frac{da_0(t)}{dt} + \frac{da_1(t)}{dt}\mathbf{x} + \frac{da_2(t)}{dt}\mathbf{y} + \frac{da_3(t)}{dt}\mathbf{z} \quad (2.38)$$

$$\int \mathbf{a}(t)dt = \int a_0(t)dt + \left(\int a_1(t)dt\right)\mathbf{x} + \left(\int a_2(t)dt\right)\mathbf{y} + \left(\int a_3(t)dt\right)\mathbf{z}. \quad (2.39)$$

¹A rotation is considered as clockwise, if an observer face to face with the axis of rotation observes the elements being rotated clockwise. Face to face, in this context, means that in this position the axis is pointing out to him.

It is worth mentioning that all calculus rules, such as the chain rule, applies normally.

It is noteworthy that derivatives of quaternions describing circular motions are equal to multiplying them by their angular momentum. So, if such a quaternion is represented in the polar form as

$$\mathbf{a} = |\mathbf{a}|e^{\mathbf{n}\theta} \quad (2.40)$$

and its angle changes over time while its norm is held constant, then

$$\frac{d\mathbf{a}(t)}{dt} = \mathbf{n}\frac{d\theta}{dt}\mathbf{a}. \quad (2.41)$$

More specifically, if the angle changes at a constant rate, it can be rewritten in terms of an angular frequency (w)

$$\theta = wt \quad (2.42)$$

then its derivative is

$$\frac{d\mathbf{a}(t)}{dt} = \mathbf{n}w\mathbf{a} \quad (2.43)$$

and its integral is

$$\int \mathbf{a}(t)dt = -\mathbf{n}\frac{1}{w}\mathbf{a}. \quad (2.44)$$

A quaternion moving circularly over time around a perpendicular axis \mathbf{n} and with a constant magnitude and constant angular speed (w) can be expressed accordingly to (2.37) as

$$\mathbf{V}(t) = e^{\mathbf{n}wt}\mathbf{V}_{t0}, \quad (2.45)$$

in which \mathbf{V}_{t0} is the quaternion value at the time instant equal to zero. Therefore, it is possible to demonstrate that

$$\frac{d\mathbf{V}(t)}{dt} = \mathbf{n}w\mathbf{V}(t) \quad (2.46)$$

$$\int \mathbf{V}(t)dt = -\mathbf{n}\frac{1}{w}\mathbf{V}(t). \quad (2.47)$$

In other words, the quaternion derivative and integral are mapped into a product.

2.2 Matrices and Quaternions

In this section the link between quaternion and matrix representations will be discussed. Since quaternions are usually employed for three dimensional representation, consider $vec(\cdot)$ as a one-by-one mapping from \mathbb{H} to \mathbb{R}^4 . Mathematically,

$$vec(\mathbf{a}) = \left[\begin{array}{cccc} a_0 & a_1 & a_2 & a_3 \end{array} \right]^T, \quad (2.48)$$

i.e. the $vec(\cdot)$ operator takes each quaternion coefficient and stacks them in a vector. The inverse operation maps from the \mathbb{R}^4 back to \mathbb{H} and is given by

$$vec^{-1}\left(\left[\begin{array}{cccc} a_0 & a_1 & a_2 & a_3 \end{array}\right]^T\right) = a_0 + a_1\mathbf{x} + a_2\mathbf{y} + a_3\mathbf{z} \quad (2.49)$$

With this mapping, a quaternion product can be rewritten in terms of a matricial product via the Hamilton operators $\overset{+}{H}(\cdot)$ and $\overset{-}{H}(\cdot)$

$$vec(\mathbf{ab}) = \overset{+}{H}(\mathbf{a}) vec(\mathbf{b}) = \overset{-}{H}(\mathbf{b}) vec(\mathbf{a}). \quad (2.50)$$

Manipulating (2.15), Hamilton operators are found to be

$$\overset{+}{H}(\mathbf{a}) = \begin{bmatrix} a_0 & -a_1 & -a_2 & -a_3 \\ a_1 & a_0 & -a_3 & a_2 \\ a_2 & a_3 & a_0 & -a_1 \\ a_3 & -a_2 & a_1 & a_0 \end{bmatrix} \quad (2.51)$$

$$\overset{-}{H}(\mathbf{b}) = \begin{bmatrix} b_0 & -b_1 & -b_2 & -b_3 \\ b_1 & b_0 & b_3 & -b_2 \\ b_2 & -b_3 & b_0 & b_1 \\ b_3 & b_2 & -b_1 & b_0 \end{bmatrix}. \quad (2.52)$$

It is noteworthy that $\overset{+}{H}$ and $\overset{-}{H}$ are anti-symmetrical matrices with non-zero diagonal. Therefore, any transformation given by a matrix in this format can be mapped into a quaternion product. Furthermore, with these operators, any quaternion expression can be rewritten in terms of matrices.

The mapping from matrices to quaternion, however, is not as straightforward. Consider the generalized condition where the matricial equality

$$\underbrace{\begin{pmatrix} p_0 \\ p_1 \\ p_2 \\ p_3 \end{pmatrix}}_{vec(\mathbf{p})} = \underbrace{\begin{pmatrix} M_{00} & M_{01} & M_{02} & M_{03} \\ M_{10} & M_{11} & M_{12} & M_{13} \\ M_{20} & M_{21} & M_{22} & M_{23} \\ M_{30} & M_{31} & M_{32} & M_{33} \end{pmatrix}}_M \underbrace{\begin{pmatrix} h_0 \\ h_1 \\ h_2 \\ h_3 \end{pmatrix}}_{vec(\mathbf{h})} \quad (2.53)$$

needs to be mapped into \mathbb{H} .

One solution is to map each element from the matrix to a quaternion product. This can be achieved using the property that the real part of \mathbf{hx} is equal to $-h_1$. Applying it in conjunction with (2.22) yields

$$h_1 = -\frac{(\mathbf{hx}) + (\mathbf{hx})^*}{2}. \quad (2.54)$$

This result can be generalized for any of \mathbf{h} elements, as

$$h_k = \frac{\mathbf{h}\delta_k + \delta_k^*\mathbf{h}^*}{2}, \forall k \in \{0, 1, 2, 3\} \quad (2.55)$$

in which

$$\delta_k = \begin{cases} 1, & \text{if } k = 0 \\ -\mathbf{x}, & \text{if } k = 1 \\ -\mathbf{y}, & \text{if } k = 2 \\ -\mathbf{z}, & \text{if } k = 3 \end{cases} \quad (2.56)$$

The first row of (2.53) can be rewritten as

$$p_0 = \sum_{k=0}^3 M_{0k} \frac{\mathbf{h}\boldsymbol{\delta}_k + \boldsymbol{\delta}_k^* \mathbf{h}^*}{2}. \quad (2.57)$$

Since $\mathbf{p} = p_0 + p_1\mathbf{x} + p_2\mathbf{y} + p_3\mathbf{z}$, then

$$\mathbf{p} = \sum_{k=0}^3 \left[\sum_{l=0}^3 M_{kl} \frac{\mathbf{h}\boldsymbol{\delta}_k + \boldsymbol{\delta}_k^* \mathbf{h}^*}{2} \right] \boldsymbol{\delta}_k^*. \quad (2.58)$$

After performing this mapping, further algebraic simplification can be achieved if necessary.

A special case worthy of note is the matrix $M \in \mathbb{R}^{3 \times 3}$ representing a rotation. In this case the matricial mapping to the quaternion domain is performed by the computation of the axis and the angle of rotation. The axis (d) is invariant to the rotation, so in the matricial form

$$Md = d, \quad (2.59)$$

$$(M - \mathbb{I})d = 0 \quad (2.60)$$

Therefore d is the eigenvector of M associated with the eigenvalue of 1.

The angle of rotation (θ_r) can be computed from the trace (*i.e.* the sum of the diagonal elements) of the rotation matrix as

$$Tr(M) = 1 + 2 \cos(\theta_r) \quad (2.61)$$

$$\theta_r = \arccos\left(\frac{Tr(M) - 1}{2}\right). \quad (2.62)$$

With the axis and angle, the quaternion implementation is given by (2.35).

Example 1 [Mapping to a real matrix product the quaternion equality $\mathbf{p} = \mathbf{R}\mathbf{h}\mathbf{R}^{-1}$, in which \mathbf{R} is given in (2.36) and $\mathbf{h} = h_0 + h_1\mathbf{x} + h_2\mathbf{y} + h_3\mathbf{z}$.]

Applying the Hamilton operators, the mapping gives

$$\begin{aligned} \text{vec}(\mathbf{p}) &= \overset{+}{H}(\mathbf{R}) \overset{-}{H}(\mathbf{R}^*) \text{vec}(\mathbf{h}) = R \text{vec}(\mathbf{h}) \\ &= \begin{pmatrix} R_0 & -R_1 & -R_2 & -R_3 \\ R_1 & R_0 & -R_3 & R_2 \\ R_2 & R_3 & R_0 & -R_1 \\ R_3 & -R_2 & R_1 & R_0 \end{pmatrix} \begin{pmatrix} R_0 & -(-R_1) & -(-R_2) & -(-R_3) \\ (-R_1) & R_0 & (-R_3) & -(-R_2) \\ (-R_2) & -(-R_3) & R_0 & (-R_1) \\ (-R_3) & (-R_2) & -(-R_1) & R_0 \end{pmatrix} \text{vec}(\mathbf{h}) \\ &= \begin{pmatrix} |\mathbf{R}|^2 & & & \\ \hline 0 & R_0^2 + R_1^2 - R_2^2 - R_3^2 & -2(R_0R_3 - R_1R_2) & 2(R_0R_2 - R_3R_1) \\ 0 & 2(R_0R_3 - R_1R_2) & R_0^2 - R_1^2 + R_2^2 - R_3^2 & -2(R_0R_1 - R_2R_3) \\ 0 & -2(R_0R_2 - R_3R_1) & 2(R_0R_1 - R_2R_3) & R_0^2 - R_1^2 - R_2^2 + R_3^2 \end{pmatrix} \text{vec}(\mathbf{h}) \end{aligned}$$

It is noteworthy that the lower matrix 3×3 indicated by the dashed lines is in the format of a

rotation matrix. Its trace, which is given by

$$\begin{aligned}
Tr \left(M^{[3 \times 3]} \right) &= 3R_0^2 - (R_1^2 + R_2^2 + R_3^2) \\
&= 3 \cos^2 \left(\frac{\theta_r}{2} \right) - |\mathbf{d}|^2 \sin^2 \left(\frac{\theta_r}{2} \right) \\
&= 3 \cos^2 \left(\frac{\theta_r}{2} \right) - \sin^2 \left(\frac{\theta_r}{2} \right) \\
&= 2 \left[\underbrace{\cos^2 \left(\frac{\theta_r}{2} \right)}_{\frac{1+\cos(\theta_r)}{2}} \right] + \underbrace{\cos^2 \left(\frac{\theta_r}{2} \right) - \sin^2 \left(\frac{\theta_r}{2} \right)}_{\cos(\theta_r)} \\
&= 1 + 2\cos(\theta_r),
\end{aligned}$$

is equivalent to (2.61), as it was expected because the given quaternion equality is the rotation formula.

The theory discussed in this chapter is sufficient to deal with most of the challenges associated with Hamiltonian algebra. In the following chapter, the electrical circuit theory proposed in this dissertation is presented.

Chapter 3

Voltage and Current: A Geometrical Analysis

In this chapter quaternion voltage and current are presented. Their geometrical loci in a complete period are investigated. Their time derivative and integral are provided. At last, the related geometrical quantities and how they are related to the unbalance are discussed via two examples. This geometrical approach is also shown to be applicable to any periodic and three-phase quantity.

3.1 Balanced Conditions

According to [36,38], three-phase quaternion voltage is denoted by

$$\mathbf{V}(t) = v_a(t)\mathbf{x} + v_b(t)\mathbf{y} + v_c(t)\mathbf{z}, \quad (3.1)$$

in which

$$v_a(t) = \sqrt{2}V_a \cos(wt) \quad (3.2)$$

$$v_b(t) = \sqrt{2}V_b \cos(wt - 120^\circ + \phi_b) \quad (3.3)$$

$$v_c(t) = \sqrt{2}V_c \cos(wt + 120^\circ + \phi_c) \quad (3.4)$$

are instantaneous voltages with reference to a neutral point, V_a , V_b , V_c are the RMS value for phases A , B and C , respectively, w is the electrical frequency in rad/s and ϕ_b and ϕ_c are phase displacements. If voltages are balanced, then $\phi_b = \phi_c = 0$ and $V_a = V_b = V_c$.

Analogously, current is denoted by

$$\mathbf{I}(t) = i_a(t)\mathbf{x} + i_b(t)\mathbf{y} + i_c(t)\mathbf{z}, \quad (3.5)$$

in which $i_a(t)$, $i_b(t)$ and $i_c(t)$ refer to line currents flowing through phases a, b and c, respectively.

If voltage and current measurements are digital, *i.e.* constituted of samples, then the continuous time is substituted by the discrete variable

$$t_{[k]} = kT_S, \quad (3.6)$$

in which T_S is the time sampling interval and k is the sample number. In this condition, voltage for phase “A” is

$$v_{a[k]} = \sqrt{2}V_a \cos(\omega kT_S). \quad (3.7)$$

In fact, any quantity can be rewritten by replacing t with kT_S . In this dissertation, variables continuous form is adopted. However, they can be easily mapped into the digital domain by applying (3.6). So, the entire theory is applicable for sampled values of either voltage or current.

The theory hereby developed applies actually to any periodic three-phase quantity. A particular case that might be of interest is the electromagnetic flux, because it is responsible for the functioning of electrical machines. Usually, the fluxes obtained in induction motors are coplanar and spaced of 120° . If they were to be perpendicular to other, a different electrical machine with the stator windings displayed in three orthogonal planes in the three-dimensional space should be built. This geometrical investigation can provide further insights on whether or not such machine would work and if it could actually be better than the actual ones.

It is worth mentioning that $\mathbf{V}(t)$ and $\mathbf{I}(t)$ are purely vectorial. Thus, it is possible to fully represent them graphically in a three dimensional reference frame. Since these quantities are time varying and periodic, their graphical representation is also time varying and periodic. The set of points resulting from the trajectory described by the end of the quaternion voltage in a complete period is named the quaternion voltage locus (QVL), and it is a closed curve. Similarly, the current trajectory is defined as the quaternion current locus (QCL). Figure 3.1 (in which \mathbf{n} is the quaternion orthogonal to the voltage plane) shows the concept of the quaternion voltage behaviour and its locus.

A time varying visualization of the quaternion voltage is given by Figure 3.2. In the digital version of this dissertation, it is an animated figure that can be visualized using an appropriate PDF reader, *e.g.* Adobe Acrobat Reader. In the printed version, it is constituted of six different frames that gives an overall idea of the dynamics involved.

Following this concept, steady-state¹ three phase voltages (or currents²) can be fully described in terms of the ellipse plane direction, major and minor semi-axis magnitude and the direction of one of those axis (since they are perpendicular to each other). Therefore, it seems that in this alternative representation four quantities are needed to represent the three phase voltages. In the phasorial domain, five real quantities are required: three magnitudes and two angles (since one is the angular reference). Comparing these two representations, a mislead conclusion is that there is a gain in the quaternion approach, in terms of reducing the required quantities needed to represent the system voltages. It is worth mentioning that the ellipse plane and its semi-axes

¹The QVL is a steady-state representation because each voltage period corresponds to a QVL.

²In this and the following two sections, voltages are considered during the development. But the developed theory is also applicable to currents

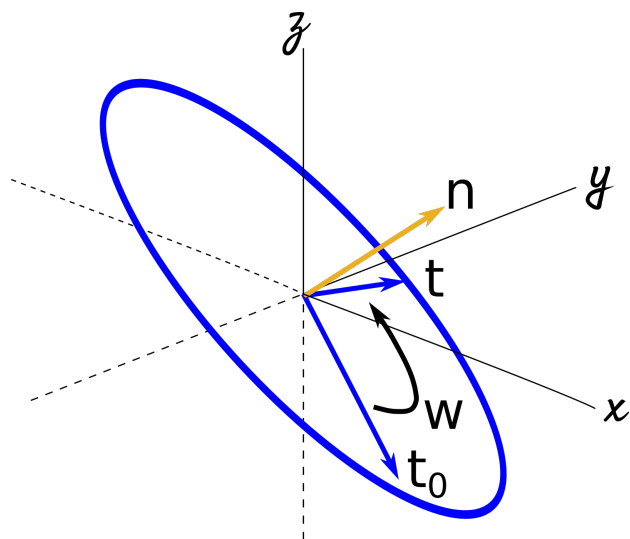


Figure 3.1: General concept of a balanced quaternion voltage and its locus.

Figure 3.2: Animated balanced quaternion voltage and its locus.

directions are given by purely vectorial quaternions, each one with three real elements. Since they have unit norm, each one can be specified by two elements. For instance, if $\mathbf{n} = n_1\mathbf{x} + n_2\mathbf{y} + n_3\mathbf{z}$ and n_1 and n_2 are defined, then n_3 is computed as

$$|\mathbf{n}| = \sqrt{n_1^2 + n_2^2 + n_3^2} = 1 \quad (3.8)$$

$$n_3 = \sqrt{1^2 - n_1^2 - n_2^2}. \quad (3.9)$$

Thus, the total amount of real quantities in the proposed representation is actually six: two for the ellipse plane orientation, two for the magnitude of both semi-axes and two for their direction. Therefore, there is a loss in terms of storage needed to fully portray the system because one more real element is needed in contrast to the five required in the phasorial representation.

Although not being efficient from the perspective of storage, this geometric quaternion-based representation may still be advantageous in some other aspects and, therefore, needs further investigation. One of the motivations was to come up with quantities that may be related to the unbalance in order to quantify it. In this sense, each of the geometric quantities and how they relate to traditional phasor variables will be presented.

Any given plane is determined by i) \mathbf{n} , which has unit norm and is orthogonal to the plane, and ii) c , that is a constant regarding a relation between \mathbf{n} coefficients and where this plane may intersect the three-dimensional axes. Mathematically, its equation is

$$\mathbf{n} \cdot [r\mathbf{x} + s\mathbf{y} + t\mathbf{z}] = c \quad (3.10)$$

in which (r, s, t) represents a point within it. So, computing the QVL plane is achieved by determining both the constant c and the quaternion \mathbf{n} . This can be done solving

$$Re(\mathbf{n}\mathbf{V}(t)) = \mathbf{n} \cdot \mathbf{V}(t) = c. \quad (3.11)$$

It is possible to prove that c is always zeros if there is not a DC value in any of the considered phases. Since we are not interested in the DC offset phenomenon, this proof will not be given for the sake of simplicity. However, it is relatively simple to prove that c is zero for balanced and unbalanced conditions.

As previously mentioned, voltages are sinusoidal, which is a bi-dimensional group of functions. This means that any sinusoidal function can be written in terms of two other functions, usually the cosine and the sine. In this sense, $v_c(t)$ is always a linear combination of $v_a(t)$ and $v_b(t)$, and vice versa. Mathematically,

$$v_c(t) = c_a v_a(t) + c_b v_b(t) \quad (3.12)$$

in which c_a and c_b are constants. Substituting

$$c_a = -\frac{n_1}{n_3} \quad (3.13)$$

$$c_b = -\frac{n_2}{n_3} \quad (3.14)$$

yields

$$n_1v_a(t) + n_2v_b(t) + n_3v_c(t) = \mathbf{n} \cdot \mathbf{V}(t) = 0 \quad (3.15)$$

that is exactly (3.11) with $c = 0$. Therefore, only \mathbf{n} need to be computed.

Although (3.15) has three unknown variables (n_1 , n_2 and n_3) and it is a single equation, it has a unique solution. From (3.15) it is possible to come up with several other equations because the equality is held for any time instant. In this case, this linear system can be composed of an unlimited number of equations and with only three variables. Thus, it is possible to solve it. In order to employ the minimum equations required, three voltage samples are considered, resulting in the homogeneous system

$$V_{abc}(t_{1,2,3}) \begin{bmatrix} n_1 \\ n_2 \\ n_3 \end{bmatrix} = \begin{bmatrix} v_a(t_1) & v_b(t_1) & v_c(t_1) \\ v_a(t_2) & v_b(t_2) & v_c(t_2) \\ v_a(t_3) & v_b(t_3) & v_c(t_3) \end{bmatrix} \begin{bmatrix} n_1 \\ n_2 \\ n_3 \end{bmatrix} = \begin{bmatrix} 0 \\ 0 \\ 0 \end{bmatrix}. \quad (3.16)$$

Since v_c is always a linear combination of v_a and v_b , one of the equations given in (3.16) can be eliminated. This means that this problem has infinite solutions, which are formed by the basis of $V_{abc}(t_{1,2,3})$. Hence, only two samples are required to solve it by determining the null space of $V_{abc}(t_{1,2})$

$$\mathbf{n} = \text{null}(V_{abc}(t_{1,2})). \quad (3.17)$$

Despite being algebraically feasible, this computation is not performed in the quaternion domain.

In this sense, a method for determining the QVL plane based on also two voltage samples and on the quaternion domain is proposed. Since the plane intersects the origin, the whole quaternion is within it. Considering that the cross product always outputs a third vector (in this case, a purely vectorial quaternion) orthogonal to the previous ones, then the vectorial part of the product between voltage at two different time instants yields a quaternion proportional to \mathbf{n} .

$$\overrightarrow{\mathbf{V}(t_1)\mathbf{V}(t_2)} = \mathbf{V}(t_1) \times \mathbf{V}(t_2) \propto \mathbf{n} \quad (3.18)$$

So, \mathbf{n} can be obtained with only two voltage samples by normalizing the product in order for it to has a unitary norm. It is noteworthy that $\mathbf{n}w$ is the angular momentum of the quaternion voltage. In this sense, computation of \mathbf{n} via the cross product method requires two samples with an angular shift lower than 180° . Otherwise it will have an opposite direction of the actual angular momentum. In other words, $wt_2 \leq wt_1 + 180^\circ$. So a general expression is

$$\mathbf{n} = \frac{\mathbf{V}(t_1) \times \mathbf{V}(t_2)}{|\mathbf{V}(t_1)||\mathbf{V}(t_2)|}. \quad (3.19)$$

For balanced voltages, $V_a = V_b = V_c = V$ and $\phi_b = \phi_c = 0$. If $wt_1 = 0$ and $wt_2 = \frac{\pi}{2}$, then

$$\mathbf{V}(t_1) = \sqrt{2}V \left[\mathbf{x} - \frac{1}{2}\mathbf{y} - \frac{1}{2}\mathbf{z} \right] \quad (3.20)$$

$$\mathbf{V}(t_2) = \sqrt{2}V \left[0 + \frac{\sqrt{3}}{2}\mathbf{y} - \frac{\sqrt{3}}{2}\mathbf{z} \right]. \quad (3.21)$$

Therefore, the orthogonal quaternion \mathbf{n} for the balanced case is proportional to

$$\mathbf{n}_{\text{bal}} \propto \mathbf{V}(t_1) \times \mathbf{V}(t_2) \quad (3.22)$$

$$\propto 2V^2 \left[\left(\frac{\sqrt{3}}{4} + \frac{\sqrt{3}}{4} \right) \mathbf{x} + \left(\frac{\sqrt{3}}{2} - 0 \right) \mathbf{y} + \left(0 + \frac{\sqrt{3}}{2} \right) \mathbf{z} \right] \quad (3.23)$$

$$\propto 2V^2 \left[\frac{\sqrt{3}}{2} \mathbf{x} + \frac{\sqrt{3}}{2} \mathbf{y} + \frac{\sqrt{3}}{2} \mathbf{z} \right]. \quad (3.24)$$

Because \mathbf{n} is unitary,

$$\mathbf{n}_{\text{bal}} = \frac{\mathbf{x} + \mathbf{y} + \mathbf{z}}{\sqrt{3}}. \quad (3.25)$$

Therefore, the QVL plane for a balanced condition is determined. This result means the QVL is equally distributed along each axis. This was expected, since each voltage is represented by an axis and they are balanced.

Both methods for determining \mathbf{n} were implemented on *Matlab* [54] and compared using the code attached in Appendix I. The demanded computational time for each method can be determined statistically. As it depends on the computer memory status and the numerical values used, it can be considered a random variable. So, a Monte Carlo simulation constituted with a thousand loops for 4096 unbalanced conditions was performed. For this purpose, a computer with a student license of *Matlab* [54] was employed. The magnitude of negative and zero sequences were uniformly varied between 0 and 0,5 pu, and the positive was varied from 0,5 to 1,5 pu. Angles between 0 and 360° were considered.

Results are presented in Table 3.1.

Table 3.1: Comparison of the computation time needed for the null space and the cross product methods for determining the QVL plane, *i.e.* \mathbf{n} .

Time	Null Space	Cross Product
Avarage (μs)	41,49	6,61
Variance (ns)	3,51	0,33

In order to verify if the amount of data is sufficient, the average demanded computational time is plotted for each iteration and shown on Figure 3.3. As it approaches smoothly the final value obtained, adding new samples would not change significantly the results obtained. Therefore, it is correctly to state that the cross product method was approximately 6 times faster than the the null space. So, the former method is better than the latter, since it is faster and needs the same amount of inputs.

In order to determine the QVL geometrical shape, its norm will be investigated. Applying (2.18) in (3.1) and considering a balanced condition,

$$|\mathbf{V}|_{\text{bal}}(t) = \sqrt{2V^2 \cos^2(\omega t) + 2V^2 \cos^2(\omega t - 120^\circ) + 2V^2 \cos^2(\omega t + 120^\circ)} \quad (3.26)$$

$$|\mathbf{V}|_{\text{bal}}(t) = \sqrt{2V^2 [\cos^2(\omega t) + \cos^2(\omega t - 120^\circ) + \cos^2(\omega t + 120^\circ)]} \quad (3.27)$$

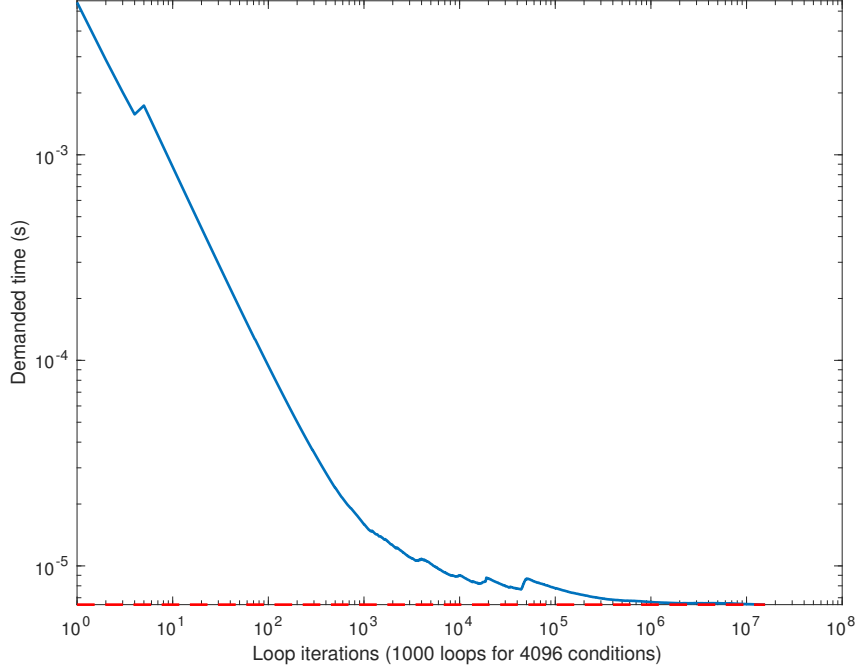


Figure 3.3: Cumulative average for the demanded computational time of the QVL plane via the cross product method.

Applying the trigonometric property

$$\cos^2(x) = \frac{1 + \cos(2x)}{2} \quad (3.28)$$

to the former equation yields

$$|\mathbf{V}|_{\text{bal}}(t) = \sqrt{2V^2 \left[\frac{3}{2} + \cos(2wt) + \cos(2wt - 240^\circ) + \cos(2wt + 240^\circ) \right]}. \quad (3.29)$$

Because $\cos(-240^\circ) = \cos(120^\circ)$, then

$$|\mathbf{V}|_{\text{bal}}(t) = \sqrt{2V^2 \left[\frac{3}{2} + \cos(2wt) + \cos(2wt + 120^\circ) + \cos(2wt - 120^\circ) \right]}. \quad (3.30)$$

and since the sum of varying over time cosines with equally spaced angular shifts is always zero, then

$$|\mathbf{V}|_{\text{bal}}(t) = \sqrt{3}V. \quad (3.31)$$

It is noteworthy that quaternion voltage norm is constant over time and is equal to the line voltage (phase-to-phase) magnitude. This means that the minimum and maximum values of the norm are the same. So, the QVL shape is a circle or equivalently an ellipse with null eccentricity (e) defined as

$$e = \sqrt{1 - \frac{b^2}{a^2}}, \quad (3.32)$$

in which a and b are the major and minor semi-axes magnitudes, respectively. In this case, there is no meaning in determining the semi-axes directions. So, the QVL for balanced conditions has been fully described.

As a result of the QVL being a circle, quaternion voltage (\mathbf{V}_{bal}) can be written in terms of quaternion rotations, accordingly to (2.35). Moreover, since rotation is executed around a perpendicular axis, it can be reduced to the format of (2.37). Therefore, this dissertation proposes

$$\mathbf{V}_{bal}(t) = \sqrt{3}V e^{\mathbf{n}wt} \mathbf{q}_p \quad (3.33)$$

in which \mathbf{q}_p is the direction of $\mathbf{V}_{bal}(t=0)$ and is computed as

$$\mathbf{q}_p \propto V \left(\mathbf{x} - \frac{1}{2}\mathbf{y} - \frac{1}{2}\mathbf{z} \right) \quad (3.34)$$

$$\mathbf{q}_p = \frac{2\mathbf{x} - \mathbf{y} - \mathbf{z}}{\sqrt{6}}. \quad (3.35)$$

All QVL parameters have been computed for balanced conditions. The locus has been proved to be a circle inside the \mathbf{n}_{bal} plane, and it represents the voltage behaviour for a cycle. Thus, the circle equation in a three dimensional frame is given by

$$\left(\frac{2x - y - z}{\sqrt{6}} \right)^2 + \left(\frac{y - z}{\sqrt{2}} \right)^2 = (\sqrt{3}V)^2 \forall (x, y, z) \in \mathbb{R}^3, s.t. \ x + y + z = 0, \quad (3.36)$$

and it conveys all of the steady-state information about the system voltage magnitudes and angles.

As a remark from (3.33), it is possible to come up with an evolution equation for a voltage state-space model. Rewriting (3.33) in the discrete form

$$\mathbf{V}[k] = \sqrt{3}V e^{\mathbf{n}wkT_s} \mathbf{q}_p, \quad (3.37)$$

then voltage at instant $k+1$ is equal to

$$\mathbf{V}[k+1] = \sqrt{3}V e^{\mathbf{n}w(k+1)T_s} \mathbf{q}_p \quad (3.38)$$

$$\mathbf{V}[k+1] = \sqrt{3}V e^{\mathbf{n}wT_s} e^{\mathbf{n}wkT_s} \mathbf{q}_p \quad (3.39)$$

$$(3.40)$$

and finally,

$$\mathbf{V}[k+1] = e^{\mathbf{n}wT_s} \mathbf{V}[k]. \quad (3.41)$$

It is worth mentioning that $\mathbf{V}[k+1]$ is linear in relation to $\mathbf{V}[k]$. Hence the state transition matrix is in this case would be equal to $e^{\mathbf{n}wT_s}$ and the model is said to be linear. This highlights the feasibility of using quaternions as voltage or current estimators. Nevertheless, this is not further investigated because it is beyond the scope of this dissertation.

Another outcome from (3.33) is that the voltage time derivative is given by

$$\frac{d\mathbf{V}_{bal}(t)}{dt} = \mathbf{n}w\mathbf{V}_{bal}(t). \quad (3.42)$$

Similarly to phasors, quaternion representation also maps derivatives into products. Moreover, (3.42) contains time derivative for all phases. This outputs was expected, since the derivative of a circular quaternion is equivalent to left multiplying it by its angular momentum, as previously discussed in (2.46).

Likewise, quaternion voltage integral with respect to the time is also mapped into a product

$$\int \mathbf{V}_{\text{bal}}(t)dt = -\frac{\mathbf{n}}{w}\mathbf{V}_{\text{bal}}(t). \quad (3.43)$$

As aforementioned, the theory hereby developed applies to any periodic three-phase quantity. A particular case that must be considered is the electromagnetic flux. Consider an electrical machine with stator windings perpendicular to each other in the three-dimensional space, instead of coplanar and spaced of 120° . In this condition, the resultant flux rotates with the electrical frequency. Moreover, it has a higher magnitude due to the orthogonality. If the windings are coplanar, some components cancel out, reducing its total value. Nonetheless, other aspects of such machine are still to be discussed, for example the construction aspects, the armature reaction and the impacts of voltage unbalance in its performance.

The methodology developed to determine the geometrical parameters of the QVL can also be applied to the analysis of the flux inside usual electrical machines with coplanar windings. A systematic investigation of such phenomenon might give physical interpretations to the effects of voltage unbalance on these equipments. As a consequence, another unbalance factor might be developed. This is suggested for future research.

3.2 Unbalanced Conditions

In this section, quaternion voltage and current are investigated under unbalanced situations. The previous development will be extended for the general case, in which magnitudes are not necessarily equal to each other, neither angles are equally shifted of 120° . Figure 3.4 shows a QVL for balanced, amplitude unbalanced and phase unbalanced conditions. It is worth mentioning that there is a change in the plane direction as well as in its eccentricity. The balanced circle becomes an ellipse.

In order to ratify those visual conclusions drawn from Figure 3.4, QVL parameters will be analytically computed. Firstly, \mathbf{n} will be computed, followed by the major and minor semi-axes magnitudes. Lastly, the direction of the semi-axes will be determined. The ellipse equation for the QVL will also be presented.

Quaternion \mathbf{n} can be computed following the cross product approach presented in (3.19).

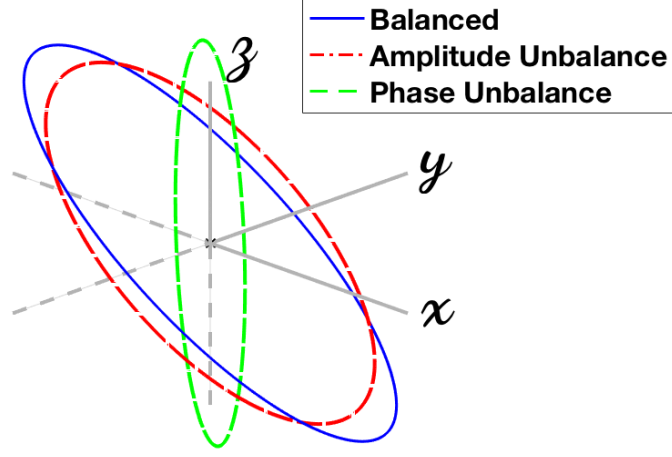


Figure 3.4: QVL for balanced, amplitude unbalanced and phase unbalanced conditions

Considering $t_1 = t$ and $t_2 = t + \Delta t$, then

$$\mathbf{n} \propto \mathbf{V}(t) \times \mathbf{V}(t + \Delta t) \quad (3.44)$$

$$\begin{aligned} \mathbf{n} \propto & [v_b(t)v_c(t + \Delta t) - v_c(t)v_b(t + \Delta t)] \mathbf{x} \\ & + [v_c(t)v_a(t + \Delta t) - v_a(t)v_c(t + \Delta t)] \mathbf{y} \\ & + [v_a(t)v_b(t + \Delta t) - v_b(t)v_a(t + \Delta t)] \mathbf{z}. \end{aligned} \quad (3.45)$$

Denoting the \mathbf{x} term as q_x for the ease of notation,

$$q_x = v_b(t)v_c(t + \Delta t) - v_c(t)v_b(t + \Delta t) \quad (3.46)$$

and expanding its terms, it is rewritten as

$$\begin{aligned} q_x = & 2V_bV_c [\cos(wt - 120^\circ + \phi_b) \cos(w(t + \Delta t) + 120^\circ + \phi_c) \\ & - \cos(wt + 120^\circ + \phi_c) \cos(w(t + \Delta t) - 120^\circ + \phi_b)]. \end{aligned} \quad (3.47)$$

Applying the property

$$\cos(a + b) = \cos(a) \cos(b) - \sin(a) \sin(b) \quad (3.48)$$

with $a = wt + 120^\circ + \phi_c$ and $b = w\Delta t$, then q_x becomes

$$\begin{aligned} q_x = & 2V_bV_c \\ & \{ \cos(wt - 120^\circ + \phi_b) [\cos(wt + 120^\circ + \phi_c) \cos(w\Delta t) - \sin(wt + 120^\circ + \phi_c) \sin(w\Delta t)] \\ & - \cos(wt + 120^\circ + \phi_c) \cos(w(t + \Delta t) - 120^\circ + \phi_b) \}. \end{aligned} \quad (3.49)$$

Applying once more the property (3.48) with $a = wt - 120^\circ + \phi_b$ and $b = w\Delta t$,

$$\begin{aligned} q_x = & 2V_bV_c \\ & \{ \cos(wt - 120^\circ + \phi_b) [\cos(wt + 120^\circ + \phi_c) \cos(w\Delta t) - \sin(wt + 120^\circ + \phi_c) \sin(w\Delta t)] \\ & - \cos(wt + 120^\circ + \phi_c) [\cos(wt - 120^\circ + \phi_b) \cos(w\Delta t) - \sin(wt - 120^\circ + \phi_b) \sin(w\Delta t)] \}. \end{aligned} \quad (3.50)$$

Notice that the terms $\cos(wt + 120^\circ + \phi_c) \cos(wt - 120^\circ + \phi_b) \cos(w\Delta t)$ cancel out. So, the expression is reduced to

$$q_x = 2V_b V_c \sin(w\Delta t) \{ \cos(wt + 120^\circ + \phi_c) \sin(wt - 120^\circ + \phi_b) - \cos(wt - 120^\circ + \phi_b) \sin(wt + 120^\circ + \phi_c) \}. \quad (3.51)$$

Applying the trigonometric property

$$\sin(a + b) = \sin(a) \cos(b) + \sin(b) \cos(a) \quad (3.52)$$

with $a = wt - 120^\circ + \phi_b$ and $b = -(wt + 120^\circ + \phi_c)$, yields

$$q_x = 2V_b V_c \sin(w\Delta t) \sin(wt - 120^\circ + \phi_b - wt - 120^\circ - \phi_c). \quad (3.53)$$

Since $\sin(-240^\circ) = \sin(120^\circ)$, then

$$q_x = 2V_b V_c \sin(w\Delta t) \sin(120^\circ + \phi_b - \phi_c) \quad (3.54)$$

The \mathbf{y} and \mathbf{z} terms are computed analogously. Hence, \mathbf{n} is proportional to

$$\begin{aligned} \mathbf{n} \propto 2 \sin(w\Delta t) [& V_b V_c \sin(120^\circ + \phi_b - \phi_c) \mathbf{x} \\ & + V_c V_a \sin(120^\circ + \phi_c) \mathbf{y} \\ & + V_a V_b \sin(120^\circ - \phi_b) \mathbf{z}] \end{aligned} \quad (3.55)$$

It is worth mentioning that an even more compact expression can be achieved by noticing that angular shifts between phases are equal to

$$\theta_{ab} = 120^\circ - \phi_b \quad (3.56)$$

$$\theta_{bc} = 120^\circ + \phi_b - \phi_c \quad (3.57)$$

$$\theta_{ca} = 120^\circ + \phi_c, \quad (3.58)$$

in which θ_{xy} refers to the angular displacement from y to x . Substituting these expressions into (3.55) and normalizing the right hand side,

$$\mathbf{n} = \frac{1}{|\mathbf{n}_0|} [V_b V_c \sin(\theta_{bc}) \mathbf{x} + V_c V_a \sin(\theta_{ca}) \mathbf{y} + V_a V_b \sin(\theta_{ab}) \mathbf{z}] \quad (3.59)$$

in which \mathbf{n}_0 is a normalization parameter given by

$$|\mathbf{n}_0| = \sqrt{V_a^2 V_b^2 \sin^2(\theta_{ab}) + V_b^2 V_c^2 \sin^2(\theta_{bc}) + V_a^2 V_c^2 \sin^2(\theta_{ca})}. \quad (3.60)$$

So, the QVL plane for any unbalanced condition has been obtained. As a way of testing (3.59), it can be applied to the balanced case and compared to the results of the previous section. It should exactly match (3.25). So, substituting $V_a = V_b = V_c = V$ and $\theta_{ab} = \theta_{bc} = \theta_{ca} = 120^\circ$ in (3.60),

$$|\mathbf{n}_0|_{\text{bal}} = V^2 \sin(120^\circ) \sqrt{3} \quad (3.61)$$

and applying this last equation in (3.59), the plane direction is found to be

$$\begin{aligned}\mathbf{n}_{bal} &= \frac{V^2 \sin(120^\circ) (\mathbf{x} + \mathbf{y} + \mathbf{z})}{V^2 \sin(120^\circ) \sqrt{3}} \\ &= \frac{\mathbf{x} + \mathbf{y} + \mathbf{z}}{\sqrt{3}}.\end{aligned}\quad (3.62)$$

As expected, results for \mathbf{n}_{bal} computed in section 3.1 and computed via the general equation in this section are exactly the same. Therefore, \mathbf{n}_{bal} is a particular case of (3.59).

It is worth mentioning that \mathbf{n} may be thought of as a indicator of the less “dominant” phase voltage. In other words, if phase “C” is equal to zero, then \mathbf{n} will have the direction of the axis associated with phase “C”, *i.e.* $\mathbf{n} = \mathbf{z}$. The “predominant” voltages, on the other hand, are those closer to the plane or equivalently those with lower \mathbf{n} coefficients. This assertive still needs further investigation because both magnitudes and angles affects this quaternion. In section 4.1, this will be discussed under the point of view of Fortecue’s theory.

Heretofore, the QVL plane has been determined. The semi-axes magnitudes and directions, nonetheless, still remains unknown. These parameters will now be determined. For this purpose, a generic ellipse equation is discussed. Then, the quaternion norm is computed in order to determine its maximum and minimum values, which are the semi-axes magnitudes. Their directions are computed by determining the moment they occur and substituting it in the voltage expression (3.1).

Since the quaternion voltage describes an ellipse, it can be written in terms of the following parametric ellipse equation

$$\mathbf{V} = V_\alpha \cos(wt) [\cos(\phi_d) \mathbf{q}_1 + \sin(\phi_d) \mathbf{q}_2] + V_\beta \sin(wt) [-\sin(\phi_d) \mathbf{q}_1 + \cos(\phi_d) \mathbf{q}_2], \quad (3.63)$$

in which its plane is $\mathbf{q}_1 \mathbf{q}_2$ and the major semi-axis is displaced of \mathbf{q}_1 by ϕ_d as shown in Figure 3.5. In the above equation, the quaternion voltage maximum absolute value (equivalently, its norm) is considered to happen in $t = 0$. However, this is a restriction that may not be satisfied. In the most general case, maximum occurs in t_{\max} , which may be rewritten as

$$t_{\max} = \frac{\phi_t}{w}. \quad (3.64)$$

Therefore, voltage ellipse is given by

$$\mathbf{V} = V_\alpha \cos(wt - \phi_t) [\cos(\phi_d) \mathbf{q}_1 + \sin(\phi_d) \mathbf{q}_2] + V_\beta \sin(wt - \phi_t) [-\sin(\phi_d) \mathbf{q}_1 + \cos(\phi_d) \mathbf{q}_2]. \quad (3.65)$$

The semi-axes directions are given by

$$\boldsymbol{\alpha} = \cos(\phi_d) \mathbf{q}_1 + \sin(\phi_d) \mathbf{q}_2 \quad (3.66)$$

$$\boldsymbol{\beta} = -\sin(\phi_d) \mathbf{q}_1 + \cos(\phi_d) \mathbf{q}_2. \quad (3.67)$$

As discussed previously, the ellipse plane has been provided. The semi-axes magnitudes and directions are yet to be determined. Namely, \mathbf{q}_1 , \mathbf{q}_2 , ϕ_t , ϕ_d , V_α and V_β are computed next.

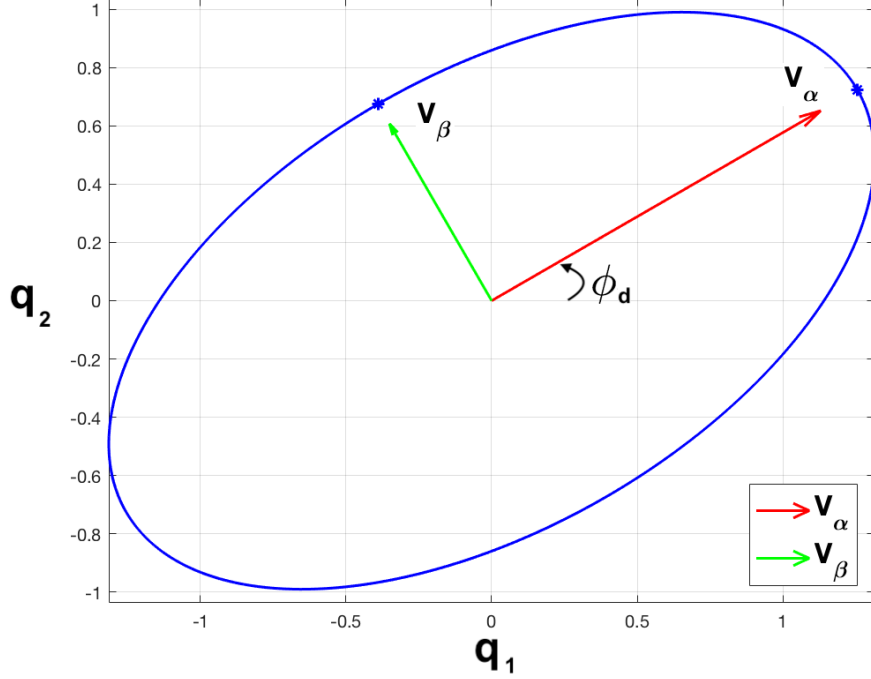


Figure 3.5: Arbitrary ellipse in the plane $\mathbf{q}_1\mathbf{q}_2$ with major and minor semi-axes denoted by V_α and v_β , respectively

Notice, that the only restrictions for \mathbf{q}_1 and \mathbf{q}_2 is that they are contained in the QVL plane and that they are perpendicular to each other. In this sense, they may be arbitrarily chosen. If \mathbf{q}_1 is chosen to be the quaternion voltage direction when its maximum occurs, then ϕ_d will be zero and $\boldsymbol{\alpha} = \mathbf{q}_1$ and $\boldsymbol{\beta} = \mathbf{q}_2$.

In order to determine $\boldsymbol{\beta}$, consider that \mathbf{n} is pointing out from the Figure 3.5 and that $\boldsymbol{\beta}$ is counter-clockwise ahead of $\boldsymbol{\alpha}$. Using the properties i) the cross products always yields an orthogonal quaternion, and ii) the quaternion product is equal to the cross product if quaternions are purely vectorial and orthogonal to each other, then $\boldsymbol{\beta}$ can be determined as $\boldsymbol{\beta} = \mathbf{n}\boldsymbol{\alpha}$. So, $\boldsymbol{\alpha}$ needs to be determined. For this purpose, maximum and minimum voltage norm will be computed, followed by the computation of the time instant they occur.

The norm can be related to the voltage magnitudes of each phase. As a matter of fact, the norm increases accordingly to the voltage levels. For an unbalanced condition, it is given by

$$|\mathbf{V}|^2(t) = v_a^2(t) + v_b^2(t) + v_c^2(t) \quad (3.68)$$

$$= 2V_a^2 \cos^2(wt) + 2V_b^2 \cos^2(wt - 120^\circ + \phi_b) + 2V_c^2 \cos^2(wt + 120^\circ + \phi_c). \quad (3.69)$$

Applying (3.28), the previous equation turns into

$$|\mathbf{V}|^2(t) = 2V_a^2 \left[\frac{1 + \cos(2wt)}{2} \right] + 2V_b^2 \left[\frac{1 + \cos(2wt - 2\theta_{ab})}{2} \right] + 2V_c^2 \left[\frac{1 + \cos(2wt + 2\theta_{ca})}{2} \right] \quad (3.70)$$

$$= V_a^2 + V_b^2 + V_c^2 + V_a^2 \cos(2wt) + V_b^2 \cos(2wt - 2\theta_{ab}) + V_c^2 \cos(2wt + 2\theta_{ca}), \quad (3.71)$$

and it can be rewritten in terms of its RMS value and an oscillating component. Voltage norm RMS value is given by

$$|\mathbf{V}|_{RMS} = \sqrt{\frac{1}{T} \int_0^T |\mathbf{V}|^2(t) dt} \quad (3.72)$$

$$= \sqrt{V_a^2 + V_b^2 + V_c^2}. \quad (3.73)$$

Therefore, voltage norm can be rewritten as

$$|\mathbf{V}|^2(t) = |\mathbf{V}|_{RMS}^2 + |\mathbf{V}|_{osc}^2 \cos(2\omega t + \phi_{osc}) \quad (3.74)$$

in which the $|\mathbf{V}|_{osc}$ represents an oscillating component of the norm and can be computed by the trigonometric sum

$$|\mathbf{V}|_{osc}^2 \cos(2\omega t + \phi_{osc}) = V_a^2 \cos(2\omega t) + V_b^2 \cos(2\omega t - 2\theta_{ab}) + V_c^2 \cos(2\omega t + 2\theta_{ca}). \quad (3.75)$$

Making use of phasors to represent this sum,

$$|\mathbf{V}|_{osc}^2 \cos(2\omega t + \phi_{osc}) = \text{Re}(|\mathbf{V}|_{osc}^2 \angle \phi_{osc}) \quad (3.76)$$

$$= \text{Re}(V_a^2 \angle 0^\circ + V_b^2 \angle -2\theta_{ab} + V_c^2 \angle 2\theta_{ca}). \quad (3.77)$$

In this sense, the following phasorial equality must be solved

$$|\mathbf{V}|_{osc}^2 \angle \phi_{osc} = V_a^2 \angle 0^\circ + V_b^2 \angle -2\theta_{ab} + V_c^2 \angle 2\theta_{ca}. \quad (3.78)$$

From (3.78), $|\mathbf{V}|_{osc}^2$ and ϕ_{osc} can be computed as the absolute and angle values, respectively. It is noteworthy that this equality can be illustrated geometrically, as in Figure 3.6. Applying the Pythagorean theorem, $|\mathbf{V}|_{osc}^2$ is

$$|\mathbf{V}|_{osc}^2 = \sqrt{[V_a^2 + V_b^2 \cos(2\theta_{ab}) + V_c^2 \cos(2\theta_{ca})]^2 + [V_b^2 \sin(2\theta_{ab}) - V_c^2 \sin(2\theta_{ca})]^2} \quad (3.79)$$

Likewise, ϕ_{osc} can be computed as the arc tangent of the vertical cathetus over the horizontal one, *i.e.*

$$\phi_{osc} = \arctan\left(\frac{V_c^2 \sin(2\theta_{ca}) - V_b^2 \sin(2\theta_{ab})}{V_a^2 + V_b^2 \cos(2\theta_{ab}) + V_c^2 \cos(2\theta_{ca})}\right). \quad (3.80)$$

It is worth mentioning that since $\arctan(\cdot)$ is limited in $[-\frac{\pi}{2}; \frac{\pi}{2}]$, then the signs of both cathetus from Figure 3.6 must be considered in order to compute the correct value of ϕ_{osc} . For instance, if $\phi_{osc} = 180^\circ$, the vertical cathetus magnitude will be nil. In this condition, if the cathetus sign are not considered, then the right hand side of (3.80) will be equal to zero. This can be solved in *Matlab* [54] by using the *atan2* function.

So, major and minor semi-axis magnitudes, *i.e.* maximum and minimum values of voltage norm, have been computed and are given by

$$V_\alpha = \sqrt{|\mathbf{V}|_{RMS}^2 + |\mathbf{V}|_{osc}^2} \quad (3.81)$$

$$V_\beta = \sqrt{|\mathbf{V}|_{RMS}^2 - |\mathbf{V}|_{osc}^2}. \quad (3.82)$$

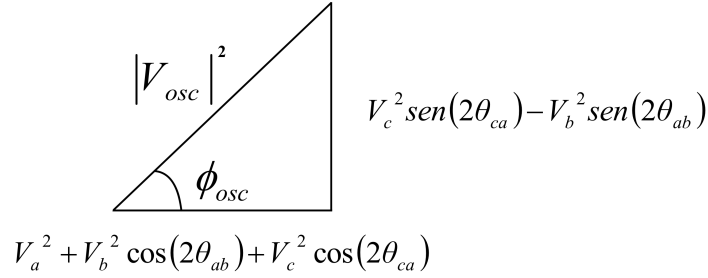


Figure 3.6: Geometric representation for the oscillatory voltage norm component in terms of its magnitude and angle.

It is noteworthy that in balanced cases $|\mathbf{V}|_{osc} = 0$. Thus, QVL is a circle with the voltage norm RMS value as its radius, in accordance with the theory developed in the previous section.

Up to now, QVL plane and semi-axes magnitudes have been determined. So, remains to be computed its semi-axes directions, which are related to the angular displacement between phase quantities. In order to do this, the time instant in which occurs the maximum voltage norm will be computed. The major semi-axis direction ($\boldsymbol{\alpha}$) is obtained by evaluating quaternion voltage given by (3.1) and then normalizing it. The minor semi-axis ($\boldsymbol{\beta}$), as previously mentioned, is obtained by the product

$$\boldsymbol{\beta} = \mathbf{n}\boldsymbol{\alpha}. \quad (3.83)$$

The time instant in which occurs the maximum norm is the value that makes the argument of the oscillating component in (3.74) equal to zero, *i.e.*

$$t_{max} = -\frac{\phi_{osc}}{2w}. \quad (3.84)$$

Substituting (3.80) in the previous equation and considering that the arctan is a pair function (*i.e.* $arctan(-x) = -arctan(x)$), then

$$t_{max} = \frac{1}{2w} arctan \left(\frac{V_b^2 \sin(2\theta_{ab}) - V_c^2 \sin(2\theta_{ca})}{V_a^2 + V_b^2 \cos(2\theta_{ab}) + V_c^2 \cos(2\theta_{ca})} \right). \quad (3.85)$$

With these equations, it is possible to determine QVL parameters for both balanced and unbalanced conditions. Its ellipse equation is given by

$$\frac{\alpha^2}{V_\alpha^2} + \frac{\beta^2}{V_\beta^2} = 1, \forall (x, y, z) \in \mathbb{R}^3, \perp n = 0 \quad (3.86)$$

in which n , α and β (not in bold letters) represents the $(x, y, z) \in \mathbb{R}^3$ of the line orthogonal to the QVL plane and the major and minor semi-axes, respectively.

Two examples are strategically defined in order to provide simple mathematical computations and also to provide insights on different unbalance conditions. They are presented hereupon.

Example 2 [*Amplitude Unbalance*]

In this example the effects of an amplitude unbalance on the QVL will be discussed. Considering

$V_a = 1$ pu and $V_b = V_c = 0,5$ pu and phases equally displaced (i.e. $\theta_{ab} = \theta_{bc} = \theta_{ca} = 120^\circ$), then the QVL plane (\mathbf{n}), computed accordingly to (3.59), is

$$\mathbf{n} = \frac{1}{\mathbf{n}_0} \left[\frac{1}{2} \cdot \frac{1}{2} \sin(120^\circ) \mathbf{x} + \frac{1}{2} \cdot 1 \sin(120^\circ) \mathbf{y} + 1 \cdot \frac{1}{2} \sin(120^\circ) \mathbf{z} \right] \quad (3.87)$$

$$= \frac{1}{\mathbf{n}_0} \left[\frac{\sqrt{3}}{8} \mathbf{x} + \frac{\sqrt{3}}{4} \mathbf{y} + \frac{\sqrt{3}}{4} \mathbf{z} \right] \quad (3.88)$$

$$= \frac{1}{\mathbf{n}_0} \cdot \frac{\sqrt{3}}{8} [\mathbf{x} + 2\mathbf{y} + 2\mathbf{z}] \quad (3.89)$$

The normalization parameter \mathbf{n}_0 , that is given by (3.60), is equal to

$$\mathbf{n}_0 = \sqrt{1^2 \left(\frac{1}{2}\right)^2 \sin^2(120^\circ) + \left(\frac{1}{2}\right)^2 \left(\frac{1}{2}\right)^2 \sin^2(120^\circ) + 1^2 \left(\frac{1}{2}\right)^2 \sin^2(120^\circ)} \quad (3.90)$$

$$= \frac{1}{2} \sin(120^\circ) \sqrt{1 + \frac{1}{4} + 1} \quad (3.91)$$

$$= \frac{1}{2} \sin(120^\circ) \sqrt{\frac{9}{4}} \quad (3.92)$$

$$= \frac{1}{2} \cdot \frac{\sqrt{3}}{2} \cdot \frac{3}{2} = 3 \frac{\sqrt{3}}{8}. \quad (3.93)$$

So,

$$\mathbf{n} = \frac{\mathbf{x} + 2\mathbf{y} + 2\mathbf{z}}{3}. \quad (3.94)$$

The quaternion \mathbf{n} is closer to those axes associated with lower magnitudes phases (V_b and V_c) because its \mathbf{y} and \mathbf{z} components are higher. Considering that \mathbf{n} is orthogonal to the QVL, it is correct to state that the plane is closer to \mathbf{x} , as shown in Figure 3.7. This was expected, since phase ‘‘A’’ voltage magnitude is higher. Thus it should influence the QVL plane the most.

The voltage norm RMS value, accordingly to (3.73), is

$$|\mathbf{V}|_{RMS} = 1^2 + \left(\frac{1}{2}\right)^2 + \left(\frac{1}{2}\right)^2 \quad (3.95)$$

$$= \sqrt{\frac{3}{2}}. \quad (3.96)$$

The oscillating component magnitude, given by (3.79), is

$$|\mathbf{V}|_{osc} = \sqrt{\sqrt{\left[1 + \left(\frac{1}{2}\right)^2 \cos(240^\circ) + \left(\frac{1}{2}\right)^2 \cos(240^\circ)\right]^2 + \left[\left(\frac{1}{2}\right)^2 \sin(240^\circ) - \left(\frac{1}{2}\right)^2 \sin(240^\circ)\right]^2}} \quad (3.97)$$

$$= \sqrt{\sqrt{\left[1 + \frac{1}{4} \left(\frac{-1}{2}\right) + \frac{1}{4} \left(\frac{-1}{2}\right)\right]^2 + 0^2}} \quad (3.98)$$

$$= \sqrt{1 - \frac{2}{8}} \quad (3.99)$$

$$= \frac{\sqrt{3}}{2} \quad (3.100)$$

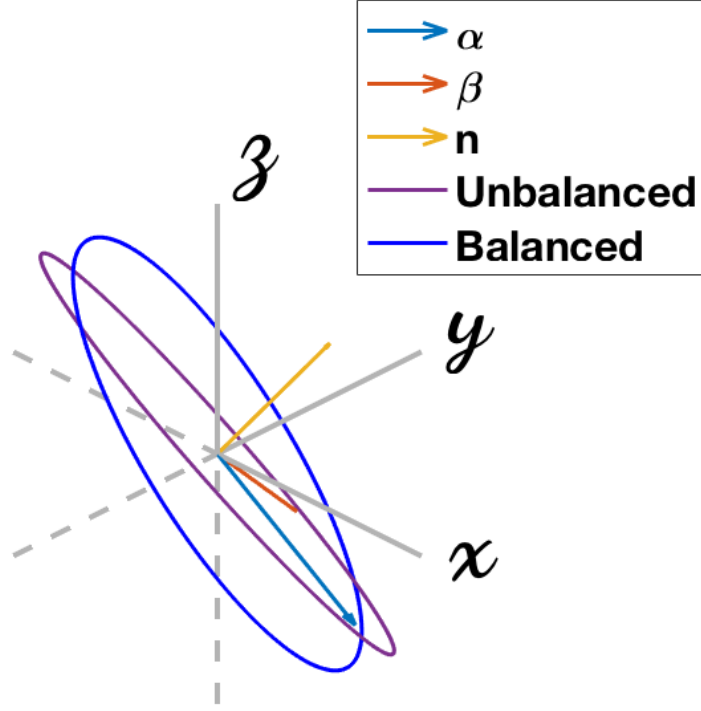


Figure 3.7: QVL for the magnitude unbalanced condition of Example 2. Balanced QVL is presented for comparison. Major and minor semi-axes denoted α and β are in blue and red colors.

and the phase computed via (3.80) is

$$\phi_{osc} = \arctan \left(\frac{\left(\frac{1}{2}\right)^2 \sin(240^\circ) - \left(\frac{1}{2}\right)^2 \sin(240^\circ)}{1 + \left(\frac{1}{2}\right)^2 \cos(240^\circ) + \left(\frac{1}{2}\right)^2 \cos(240^\circ)} \right) \quad (3.101)$$

$$= \arctan \left(\frac{0}{1 + \left(\frac{1}{2}\right)^2 \cos(240^\circ) + \left(\frac{1}{2}\right)^2 \cos(240^\circ)} \right) \quad (3.102)$$

$$= \arctan(+0). \quad (3.103)$$

Since the vertical cathetus of the Figure (3.6) is zero and the horizontal is positive, the angle from the geometrical interpretation is

$$\phi_{osc} = 0. \quad (3.104)$$

Therefore, voltage norm maximum occurs at $t_{max} = 0$.

Quaternion major semi-axis direction is parallel (denoted by the \parallel symbol) to the quaternion voltage direction at $t = t_{max}$.

$$\alpha \parallel \mathbf{V}(t = t_{max} = 0) \quad (3.105)$$

$$\parallel (1 \cos(0)) \mathbf{x} + \left(\frac{1}{2} \cos(0 - 120^\circ)\right) \mathbf{y} + \left(\frac{1}{2} \cos(0 + 120^\circ)\right) \mathbf{z} \quad (3.106)$$

$$\parallel \mathbf{x} - \frac{1}{4} \mathbf{y} - \frac{1}{4} \mathbf{z} \quad (3.107)$$

Normalizing the right hand side of the previous equation,

$$\boldsymbol{\alpha} = \frac{4\mathbf{x} - \mathbf{y} - \mathbf{z}}{3\sqrt{2}} \quad (3.108)$$

The direction of the minor semi-axis is determined applying (3.83)

$$\boldsymbol{\beta} = \mathbf{n}\boldsymbol{\alpha} \quad (3.109)$$

$$= \frac{\mathbf{x} + 2\mathbf{y} + 2\mathbf{z}}{3} \frac{4\mathbf{x} - \mathbf{y} - \mathbf{z}}{3\sqrt{2}} \quad (3.110)$$

$$= \frac{[2\mathbf{y}(-\mathbf{z}) - 2\mathbf{z}(-\mathbf{y})] + [2\mathbf{z}4\mathbf{x} - \mathbf{x}(-\mathbf{z})] + [\mathbf{x}(-\mathbf{y}) - 2\mathbf{y}4\mathbf{x}]}{9\sqrt{2}} \quad (3.111)$$

$$= \frac{0\mathbf{x} + 9\mathbf{y} - 9\mathbf{z}}{9\sqrt{2}} \quad (3.112)$$

$$= \frac{\mathbf{y} - \mathbf{z}}{\sqrt{2}}. \quad (3.113)$$

The last quantity to be determined are the semi-axes magnitudes. By (3.81) and (3.82), they are equal to

$$V_{\alpha} = \sqrt{\left(\frac{\sqrt{3}}{2}\right)^2 + \left(\frac{\sqrt{3}}{2}\right)^2} \quad (3.114)$$

$$= \sqrt{\frac{3}{2} + \frac{3}{4}} = \frac{3}{2} \quad (3.115)$$

$$V_{\beta} = \sqrt{\left(\frac{\sqrt{3}}{2}\right)^2 - \left(\frac{\sqrt{3}}{2}\right)^2} \quad (3.116)$$

$$= \sqrt{\frac{3}{2} - \frac{3}{4}} = \frac{\sqrt{3}}{2} \quad (3.117)$$

Eccentricity in this case is given by

$$e = \sqrt{1 - \frac{3}{9}} \quad (3.118)$$

$$e = \frac{\sqrt{6}}{3} \approx 0,82. \quad (3.119)$$

Therefore, all quantities related to the QVL with magnitude unbalance have been computed. The ellipse equation for this example is

$$\frac{\left(\frac{4x-y-z}{3\sqrt{2}}\right)^2}{\left(\frac{3}{2}\right)^2} + \frac{\left(\frac{y-z}{\sqrt{2}}\right)^2}{\left(\frac{\sqrt{3}}{2}\right)^2} = 1, \forall (x, y, z) \in \mathbb{R}^3, x + 2y + 2z = 0. \quad (3.120)$$

Example 3 [Phase Unbalance]

In this example the effects of a phase unbalance on the QVL will be discussed. Considering $V_a = V_b = V_c = 1$ pu and $\theta_{ab} = \theta_{ca} = 90^\circ$ and $\theta_{bc} = 180^\circ$, then the QVL plane (\mathbf{n}), computed

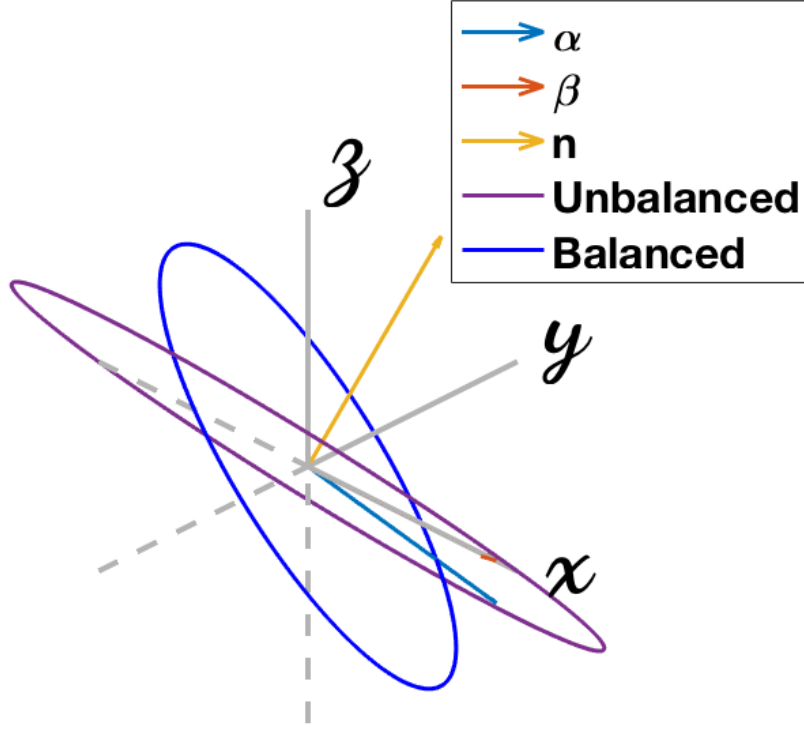


Figure 3.8: QVL for the phase unbalanced condition of Example 3. Balanced QVL is presented for comparison. Major and minor semi-axes are denoted α and β in blue and red colors.

accordingly to (3.59), is

$$\mathbf{n} = \frac{1}{\mathbf{n}_0} [1 \sin(180^\circ) \mathbf{x} + 1 \sin(90^\circ) \mathbf{y} + 1 \sin(90^\circ) \mathbf{z}] \quad (3.121)$$

$$= \frac{1}{\mathbf{n}_0} [0\mathbf{x} + \mathbf{y} + \mathbf{z}]. \quad (3.122)$$

The normalization parameter \mathbf{n}_0 , that is given by (3.60), is equal to

$$\mathbf{n}_0 = \sqrt{1 \sin^2(90^\circ) + 1^2 \sin^2(180^\circ) + 1^2 \sin^2(90^\circ)} \quad (3.123)$$

$$= \sqrt{1 + 0 + 1} = \sqrt{2}. \quad (3.124)$$

So,

$$\mathbf{n} = \frac{\mathbf{y} + \mathbf{z}}{\sqrt{2}} \quad (3.125)$$

The quaternion \mathbf{n} is closer to the \mathbf{y} and \mathbf{z} directions, since its coefficients are higher. Considering that \mathbf{n} is orthogonal to the QVL, it is correct to say that the plane is closer to \mathbf{x} , as shown in Figure 3.8. This can be thought of as a result from phases b and c being closer (angularly) to phase a , which is parallel to \mathbf{x} .

The voltage norm RMS value, accordingly to (3.73), is

$$|\mathbf{V}|_{RMS} = \sqrt{1^2 + 1^2 + 1^2} \quad (3.126)$$

$$= \sqrt{3}. \quad (3.127)$$

The oscillating component magnitude, given by (3.79), is

$$|\mathbf{V}|_{osc} = \sqrt{\sqrt{[1 + 1^2 \cos(180^\circ) + 1^2 \cos(180^\circ)]^2 + [1^2 \sin(180^\circ) - 1^2 \sin(180^\circ)]^2}} \quad (3.128)$$

$$= \sqrt{\sqrt{[1 + (-1) + (-1)]^2 + 0^2}} \quad (3.129)$$

$$= 1 \quad (3.130)$$

and the phase computed via (3.80) is

$$\phi_{osc} = \arctan\left(\frac{1^2 \sin(180^\circ) - 1^2 \sin(180^\circ)}{1 + 1^2 \cos(180^\circ) + 1^2 \cos(180^\circ)}\right) \quad (3.131)$$

$$= \arctan\left(\frac{0}{1 + (-1) + (-1)}\right) \quad (3.132)$$

$$= \arctan(-0) \quad (3.133)$$

$$= 180^\circ. \quad (3.134)$$

Therefore, voltage norm maximum occurs at $t_{max} = \frac{180^\circ}{2w}$.

Quaternion major semi-axis direction is parallel to the quaternion voltage direction at $t = t_{max}$. Thus,

$$\boldsymbol{\alpha} \parallel \mathbf{V}(t = t_{max} = \frac{180^\circ}{w}) \quad (3.135)$$

$$\parallel (1 \cos(90^\circ)) \mathbf{x} + 1 \cos(90^\circ - 90^\circ) \mathbf{y} + 1 \cos(90^\circ + 90^\circ) \mathbf{z} \quad (3.136)$$

$$\parallel 0\mathbf{x} + 1\mathbf{y} - 1\mathbf{z} \quad (3.137)$$

$$= \frac{\mathbf{y} - \mathbf{z}}{\sqrt{2}}. \quad (3.138)$$

The direction of the minor semi-axis is determined applying (3.83)

$$\boldsymbol{\beta} = \mathbf{n}\boldsymbol{\alpha} \quad (3.139)$$

$$= \left(\frac{\mathbf{y} + \mathbf{z}}{\sqrt{2}}\right) \left(\frac{\mathbf{y} - \mathbf{z}}{\sqrt{2}}\right) \quad (3.140)$$

$$= \frac{[\mathbf{y}(-\mathbf{z}) - \mathbf{z}\mathbf{y}] + [0] + [0]}{2} \quad (3.141)$$

$$= -\mathbf{x}. \quad (3.142)$$

The last quantity to be determined are the semi-axes magnitudes. By (3.81) and (3.82), they are equal to

$$V_\alpha = \sqrt{(\sqrt{3})^2 + (1)^2} \quad (3.143)$$

$$= \sqrt{4} = 2 \quad (3.144)$$

$$V_\beta = \sqrt{(\sqrt{3})^2 - (1)^2} \quad (3.145)$$

$$= \sqrt{2} \quad (3.146)$$

Eccentricity, in this case, is given by

$$e = \sqrt{1 - \frac{2}{4}} \quad (3.147)$$

$$e = \frac{\sqrt{2}}{2} \approx 0,71. \quad (3.148)$$

Therefore, all quantities related to the QVL with angular unbalance have been computed.

The ellipse equation for this example is

$$\frac{\left(\frac{y-z}{\sqrt{2}}\right)^2}{(2)^2} + \frac{\left(\frac{-x}{\sqrt{2}}\right)^2}{(\sqrt{2})^2} = 1, \forall (x, y, z) \in \mathbb{R}^3, y + z = 0 \quad (3.149)$$

The results from examples 2 and 3 are summarized in Table 3.2. It is noteworthy that phase unbalance doesn't change the norm rms value. This was expected due to the fact that (3.73) depends only on phase magnitudes. Therefore, it measures the system voltage levels. Additionally, it can be used to identify the type of unbalance occurring.

The QVL plane displacement (θ_n) with regard to the balanced plane is shown to be related to the zero sequence component, expressed in terms of

$$VUF_0 = \frac{V_0}{V_1}, \quad (3.150)$$

in which V_0 and V_1 are the zero and positive sequence magnitudes from Fortescue's theory. This will be further explained in the next sections. But, the basic idea is that this component is the only one that acts perpendicularly to the QVL balanced plane. So, it is responsible for the increase in θ_n .

The major semi-axis magnitude was higher in the phase unbalanced condition, which also presented a slightly higher unbalance factor VUF , which is given by

$$VUF = \frac{V_2}{V_1}, \quad (3.151)$$

being V_2 the negative sequence. For this analysis, it is important to notice that VUF quantifies the unbalance. Comparing both unbalanced cases, example 3 presented quantities with higher value, with exception of the eccentricity. This analysis suggests, therefore, several quantities that may be employed as unbalance factors in substitution to the traditional VUF . A thorough investigation, however, still needs to be performed. The relationship of these quantities with electrical phenomena on loads supplied by unbalanced sources (the temperature on an induction motor, for example) is suggested for evaluation in future researches.

Considering the QVL plane of each example, example 3 presented a higher plane displacement in relation to the balanced condition. It also presented a higher zero sequence component in relation to the positive,

$$VUF_0 = \frac{V_0}{V_1}, \quad (3.152)$$

in which V_0 is the zero sequence symmetrical component magnitude from Fortescue's theory. This may indicate a relation between these two quantities. As aforementioned, section 4.1 will analytically show that the QVL plane is indeed associated with the zero sequence.

Table 3.2: QVL parameters for different conditions.

Quantity	Balanced case	Amplitude Unbalance (Ex 2)	Phase Unbalance (Ex 3)
VUF	0	0,25	0,27
VUF0	0	0,25	0,37
\mathbf{n}	$\frac{\mathbf{x}+\mathbf{y}+\mathbf{z}}{\sqrt{3}}$	$\frac{\mathbf{x}+2\mathbf{y}+2\mathbf{z}}{3}$	$\frac{\mathbf{y}+\mathbf{z}}{\sqrt{2}}$
θ_n	0	15, 79°	35, 26°
$ \mathbf{V} _{RMS}$	$\sqrt{3}$	$\sqrt{\frac{3}{2}}$	$\sqrt{3}$
$ \mathbf{V} _{osc}$	0	$\frac{\sqrt{3}}{2}$	1
V_α	$\sqrt{3}$	$\frac{3}{2}$	2
V_β	$\sqrt{3}$	$\frac{\sqrt{3}}{2}$	$\sqrt{2}$
e	0	0,82	0,71

Chapter 4

Symmetrical Components, Passive Elements and Power

In this chapter, a quaternion time-domain version of Fortescue's symmetrical components is proposed. A three-phase quaternion impedance is defined for both balanced and unbalanced conditions. A novel hypercomplex model for transmission lines with and without mutual coupling is also presented. For this purpose, electrical circuits equations in the time domain are investigated and then rewritten by means of quaternions.

4.1 Symmetrical Components

In this section, symmetrical components, introduced by Fortescue [52], are presented. Then, a corresponding quaternion version is proposed, and its relation with the traditional theory is discussed. Moreover, the proposed version allows to model symmetrical components in a linear state-space model.

According to [12], supply quality is associated with the utility voltages deviation from their nominal parameters. Loading quality, on the other hand, is associated with the loads distorted generated currents. Usually, both phenomena generate unbalanced currents and, consequently, deteriorate power supply of nearby region. This shows the electrical coupling between phases. Therefore, a per phase approach is not possible. As a workaround, Fortescue introduced the symmetrical components [52]. With it, he was able to represent one set of n unbalanced phasors into n sets of n balanced phasors. Furthermore, electrical coupling can be eliminated for several conditions. Hence, it is also considered a decoupling method.

For three phase systems, the balanced sets are named positive, negative and zero sequences, as illustrated by Figure 4.1. Since these sets are also balanced, only one phasor of each set is actually meaningful. In other words, any system can be completely characterized by \hat{V}_{a0} , \hat{V}_{a1} and \hat{V}_{a2} . Subscript “ a ” is usually dropped for the ease of representation.

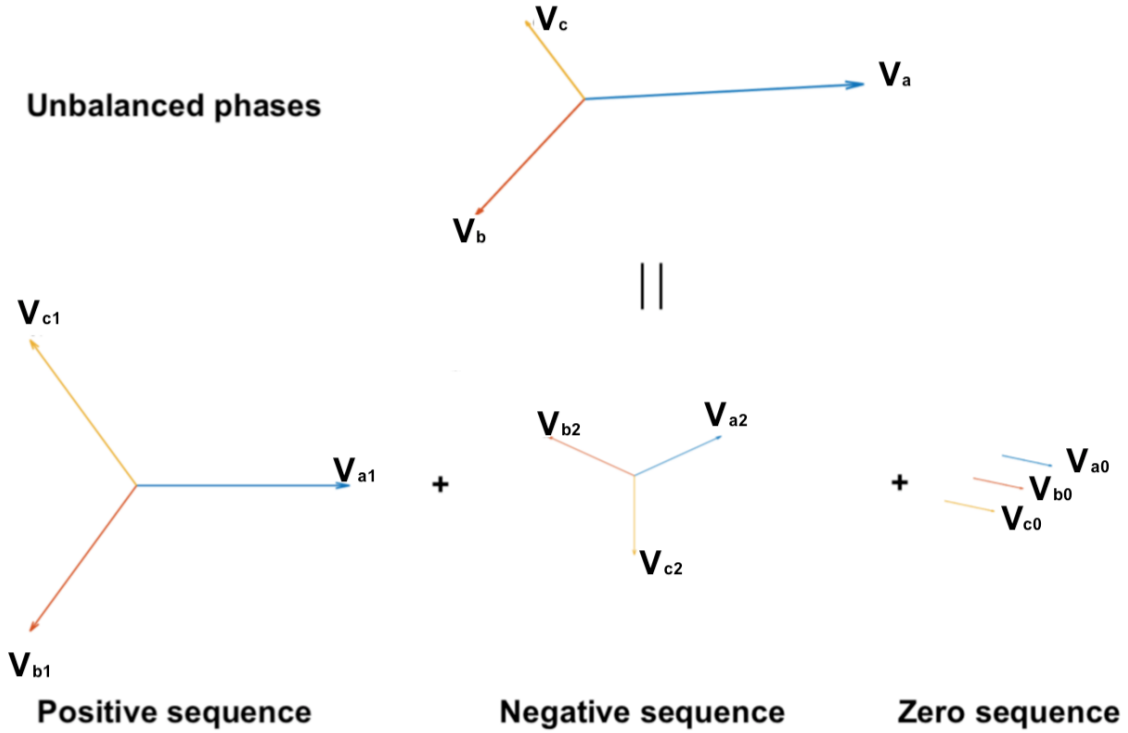


Figure 4.1: Unbalanced set of three phasors being represent by three sets of three balanced phasors. The first set is the positive sequence, the second is the negative and the third is the zero.

In this dissertation, complex numbers are denoted with a hat above it. Consequently, phasors notation is also a hat. Symmetrical components are computed via the Fortescue inverse matrix (F^{-1}) as

$$\underbrace{\begin{bmatrix} \hat{V}_0 \\ \hat{V}_1 \\ \hat{V}_2 \end{bmatrix}}_{V_{012}} = \frac{1}{3} \underbrace{\begin{bmatrix} 1 & 1 & 1 \\ 1 & \hat{a} & \hat{a}^2 \\ 1 & \hat{a}^2 & \hat{a} \end{bmatrix}}_{F^{-1}} \underbrace{\begin{bmatrix} \hat{V}_a \\ \hat{V}_b \\ \hat{V}_c \end{bmatrix}}_{V_{abc}}, \quad (4.1)$$

in which \hat{a} is the rotation element given by $\hat{a} = 1/\underline{120^\circ}$. It should be noticed that Fortescue matrix is composed of complex numbers, not phasors. In other words, although \hat{a} is a complex element, it is not associated with the rotating complex exponential $e^{j\omega t}$, in which j is the imaginary unit.

The positive sequence can be thought of as a set of phasors with sequence ABC rotating clockwise. Negative sequence might be considered as i) a set of CBA phasors rotating clockwise, or ii) ABC phasors rotating counter-clockwise. Finally, zero sequence is interpreted as a set of parallel phasors, *i.e.* with the same angle, rotating clockwise.

It is noteworthy that (4.1) is the power variant transformation. In other words, power computed with phase quantities is different by a scale factor from that computed with sequence components. According to [5], complex power is given by

$$\hat{S}_{abc} = V_{abc}^T I_{abc}^*, \quad (4.2)$$

in which V_{abc} is a column vector formed by stacking voltage phasors, I_{abc} likewise. So, they are not represented with the hat notation. Rewriting the right hand side in terms of voltage and current sequences

$$\hat{S}_{abc} = (FV_{012})^T F^* I_{012}^* \quad (4.3)$$

$$= V_{012}^T F^T F^* I_{012}^* \quad (4.4)$$

$$(4.5)$$

and since $F^T F^* = 3\mathbb{I}_{3 \times 3}$, then

$$\hat{S}_{abc} = 3V_{012}^T I_{012}^* = 3\hat{S}_{012} \quad (4.6)$$

$$(4.7)$$

A power invariant transform version is given by

$$F_{inv} = \frac{1}{\sqrt{3}} \begin{bmatrix} 1 & 1 & 1 \\ 1 & \hat{a}^2 & \hat{a} \\ 1 & \hat{a} & \hat{a}^2 \end{bmatrix} = \frac{1}{\sqrt{3}} F. \quad (4.8)$$

This matrix fulfills the following property of invariant complex transformations

$$F_{inv}^H F_{inv} = \mathbb{I}, \quad (4.9)$$

in which the H superscript denote the hermitian, and it is computed as its conjugate transposed. With this transformation, power in both domain are equivalent

$$\hat{S}_{abc} = \hat{S}_{012}. \quad (4.10)$$

With these concepts in mind, a quaternion version of this theory will be investigated.

For a balanced set of voltages with ABC sequence, it was possible to rewrite them as a rotating element, as presented in section 3.1. This condition yields a positive sequence component. In the quaternion domain, it is, therefore, expressed as

$$\mathbf{V}_1(t) = \sqrt{3}V_1 e^{\mathbf{n}_{bal}wt} \mathbf{q}_p, \quad (4.11)$$

in which \mathbf{n}_{bal} is given by (3.25) and \mathbf{q}_p by (3.35).

As previously stated, negative sequence can be thought of as a CBA voltage system. In this condition, the QVL is equal to the previous case. The quaternion angular momentum will also be equal, but with opposite sign, *i.e.* $(-\mathbf{n}_{bal})w$. In other words, it will rotate in the opposite direction of the previous case.

In this condition, voltages are given by

$$v_{a,CBA}(t) = \sqrt{2}V \cos(wt) \quad (4.12)$$

$$v_{b,CBA}(t) = \sqrt{2}V \cos(wt + 120^\circ) \quad (4.13)$$

$$v_{c,CBA}(t) = \sqrt{2}V \cos(wt - 120^\circ). \quad (4.14)$$

The QVL plane \mathbf{n} can be computed via the cross product method, with samples at the time instants $wt_1 = 0$ and $wt_2 = 90^\circ$. Applying it for the CBA systems and considering the voltage norm is equal to (3.31), then \mathbf{n}_{bal} is

$$\mathbf{n}_{\text{CBA}} = \frac{1}{3V^2} \left[\sqrt{2}V \left(1\mathbf{x} - \frac{1}{2}\mathbf{y} - \frac{1}{2}\mathbf{z} \right) \right] \times \left[\sqrt{2}V \left(0\mathbf{x} - \frac{\sqrt{3}}{2}\mathbf{y} + \frac{\sqrt{3}}{2}\mathbf{z} \right) \right] \quad (4.15)$$

$$= \frac{2}{3} \left(-\frac{\sqrt{3}}{4} - \frac{\sqrt{3}}{4} \right) \mathbf{x} + \left(-\frac{\sqrt{3}}{2} \right) \mathbf{y} + \left(-\frac{\sqrt{3}}{2} \right) \mathbf{z} \quad (4.16)$$

$$= -\frac{\mathbf{x} + \mathbf{y} + \mathbf{z}}{3} \quad (4.17)$$

$$= -\mathbf{n}_{\text{bal}}. \quad (4.18)$$

The quaternion orthonormal to the plane in this condition was found to be the negative of the one found in the ABC balanced condition. This means that the angular momentum in this case is the negative of the ABC sequence. In other words, quaternion voltage is rotating in the opposite direction.

In this condition, QVL is also a circle. Hence, the negative sequence quaternion is given by

$$\mathbf{V}_2(t) = \sqrt{3}V_2 e^{-\mathbf{n}_{\text{bal}}wt} \mathbf{q}_p \quad (4.19)$$

If voltages have the same magnitude and angle, then they represent a zero sequence component, and they are given by

$$v_{a,0}(t) = \sqrt{2}V \cos(wt + \phi) \quad (4.20)$$

$$v_{b,0}(t) = \sqrt{2}V \cos(wt + \phi) \quad (4.21)$$

$$v_{c,0}(t) = \sqrt{2}V \cos(wt + \phi). \quad (4.22)$$

The zero sequence quaternion voltage can be written as

$$\mathbf{V}_0(t) = \sqrt{3}\sqrt{2}V \cos(wt + \phi) \mathbf{n}_{\text{bal}}. \quad (4.23)$$

Combining the polar representation in (2.34) and the method for extracting its real part presented in (2.22), the previous equation turns into

$$\mathbf{V}_0(t) = \sqrt{3}V_0 \frac{e^{\mathbf{n}_{\text{bal}}(wt+\phi)} + e^{-\mathbf{n}_{\text{bal}}(wt+\phi)}}{\sqrt{2}} \mathbf{n}_{\text{bal}}. \quad (4.24)$$

Considering that all symmetrical components may occur simultaneously and with different magnitudes and angles, then a general equation for quaternion voltage is given by

$$\mathbf{V}_{\text{sym}}(t) = \underbrace{\sqrt{3}V_0 \frac{e^{\mathbf{n}_{\text{bal}}(wt+\theta_0)} + e^{-\mathbf{n}_{\text{bal}}(wt+\theta_0)}}{\sqrt{2}} \mathbf{n}_{\text{bal}}}_{\text{zero sequence}} + \underbrace{\sqrt{3}V_1 e^{\mathbf{n}_{\text{bal}}(wt+\theta_1)} \mathbf{q}_p}_{\text{positive sequence}} + \underbrace{\sqrt{3}V_2 e^{-\mathbf{n}_{\text{bal}}(wt+\theta_2)} \mathbf{q}_p}_{\text{negative sequence}} \quad (4.25)$$

$$= \mathbf{V}_0 + \mathbf{V}_1 + \mathbf{V}_2, \quad (4.26)$$

in which θ_0 , θ_1 and θ_2 are the angles of each sequence computed by the F^{-1} matrix.

In order to determine how these components are related to Fortescue's theory, it will be considered that the quaternion voltage \mathbf{x} , \mathbf{y} and \mathbf{z} components are equal to voltage on phases A , B and C , respectively. Exponential quaternions, \mathbf{q}_p and \mathbf{n}_{bal} in (4.25) are rewritten in terms of the \mathbf{x} , \mathbf{y} and \mathbf{z} . So, applying (2.34) in (4.25) and considering $\mathbf{q}_n = \mathbf{n}_{\text{bal}}\mathbf{q}_p$

$$\begin{aligned} \mathbf{V}_{\text{sym}}(t) = \sqrt{3} \{ & V_0 [\cos (wt + \theta_0) \mathbf{n}] + \\ & V_1 [\cos (wt + \theta_1) \mathbf{q}_p + \sin (wt + \theta_1) \mathbf{q}_n] + \\ & V_2 [\cos (wt + \theta_2) \mathbf{q}_p - \sin (wt + \theta_2) \mathbf{q}_n] \}. \end{aligned} \quad (4.27)$$

Substituting the values of \mathbf{n}_{bal} (3.25) and \mathbf{q}_p (3.35) and $\mathbf{q}_n = \frac{\mathbf{y}-\mathbf{z}}{\sqrt{2}}$ in the previous equations, then the term of \mathbf{x} is given by

$$\sqrt{2}V_a \cos (wt) = \sqrt{2} [V_0 \cos (wt + \theta_0) + V_1 \cos (wt + \theta_1) + V_2 \cos (wt + \theta_2)]. \quad (4.28)$$

If the above elements are rewritten as phasors, then

$$\hat{V}_a = V_0 \angle \theta_0 + V_1 \angle \theta_1 + V_2 \angle \theta_2. \quad (4.29)$$

It is noteworthy that this is equivalent to the obtained via Fortescue matrix. Analysing phase "B" voltage, or equivalently, the \mathbf{y} term of (4.27),

$$\begin{aligned} \sqrt{2}V_b \cos (wt - 120 + \phi_b) = \sqrt{2} \{ & V_0 \cos (wt + \theta_0) + \\ & V_1 \left[\cos (wt + \theta_1) \left(-\frac{1}{2} \right) + \sin (wt + \theta_1) \frac{\sqrt{3}}{2} \right] + \\ & V_2 \left[\cos (wt + \theta_2) \left(-\frac{1}{2} \right) - \sin (wt + \theta_2) \frac{\sqrt{3}}{2} \right] \} \end{aligned} \quad (4.30)$$

applying the cosine of the sum property (3.48), then

$$\sqrt{2}V_b \cos (wt - 120 + \phi_b) = \sqrt{2} [V_0 \cos (wt + \theta_0) + V_1 \cos (wt + \theta_1 - 120^\circ) + V_2 \cos (wt + \theta_2 + 120^\circ)]. \quad (4.31)$$

Using phasorial notation,

$$\hat{V}_b = V_0 \angle \theta_0 + \hat{a}^2 V_1 \angle \theta_1 + \hat{a} V_2 \angle \theta_2. \quad (4.32)$$

Likewise for phase "C",

$$\hat{V}_c = V_0 \angle \theta_0 + \hat{a} V_1 \angle \theta_1 + \hat{a}^2 V_2 \angle \theta_2. \quad (4.33)$$

Gathering these phasorial equalities in a matrix form, yields

$$\begin{bmatrix} \hat{V}_a \\ \hat{V}_b \\ \hat{V}_c \end{bmatrix} = \underbrace{\begin{bmatrix} 1 & 1 & 1 \\ 1 & \hat{a}^2 & \hat{a} \\ 1 & \hat{a} & \hat{a}^2 \end{bmatrix}}_F \begin{bmatrix} V_0 \angle \theta_0 \\ V_1 \angle \theta_1 \\ V_2 \angle \theta_2 \end{bmatrix}, \quad (4.34)$$

which is equal to (4.1) inverse. So, the symmetrical components (V_0 , V_1 , V_2 , θ_0 , θ_1 and θ_2) in the quaternion formulation given by (4.25) have been proved to be the same as those provided by the

Figure 4.2: Animated unbalanced quaternion voltage and its locus in terms of its symmetrical quaternion components.

Fortescue's power variant transformation. It is noteworthy that if the $\sqrt{3}$ factor was neglected in (4.25), then the obtained components would be equal to those obtained with the power invariant transformation.

The quaternion symmetrical components dynamics and how they add up to the voltage are shown in Figure 4.2. In the virtual version of this dissertation, it is an animated figure that may be visualized using an appropriate PDF reader, such as Adobe Acrobat Reader DC. In the printed version, several frames are shown in order to give an intuition of the dynamics involved. As indicated by (4.25) and visible in Figure 4.2, quaternion positive and negative sequences rotates in opposite directions and are contained in the balanced QVL plane. It is also observable that the zero component oscillates parallel to \mathbf{n}_{bal} . So, the results obtained analytically in (4.25) are supported by Figure 4.2.

Since the only component that is not contained in the QVL balanced plane is the zero sequence, then this component is responsible for plane changes. The negative sequence is the main responsible for changing the QVL format. If $\theta_2 = \theta_1$, then maximum of both positive and negative sequence occurs at the same time instant. As a result, the ellipse major semi-axis is given by the time instant related to their angle, *i.e.* $t_{\text{max}} = \frac{\theta_1}{w}$. So, it is clear that these angles are related to

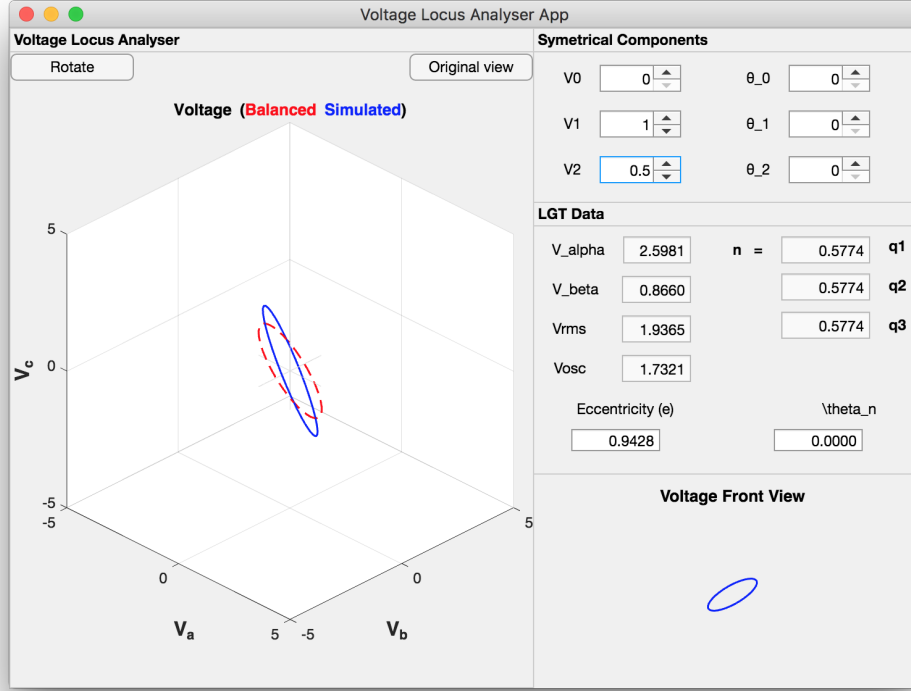


Figure 4.3: QVL Analyser app designed in *Matlab*.

the ellipse semi-axes directions.

In order to confirm these results, a QVL analyser application (app) was developed using *Matlab* [54]. This app takes as inputs Fortescue's symmetrical components magnitudes and angles. It outputs a three dimensional visualization of the unbalanced QVL and the balanced one, along with a two dimensional front view of the ellipse. It also computes the major and minor semi-axes magnitudes, the voltage norm RMS value and the magnitude of its oscillating part and the plane direction. Figure 4.3 shows the app window.

It was possible to note that if $V_0 = 0$, then \mathbf{n} is always the balanced one. In this condition, V_2 changes the ellipse eccentricity, deforming the QVL shape. However, if $V_0 \neq 0$, then the negative sequence also alters the \mathbf{n} direction. This can be explained by the fact that adding any quaternion that is not on the same plane as the voltage will result in a plane direction change. It was also noted that V_0 does influence the ellipse eccentricity, because under unbalanced situations the zero sequence is not totally perpendicular to the balanced QVL. The negative sequence effects on its format, however, is considerably higher. For example, if $V_1 = 1 pu$, $V_2 = 0 pu$ and $V_0 = 0,5 pu$, then $e \approx 0,5774$. In the opposite condition, in which $V_2 = 0,5 pu$ and $V_0 = 0 pu$, then $e \approx 0,9428$.

A remark from (4.25) is that voltage derivative can be computed by

$$\frac{d\mathbf{V}(t)}{dt} = \sqrt{3}V_0w \sin(wt + \theta_0) \mathbf{n}_{\text{bal}} + \mathbf{n}_{\text{bal}}w\mathbf{V}_1 - \mathbf{n}_{\text{bal}}w\mathbf{V}_2 \quad (4.35)$$

$$= \mathbf{n}_{\text{bal}}w\mathbf{V}_0^+ - \mathbf{n}_{\text{bal}}w\mathbf{V}_0^- + \mathbf{n}_{\text{bal}}w\mathbf{V}_1 - \mathbf{n}_{\text{bal}}w\mathbf{V}_2, \quad (4.36)$$

in which \mathbf{V}_0^+ and \mathbf{V}_0^- are

$$\mathbf{V}_0^+ = \sqrt{3}V_0 \frac{e^{\mathbf{n}_{\text{bal}}(wt+\theta_0)}}{\sqrt{2}} \mathbf{n}_{\text{bal}} \quad (4.37)$$

$$\mathbf{V}_0^- = \sqrt{3}V_0 \frac{e^{-\mathbf{n}_{\text{bal}}(wt+\theta_0)}}{\sqrt{2}} \mathbf{n}_{\text{bal}}, \quad (4.38)$$

and they represent zero sequence associated to the quaternion exponential with positive and negative \mathbf{n}_{bal} , respectively. Notice that they are the output of a mathematical decomposition. Actually, they do not have a clear interpretation.

It is noteworthy that quaternions maps three-phase voltage derivatives, for both balanced and unbalanced conditions, into products. Integrals can be computed likewise. It is highlighted that phasors also have the capability of turning a time derivative into a product. However, they operate only one phase at a time. So, the former tool is better than the latter because it allows calculus on all phases simultaneously with quaternion products. Moreover, it may be an appropriate framework for the development of power theories, since it is in the time domain and yet retain phasor simplification properties.

As a consequence from (4.36), it is possible to come up with a linear state space model for the quaternion symmetrical components. Consider the following vector of quaternion variables

$$x = \left[\mathbf{V}_0^+ \quad \mathbf{V}_0^- \quad \mathbf{V}_1 \quad \mathbf{V}_2 \right]^T. \quad (4.39)$$

Its evolution equation is given by

$$\dot{x} = \underbrace{\begin{bmatrix} \mathbf{n}w & 0 & 0 & 0 \\ 0 & -\mathbf{n}w & 0 & 0 \\ 0 & 0 & \mathbf{n}w & 0 \\ 0 & 0 & 0 & -\mathbf{n}w \end{bmatrix}}_A x + \eta, \quad (4.40)$$

in which A is the evolution matrix and $\eta \in \mathbb{H}^4$ is the state noise. An appropriate observation model could be

$$\mathbf{V} = \underbrace{\begin{bmatrix} 1 & 1 & 1 & 1 \end{bmatrix}}_H x + \mathbf{v}, \quad (4.41)$$

in which H is the observation matrix and $\mathbf{v} \in \mathbb{H}$ is the measurement noise. It is noteworthy that this proposed state space model is linear. It is possible to apply it for estimating the symmetrical components and, indirectly, the phasors magnitudes and angles, via the Fortescue transformation. This discussion, nevertheless, is beyond the scope of this dissertation and it is suggested for further investigations.

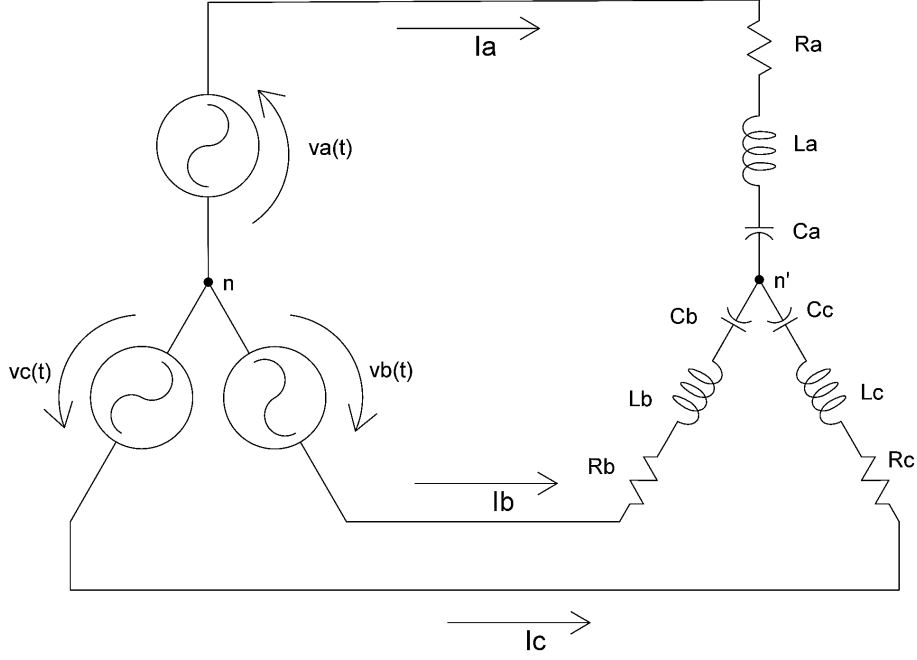


Figure 4.4: System consisting of an ideal power supply connected via three wires to a balanced load consisting of three RLC impedances connected in wye.

4.2 Loads

4.2.1 Without Mutual Coupling

This subsection is based on [41], in which a three-phase balanced wye load is studied. This approach also applies to delta (Δ) loads and works both on three and four wire systems as will be shown.

The author of this dissertation proposed a balanced quaternion impedance in [41]. For this purpose, he considered a load consisting of three RLC impedances connected in wye as shown in Figure 4.4. In this case, $R_a = R_b = R_c = R$, $L_a = L_b = L_c = L$ and $C_a = C_b = C_c = C$. Then he applied the Kirchhoff Voltage Law (KVL) for each phase. Since the system is balanced, the set of equations obtained are equal to

$$v_a(t) = Ri_a(t) + L \frac{di_a(t)}{dt} + \frac{1}{C} \int i_a(t) dt \quad (4.42)$$

$$v_b(t) = Ri_b(t) + L \frac{di_b(t)}{dt} + \frac{1}{C} \int i_b(t) dt \quad (4.43)$$

$$v_c(t) = Ri_c(t) + L \frac{di_c(t)}{dt} + \frac{1}{C} \int i_c(t) dt. \quad (4.44)$$

In the quaternion format, the three-phase voltage and current, given by (3.1) and (3.5), are related by (the time index is dropped for the ease of representation, however quantities are still in the

time domain)

$$\mathbf{V} = R\mathbf{I} + L\frac{d\mathbf{I}}{dt} + \int \mathbf{I}dt. \quad (4.45)$$

Applying (3.42) and (3.43) for the current in the former equation,

$$\mathbf{V} = \left(R + \mathbf{n}wL - \frac{\mathbf{n}}{wC} \right) \mathbf{I}, \quad (4.46)$$

in which \mathbf{n} is considered equal to \mathbf{n}_{bal} . The subscript “bal” is omitted for notation simplification.

Just as in single-phase circuits, the three-phase quaternion impedance is defined as the element relating voltage and current, more specifically, voltage right divided by current.

$$\mathbf{Z} = \mathbf{V}\mathbf{I}^{-1} \quad (4.47)$$

It is worth mentioning that despite voltage and current being time variant in (4.47), the impedance is constant for balanced conditions and depends only on load parameters. This is expected since the load is linear and time invariant (LTI). If the quaternion element was found to be a time varying element, this would be an inappropriate definition because it could lead to the misunderstanding that the load is time variant, though it is not.

Additionally, all impedance association rules applies similarly to the phasorial theory. However, the fact that the product is not commutative should be regarded. For the series RLC circuit under discussion, the impedance is

$$\mathbf{Z} = R + \mathbf{n} \left(wL - \frac{1}{wC} \right). \quad (4.48)$$

Its real part is equal to the resistive elements in the circuit. Its vectorial part, which have \mathbf{x} , \mathbf{y} and \mathbf{z} components, is equivalent to the reactive elements. So, it is correct to state that the imaginary unit employed via phasors is substituted by the complex element \mathbf{n} .

The quaternion admittance can be defined as the inverse of the impedance,

$$\mathbf{Y} = \mathbf{Z}^{-1} \quad (4.49)$$

$$\mathbf{Y} = \mathbf{I}\mathbf{V}^{-1}. \quad (4.50)$$

In this specific case,

$$\mathbf{Y} = \frac{R - \mathbf{n} \left(wL - \frac{1}{wC} \right)}{R^2 + \left(wL - \frac{1}{wC} \right)^2}. \quad (4.51)$$

Theorem 1 [*Parallel association rule*]

If two three-phase loads are in parallel, then the equivalent admittance is equal to the sum of the individual ones. The voltage over both loads is equal and the total amount of current drawn from the source (\mathbf{I}) is the sum of the currents of each load (\mathbf{I}_{L1} and \mathbf{I}_{L2}). So,

$$\mathbf{Y}_{eq} = \mathbf{I}\mathbf{V}^{-1} \quad (4.52)$$

$$= (\mathbf{I}_{L1} + \mathbf{I}_{L2}) \mathbf{V}^{-1} \quad (4.53)$$

$$= \mathbf{Y}_{L1} + \mathbf{Y}_{L2}. \quad (4.54)$$

□

This dissertation further the results presented both in [6,41] because unbalanced conditions are considered. If the supply voltage is unbalanced, then the currents are likely to be also unbalanced. Hence, (4.46) does not apply because (3.42) is valid only for balanced conditions. In this case, symmetrical components proposed in this work can be used. Although (3.42) does not apply, the quaternion voltage derivative can be rewritten according to (4.36). So the impedance must be computed in the sequence domain, rather than the phase domain. Making use of phasor as an auxiliary tool,

$$\underbrace{\begin{bmatrix} \hat{V}_a \\ \hat{V}_b \\ \hat{V}_c \end{bmatrix}}_{V_{abc}} = \underbrace{\begin{bmatrix} \hat{Z}_p & 0 & 0 \\ 0 & \hat{Z}_p & 0 \\ 0 & 0 & \hat{Z}_p \end{bmatrix}}_{Z_{abc}} \underbrace{\begin{bmatrix} \hat{I}_a \\ \hat{I}_b \\ \hat{I}_c \end{bmatrix}}_{I_{abc}} \quad (4.55)$$

$$\underbrace{(F^{-1}V_{abc})}_{V_{012}} = \underbrace{(F^{-1}Z_{abc}F)}_{Z_{012}} \underbrace{(F^{-1}I_{abc})}_{I_{012}} \quad (4.56)$$

$$V_{012} = Z_{012}I_{012}, \quad (4.57)$$

in which

$$Z_{012} = \begin{bmatrix} \hat{Z}_p & 0 & 0 \\ 0 & \hat{Z}_p & 0 \\ 0 & 0 & \hat{Z}_p \end{bmatrix}. \quad (4.58)$$

In this case, positive, negative and zero sequence impedances are equal to the phase impedance. The imaginary part of the complex impedance, its reactive part, is associated with the time derivative/integral of the voltage. Applying the derivatives of (4.36) each complex sequence impedance can be rewritten as a quaternion. Besides changing the imaginary unit j multiplying the reactances into the quaternion axis \mathbf{n} , there are also sign changes, accordingly to the sequence multiplying it. For example, if the impedance is being multiplied by the negative sequence, the imaginary unit is substituted by the negative of \mathbf{n} . So, it can be shown that voltage is

$$\mathbf{V} = \mathbf{Z}_0\mathbf{I}_0^+ + \mathbf{Z}_0^*\mathbf{I}_0^- + \mathbf{Z}_1\mathbf{I}_1 + \mathbf{Z}_2\mathbf{I}_2, \quad (4.59)$$

in which the quaternion impedances in the sequence domain are

$$\mathbf{Z}_1 = \mathbf{Z}_2^* = \mathbf{Z}_0 = \mathbf{Z} = \left[R + \mathbf{n} \left(wL - \frac{1}{wC} \right) \right]. \quad (4.60)$$

It is noteworthy that since the system has only three wires, the zero sequence current is always null.

A four-wire system can be generalized from a wye load with an impedance to the ground ($\hat{Z}_n = R_n + jX_n$). Considering a per phase complex impedance $\hat{Z}_p = R + jX$, the impedance matrix (Z_{abc}) is

$$Z_{abc} = \begin{bmatrix} \hat{Z}_p + \hat{Z}_n & \hat{Z}_n & \hat{Z}_n \\ \hat{Z}_n & \hat{Z}_p + \hat{Z}_n & \hat{Z}_n \\ \hat{Z}_n & \hat{Z}_n & \hat{Z}_p + \hat{Z}_n \end{bmatrix}. \quad (4.61)$$

Applying the Fortescue transformation,

$$Z_{012} = \begin{bmatrix} \hat{Z}_p + 3\hat{Z}_n & 0 & 0 \\ 0 & \hat{Z}_p & 0 \\ 0 & 0 & \hat{Z}_p \end{bmatrix}. \quad (4.62)$$

So, quaternion voltage is given by

$$\mathbf{V} = \mathbf{Z}_0 \mathbf{I}_0^+ + \mathbf{Z}_0^* \mathbf{I}_0^- + \mathbf{Z}_1 \mathbf{I}_1 + \mathbf{Z}_2 \mathbf{I}_2, \quad (4.63)$$

in which

$$\mathbf{Z}_0 = (R + 3R_n) + \mathbf{n}(X + 3X_n) \quad (4.64)$$

$$\mathbf{Z}_1 = \mathbf{Z}_2^* = R + \mathbf{n}X \quad (4.65)$$

A similar approach for the admittance can be developed and results are analogous. So, this will not be shown in this dissertation for the sake of simplicity.

4.2.2 With Mutual Coupling

As an outcome of (4.25) proposed in this dissertation, the mutual coupling can also be considered in the quaternion representation.

Consider a balanced load with a proper complex impedance denoted by $Z_p = R_p + jX_p$ and with mutual coupling denoted by $\hat{Z}_m = R_m + jX_m$. Fortescue symmetrical transformation can be applied to decouple the system. So, following the method applied in (4.55 through 4.57) and considering

$$Z_{abc} = \begin{bmatrix} \hat{Z}_p & \hat{Z}_m & \hat{Z}_m \\ \hat{Z}_m & \hat{Z}_p & \hat{Z}_m \\ \hat{Z}_m & \hat{Z}_m & \hat{Z}_p \end{bmatrix}, \quad (4.66)$$

then the sequence impedances are

$$Z_{012} = \begin{bmatrix} \hat{Z}_p + 2\hat{Z}_m & 0 & 0 \\ 0 & \hat{Z}_p - \hat{Z}_m & 0 \\ 0 & 0 & \hat{Z}_p - \hat{Z}_m \end{bmatrix}. \quad (4.67)$$

Expressing current as a combination of positive and negative sequences and applying (4.36), then the quaternion voltage can be expressed as

$$\mathbf{V} = [(R_p - R_m) + \mathbf{n}(X_p - X_m)] \mathbf{I}_1 + [(R_p - R_m) - \mathbf{n}(X_p - X_m)] \mathbf{I}_2. \quad (4.68)$$

The zero sequence is not considered due to the fact of the analysis being performed on a three-wire system. Nevertheless, a four-wire system can be considered by including this impedance in this last equation.

4.2.3 Unbalanced Impedance

Any unbalanced passive element can be represented by the $\mathbb{C}^{3 \times 3}$ impedance matrix

$$Z_{abc} = \begin{bmatrix} \hat{Z}_{aa} & \hat{Z}_{ab} & \hat{Z}_{ca} \\ \hat{Z}_{ab} & \hat{Z}_{bb} & \hat{Z}_{bc} \\ \hat{Z}_{ca} & \hat{Z}_{bc} & \hat{Z}_{cc} \end{bmatrix}, \quad (4.69)$$

in which \hat{Z}_{xx} is the proper impedance of phase ‘‘X’’, and \hat{Z}_{xy} is the mutual impedance between phases ‘‘X’’ and ‘‘Y’’. Since voltage and current can be unbalanced, the system will be investigated in the symmetrical sequences domain. So, the impedance matrix is now given by

$$Z_{012} = \begin{bmatrix} \hat{Z}_{00} & \hat{Z}_{01} & \hat{Z}_{02} \\ \hat{Z}_{10} & \hat{Z}_{11} & \hat{Z}_{12} \\ \hat{Z}_{20} & \hat{Z}_{21} & \hat{Z}_{22} \end{bmatrix}. \quad (4.70)$$

The expressions for each matrix term are not shown for the sake of simplicity. Notice that Z_{012} is not a symmetrical matrix like Z_{abc} . As previously discussed, each of this terms can have their equivalent in the quaternion domain by simply changing the imaginary unit for the quaternion plane direction of the term multiplying it. For example, the term \hat{Z}_{01} relates zero sequence voltage to the positive sequence current. Therefore, its quaternion version is given by

$$\mathbf{Z}_{01} = R_{01} + \mathbf{n}wX_{01}, \quad (4.71)$$

in which R and X are the resistive and reactive components, respectively. If the term \hat{Z}_{02} is considered, then it can be given by

$$\mathbf{Z}_{02} = R_{02} - \mathbf{n}wX_{02}. \quad (4.72)$$

Considering the aforementioned modifications, the quaternion impedance matrix is defined as

$$\mathbf{Z}_{012} = \begin{bmatrix} \mathbf{Z}_{00} & \mathbf{Z}_{01} & \mathbf{Z}_{02} \\ \mathbf{Z}_{10} & \mathbf{Z}_{11} & \mathbf{Z}_{12} \\ \mathbf{Z}_{20} & \mathbf{Z}_{21} & \mathbf{Z}_{22} \end{bmatrix}. \quad (4.73)$$

Differently from a balanced element, the off-diagonal elements may not be nil. This means that a positive sequence current can generate zero and/or negative sequences voltages and vice-versa. However, each element rotates in a different direction or plane. In other words, multiplying \mathbf{I}_1 by \mathbf{Z}_{01} generates a positive sequence voltage, rather than the expected zero sequence. Consequently, the system cannot be solved in the time domain. At least, not in the usual way.

As a workaround, the basis matrix

$$\mathbf{B} = \begin{bmatrix} \mathbf{n}_{\text{bal}} & 0 & 0 \\ 0 & \mathbf{q}_p & 0 \\ 0 & 0 & 1 \end{bmatrix} \quad (4.74)$$

can be employed to change the rotation of the sequence components in conjunction with a modified impedance given by

$$\mathbf{Z}_{\text{mod}} = \begin{bmatrix} \mathbf{Z}_{00} & \frac{\mathbf{Z}_{01}}{\sqrt{2}} & \frac{-\mathbf{q}_p \mathbf{Z}_{02}}{\sqrt{2}} \\ \sqrt{2} \mathbf{Z}_{10} & \mathbf{Z}_{11} & -\mathbf{q}_p \mathbf{Z}_{12} \\ \sqrt{2} \mathbf{q}_p \mathbf{Z}_{20} & \mathbf{q}_p \mathbf{Z}_{21} & \mathbf{Z}_{22} \end{bmatrix}. \quad (4.75)$$

After some algebraical manipulations, the quaternion voltage in terms of the system current is

$$\mathbf{V}_{012} = \left\{ \left[\mathbf{Z}_{\text{mod}} (\mathbf{I}_{012}^T \mathbf{B}^H)^T \right]^T \mathbf{B} \right\}^T, \quad (4.76)$$

with $\mathbf{V}_{012} = \left[\mathbf{V}_0^+ \quad \mathbf{V}_1 \quad \mathbf{V}_2 \right]^T$ and with \mathbf{I}_{012} defined likewise. The upper index H denotes the hermitian operation, which is achieved by a conjugation followed by a transposition. As \mathbf{V}_0 is composed of two rotating elements with equal magnitudes, only \mathbf{V}_0^+ is used for computations. And the quaternion voltage is obtained as

$$\mathbf{V} = \mathbf{V}_0^+ - (\mathbf{V}_0^+)^* + \mathbf{V}_1 + \mathbf{V}_2 \quad (4.77)$$

Given the system impedance and voltage, the current can be computed analogously using the admittance instead of the impedance.

It is noteworthy that this method allows to operate the system in the time domain rather than the frequency as it is usually performed with phasors. Although operating all phases simultaneously, each of the symmetrical components is solved separately. If the voltage is unbalanced, \mathbf{V}_{012} needs to be first estimated in order to apply this method. On the other hand, if the source is balanced, the voltage samples can be directly substituted in \mathbf{V}_{012} , eliminating the aforementioned estimation process.

4.3 Transmission lines

In this section, a quaternion model for transmission lines with and without mutual electrical coupling is proposed. It is worth emphasizing that the results presented in this section are an outcome of the proposed symmetrical components theory.

Consider the same system employed in section 4.2, but with a transmission line connecting the supply and the load, as shown in Figure 4.5. If the transmission line is balanced and perfectly transposed, its complex impedance matrix is equal to (4.66). in which \hat{Z}_p is the cable proper impedance, and \hat{Z}_m is the mutual impedance between cables. In order to decouple this system, the Fortescue transformation can be applied resulting in (4.67). The voltage drop over the line is equivalently to (4.63). Therefore, the quaternion impedance for a transmission line has been presented.

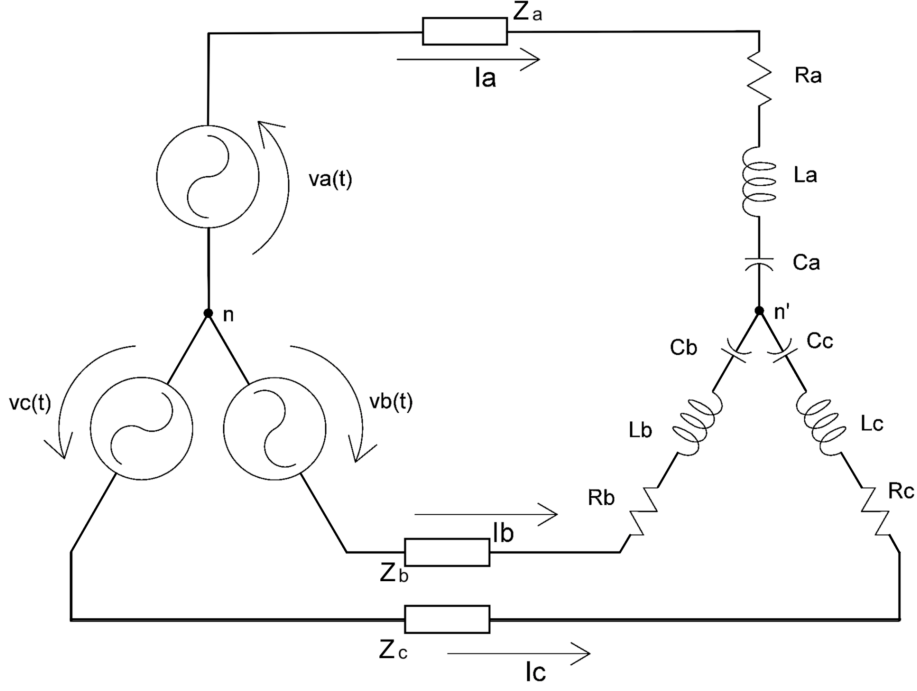


Figure 4.5: Three-phase system consisting of a source, a transmission line and a load.

4.4 Active, Reactive and Apparent Power

In this section, the quaternion power, as defined by [6, 41], is presented and discussed. Afterwards, a symmetrical decomposition of the power is proposed.

According to [6, 41], power is defined as

$$\mathbf{S}(t) = \mathbf{V}(t)\mathbf{I}^*(t). \quad (4.78)$$

Substituting the values of voltage (3.1) and current (3.5),

$$\mathbf{S}(t) = p_{abc}(t) + \mathbf{Q}(t), \quad (4.79)$$

in which the real part $p_{abc}(t)$ is the instantaneous active power given by

$$p_{abc}(t) = v_a i_a + v_b i_b + v_c i_c \quad (4.80)$$

and the vectorial part $\mathbf{Q}(t)$ is the quaternion instantaneous reactive power given by

$$\mathbf{Q}(t) = -\vec{\mathbf{U}} \times \vec{\mathbf{I}} = q_a \mathbf{x} + q_b \mathbf{y} + q_c \mathbf{z}, \quad (4.81)$$

$$q_a = v_c i_b - v_b i_c, \quad (4.82)$$

$$q_b = v_a i_c - v_c i_a, \quad (4.83)$$

$$q_c = v_b i_a - v_a i_b. \quad (4.84)$$

It is noteworthy that the proposed definition for the quaternion power employs the current conjugate, rather than the current itself employed in [37]. As a consequence, (4.81) is equivalent to

the negative of Peng's reactive power presented in [22]. This will be shown to be more appropriate in the following analysis.

Considering the RLC circuit from Figure 4.4, and substituting the voltage by (4.46),

$$\mathbf{S} = \mathbf{Z}\mathbf{I}\mathbf{I}^* \quad (4.85)$$

$$\mathbf{S} = \left[R + \mathbf{n} \left(wL - \frac{1}{wC} \right) \right] \mathbf{I}\mathbf{I}^*. \quad (4.86)$$

Applying the property (2.21), the power is

$$\mathbf{S} = (R|\mathbf{I}|^2) + \mathbf{n} \left[\left(wL - \frac{1}{wC} \right) |\mathbf{I}|^2 \right]. \quad (4.87)$$

It is observable that the reactive power is in the same direction of the impedance vectorial part, which corresponds to the reactance effects. This relation is equivalent to the existing in the phasorial domain. So, the predominance of capacitors or inductors is clearly shown through the direction of the quaternion reactive power. Nonetheless, the proposed definition is more appropriate than Nos'. Additionally, it gives a meaning to the reactive power direction that lacks in vectorial power theories, such as [8, 9, 22]. It is worth mentioning that this quantity accounts for any phenomena that displaces the quaternion current in relation to the voltage, for example any distortion that may occur.

The power norm will now be investigated and its relation to others theories will be discussed. Since the real and vectorial parts are orthogonal to each other,

$$|\mathbf{S}|^2 = p_{abc}^2 + |\mathbf{Q}|^2. \quad (4.88)$$

The power norm can be rewritten in terms of voltage and current norm, which are given by (3.74), as

$$|\mathbf{S}|(t) = |\mathbf{V}||\mathbf{I}|. \quad (4.89)$$

It is noteworthy that under unbalanced conditions, they present an oscillatory behaviour. So, power norm will behave likewise. If the apparent power is defined as the RMS value of this norm, then

$$S_Q = |\mathbf{S}|_{RMS} = \sqrt{\frac{1}{T} \int_0^T |\mathbf{S}|^2 dt} \quad (4.90)$$

$$= \sqrt{\frac{1}{T} \int_0^T |\mathbf{V}|^2 |\mathbf{I}|^2 dt} \quad (4.91)$$

$$= \sqrt{\frac{1}{T} \int_0^T [|\mathbf{V}|_{RMS}^2 + |\mathbf{V}|_{osc}^2 \cos(2wt + \phi_{osc})] [|\mathbf{I}|_{RMS}^2 + |\mathbf{I}|_{osc}^2 \cos(2wt + \phi_{I,osc})] dt}. \quad (4.92)$$

The mean value of a cosine harmonic is null, so the integration of the product of $|\mathbf{V}|_{RMS}$ and $|\mathbf{I}|_{osc}$ is null. Therefore, the apparent power is rewritten as

$$S_Q = \sqrt{\frac{1}{T} \int_0^T [|\mathbf{V}|_{RMS}^2 |\mathbf{I}|_{RMS}^2 + |\mathbf{V}|_{osc}^2 |\mathbf{I}|_{osc}^2 \cos(2wt + \phi_{osc}) \cos(2wt + \phi_{I,osc})] dt} \quad (4.93)$$

and applying the property

$$\cos(a)\cos(b) = \frac{1}{2} [\cos(a+b) + \cos(a-b)] \quad (4.94)$$

with $a = 2wt + \phi_{osc}$ and $b = 2wt + \phi_{I,osc}$

$$S_Q = \sqrt{\frac{1}{T} \int_0^T \left\{ |\mathbf{V}|_{RMS}^2 |\mathbf{I}|_{RMS}^2 + |\mathbf{V}|_{osc}^2 |\mathbf{I}|_{osc}^2 \frac{1}{2} [\cos(\phi_{osc} - \phi_{I,osc}) + \cos(4wt + \phi_{osc}\phi_{I,osc})] \right\} dt} \quad (4.95)$$

$$= \sqrt{\left[|\mathbf{V}|_{RMS}^2 |\mathbf{I}|_{RMS}^2 + \frac{1}{2} |\mathbf{V}|_{osc}^2 |\mathbf{I}|_{osc}^2 \cos(\phi_{osc} - \phi_{I,osc}) \right]} \quad (4.96)$$

Under unbalanced voltage conditions, $|\mathbf{V}|_{osc}$ is not zero. Thus, $|\mathbf{I}|_{osc}$ may not be zero, even for a balanced resistive load. If the load is unbalanced, then the currents generated are likewise. Therefore, the proposed apparent power S_Q accounts for both supply and load unbalance.

It is noteworthy that, under conditions that generate a null oscillatory norm component, this definition is equivalent to Buchholz's (S_B) and that was extended by Czarnecki (S_C) in [13]. Czarnecki's definition is based on vectors inner product. However, it can be rewritten in the quaternion theory because quaternions are used for representing the same three-dimensional, or three-phase, voltage vector. It is given by

$$S_C = |\mathbf{V}|_{RMS} |\mathbf{I}|_{RMS}. \quad (4.97)$$

The main difference between these two definitions is that in Czarnecki's the RMS is computed before the voltage and current product and in the proposed one the RMS is computed after their product. It is noteworthy that the RMS values of three-phase voltage and current are not influenced by phase unbalance as shown in (3.73). So, S_Q , in contrast to S_C , accounts for any given unbalance. Whether or not the angle unbalance should be accounted in the apparent power is still under investigation.

Power can also be computed in terms of symmetrical components as follows

$$\mathbf{S} = (\mathbf{V}_0^+ + \mathbf{V}_0^- + \mathbf{V}_1 + \mathbf{V}_2) (\mathbf{I}_0^+ + \mathbf{I}_0^- + \mathbf{I}_1 + \mathbf{I}_2)^* \quad (4.98)$$

$$= \mathbf{V}_1 \mathbf{I}_1^* + \mathbf{S}_U, \quad (4.99)$$

in which the first term of the right hand side is the quaternion power for balanced conditions and the last term is the unbalanced power.

It can be shown that \mathbf{S}_U is not decoupled. In other words, a given sequence voltage multiplies a different sequence current. This happens even for a circuit that can be decoupled. In the phasorial theory, however, power is expected to be the sum of each individual sequence contribution, without these crossed terms.

The real part of \mathbf{S}_U represents an active power $p_u(t)$, and it is given by the inner products of voltage and current elements (except for the term $\mathbf{V}_1 \cdot \mathbf{I}_1$). Since \mathbf{V}_1 and \mathbf{V}_2 are on the same plane, which is perpendicular to \mathbf{V}_0 , then

$$p_u(t) = p_0(t) + \mathbf{V}_1 \cdot \mathbf{I}_2^* + \mathbf{V}_2 \cdot \mathbf{I}_1^* + p_2(t), \quad (4.100)$$

in which $p_0(t)$ and $p_2(t)$ are the zero and negative sequence active powers, respectively. It is noteworthy that $\mathbf{V}_1\mathbf{I}_2$ and $\mathbf{V}_2\mathbf{I}_1$ have nil mean value. So, these terms are not responsible for load energy consumption. Actually, they represent only a power exchange between source and load.

The instantaneous active power can be related to Czarnecki's CPC power theory, first presented in [13] and later discussed in [55]. As shown in [55], in three-wire systems, $p(t)$ is reduced into

$$p(t) = P + D \cos(2\omega t + \varphi), \quad (4.101)$$

in which D is the Czarnecki's unbalanced power and φ is function of the ratio between positive and negatives components. It should be highlighted that the CPC power theory does not clarify the relationship of D and the symmetrical components. This relation is first presented in this dissertation, and it was possible due to the geometrical visualization provided by quaternions. The term P is composed of the active power, and it is responsible for the energy consumption. The term D corresponds to the unbalanced terms $\mathbf{V}_1\mathbf{I}_2$ and $\mathbf{V}_2\mathbf{I}_1$.

The vectorial part of \mathbf{S}_U accounts only the cross products terms. The positive and negatives sequence interactions outputs a quaternion parallel to \mathbf{n}_{bal} . On the other hand, the products involving the zero sequence are perpendicular to \mathbf{n}_{bal} , as shown on (4.102) through (4.104).

$$\mathbf{Q} = \mathbf{Q}_1 + \underbrace{\mathbf{Q}_{u0} + \mathbf{Q}_{u2}}_{\mathbf{Q}_u} \quad (4.102)$$

$$\mathbf{Q}_{u0} = \mathbf{V}_0 \times (\mathbf{I}_1 + \mathbf{I}_2) + (\mathbf{V}_1 + \mathbf{V}_2) \times \mathbf{I}_0 \underbrace{\mathbf{V}_0 \times (\mathbf{I}_1 + \mathbf{I}_2) + (\mathbf{V}_1 + \mathbf{V}_2) \times \mathbf{I}_0}_{\text{Term perpendicular to } \mathbf{n}_{\text{bal}}} \quad (4.103)$$

$$\mathbf{Q}_{u2} = \mathbf{V}_1 \times \mathbf{I}_2^* + \mathbf{V}_2 \times (\mathbf{I}_1^* + \mathbf{I}_2^*) \underbrace{\mathbf{V}_1 \times \mathbf{I}_2^* + \mathbf{V}_2 \times (\mathbf{I}_1^* + \mathbf{I}_2^*)}_{\text{Term parallel to } \mathbf{n}_{\text{bal}}} \quad (4.104)$$

Therefore, the direction of \mathbf{Q} indicates the system unbalance.

In summary, the quaternion representation allows to portray the instantaneous power as well as i) the active, ii) the reactive, and iii) the unbalanced power. Additionally, these terms are associated with the i) real axis, ii) \mathbf{n}_{bal} , and iii) $(\mathbf{q}_p, \mathbf{q}_n)$ plane. So, they are orthogonal to each other. This is expected to simplify the process of filtering out these elements.

Chapter 5

Signal Transformation

This chapter will discuss Clarke and Park transformations in a geometrical framework. Afterwards, a quaternion implementation of both of them is proposed.

In the study of electrical machines, transformations are usually applied in order to simplify mathematical operations [56]. As previously discussed, they can also be applied to map the three-phase voltage into a bi-dimensional complex signal, which can be processed by means of complex algebra algorithms [29–32].

The study of electrical machines needs a geometrical perspective due to the machine construction aspects. As a result, the Clarke transformation was developed for a two-dimensional (\mathbb{R}^2) analysis [57]. However, this specific \mathbb{R}^2 analysis can be considered as one among other possible approaches. Gataric in [58], extended this cartesian analysis for polyphase systems by using the three-dimensional space (\mathbb{R}^3). As a result, both Clarke and Park transformations can be interpreted in the \mathbb{R}^3 , as presented in [53].

Three-phase voltage without zero sequence component is within the plane that is orthogonal to \mathbf{n}_{bal} , as discussed in sections 3.1 and 4.1. Moreover, section 4.1 proved that quaternion zero sequence component is parallel to \mathbf{n}_{bal} and perpendicular to the QVL balanced plane. It can be shown that the Clarke transformation is equivalent to rotating the reference frame to lie within this plane. In other words, \mathbf{x} , \mathbf{y} and \mathbf{z} are mapped to \mathbf{q}_p , \mathbf{q}_n and \mathbf{n}_{bal} .

This equivalence will be shown step-by-step based on [53]. The initial reference frame is illustrated in Figure 5.1, extracted from [53]. The axis nomenclature in the figure are the same used in the reference. They are equivalent to the \mathbf{x} , \mathbf{y} and \mathbf{z} used in this dissertation. Making \mathbf{z} or C orthogonal to the QVL balanced plane is achieved by moving C to the corner of the box of Figure 5.1. This can be performed in terms of elementary rotations¹.

Rotating C clockwise around A by 45° yields Figure 5.2, extracted from [53]. This can be

¹These are said to be elementary because they are executed around one of the system coordinates axes.

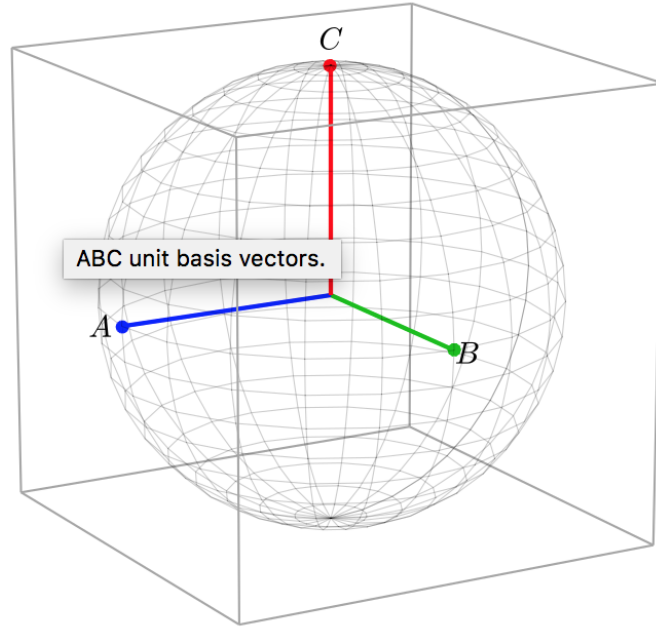


Figure 5.1: Initial reference frame before Clarke Transformation.

achieved through the following matrix

$$K1 = \begin{bmatrix} 1 & 0 & 0 \\ 0 & \cos(-45^\circ) & \sin(-45^\circ) \\ 0 & -\sin(-45^\circ) & \cos(-45^\circ) \end{bmatrix}. \quad (5.1)$$

Rotating the AYC' frame counter clockwise around Y by $35,26^\circ$ yields the Clarke reference frame shown in Figure 5.3, extracted from [53]. This is achieved by

$$K2 = \begin{bmatrix} \cos(35,26^\circ) & 0 & -\sin(35,26^\circ) \\ 0 & 1 & 0 \\ \sin(35,26^\circ) & 0 & \cos(35,26^\circ) \end{bmatrix}. \quad (5.2)$$

So, the equivalent matrix is obtained by the product $T_C = (K2)(K1)$

$$T_C = \sqrt{\frac{2}{3}} \begin{bmatrix} 1 & -\frac{1}{2} & -\frac{1}{2} \\ 0 & \frac{\sqrt{3}}{2} & -\frac{\sqrt{3}}{2} \\ \frac{1}{\sqrt{2}} & \frac{1}{\sqrt{2}} & \frac{1}{\sqrt{2}} \end{bmatrix}. \quad (5.3)$$

It is noteworthy that (5.3) is equivalent to the Clarke power invariant transformation matrix, as it was the objective. Additionally, applying this to the frame \mathbf{x} , \mathbf{y} and \mathbf{z} outputs \mathbf{q}_p , \mathbf{q}_n and \mathbf{n}_{bal} ,

$$\sqrt{\frac{2}{3}} \begin{bmatrix} 1 & -\frac{1}{2} & -\frac{1}{2} \\ 0 & \frac{\sqrt{3}}{2} & -\frac{\sqrt{3}}{2} \\ \frac{1}{\sqrt{2}} & \frac{1}{\sqrt{2}} & \frac{1}{\sqrt{2}} \end{bmatrix} \begin{bmatrix} \mathbf{x} \\ \mathbf{y} \\ \mathbf{z} \end{bmatrix} = \begin{bmatrix} \frac{2\mathbf{x}-\mathbf{y}-\mathbf{z}}{\sqrt{6}} \\ \frac{\mathbf{y}-\mathbf{z}}{\sqrt{2}} \\ \frac{\mathbf{x}+\mathbf{y}+\mathbf{z}}{\sqrt{3}} \end{bmatrix} = \begin{bmatrix} \mathbf{q}_p \\ \mathbf{q}_n \\ \mathbf{n}_{bal} \end{bmatrix}. \quad (5.4)$$

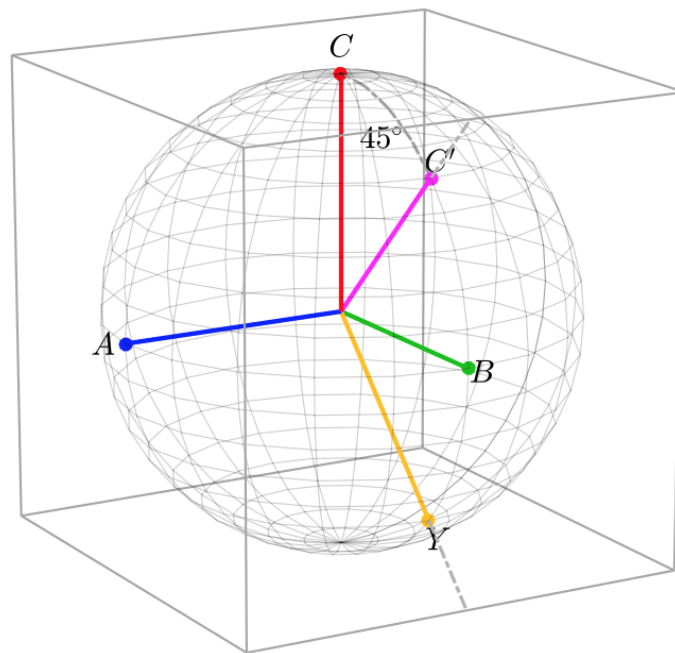


Figure 5.2: Reference frame after a clockwise rotation of C around A by 45° .

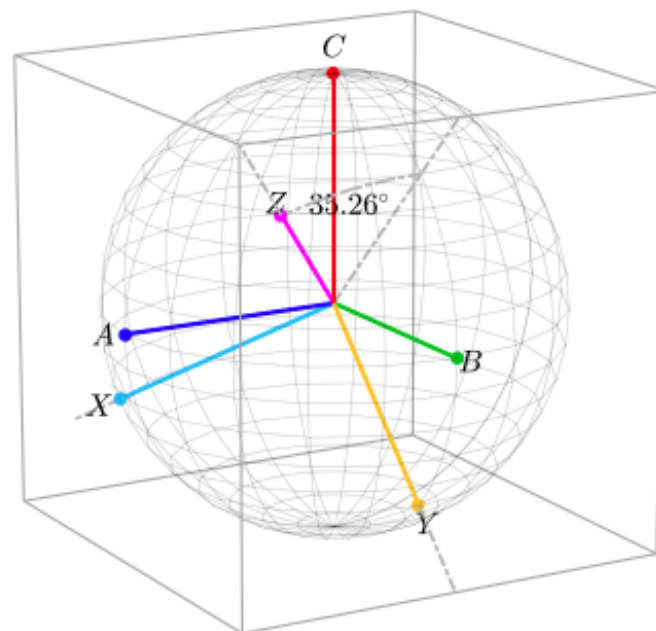


Figure 5.3: Resulting reference frame after Clarke transformation.

Therefore it is proven that the Clarke transformation is equivalent to translating the reference frame to the QVL plane.

Since the Clarke transformation can be interpreted as a rotation, it can be performed in the quaternion domain. In order to do so, the equivalent axis and angle of rotation must be determined. It is worth mentioning that there are an infinite number of transformations that maps the \mathbf{z} axis to be perpendicular to the QVL balanced plane, and Clarke is one of them.

The axis of rotation ($d \in \mathbb{R}^3$) can be computed as the eigenvector of the rotation matrix associated with the eigenvalue of 1, accordingly to (2.60). In this case it is

$$d = \text{vec}(\mathbf{d}) \approx \begin{bmatrix} 0,7693 & -0,5903 & 0,2445 \end{bmatrix}. \quad (5.5)$$

The angle of rotation, given by (2.62), is

$$\theta_r \approx 56,60^\circ. \quad (5.6)$$

In the quaternion domain, the reference change can be achieved through the product

$$\text{vec}^{-1}(T_C(\mathbf{v})) = \mathbf{R}_{fC} \mathbf{v} \mathbf{R}_{fC}^{-1}, \quad (5.7)$$

in which \mathbf{v} represents an arbitrary axis and

$$\mathbf{R}_{fC} = e^{\mathbf{d} \frac{\theta_r}{2}}. \quad (5.8)$$

In order to confirm these results, this quaternion rotation can be applied to each axis separately and then check if they are correctly mapped to \mathbf{q}_p , \mathbf{q}_n and \mathbf{n}_{bal} . These computations were made in Matlab and are not presented here for the sake of simplicity. The results obtained were

$$\mathbf{R}_{fC} \mathbf{x} \mathbf{R}_{fC}^{-1} = \mathbf{q}_p \quad (5.9)$$

$$\mathbf{R}_{fC} \mathbf{y} \mathbf{R}_{fC}^{-1} = \mathbf{q}_n \quad (5.10)$$

$$\mathbf{R}_{fC} \mathbf{z} \mathbf{R}_{fC}^{-1} = \mathbf{n}_{bal} \quad (5.11)$$

as it was expected. However, the α and β components are obtained by applying this transformation on the quaternion voltage, rather than the reference frame itself.

Rotating the reference while keeping a vector still is equivalent to rotating the vector in the opposite direction. This is shown in the example 4.

Example 4 [*Difference between reference and vector rotation*]

Consider rotating the vector $\mathbf{v} = \mathbf{x}$ around \mathbf{y} by 90° . The result is $\mathbf{v}_{rot} = -\mathbf{z}$. On the other hand, if the reference is rotated around \mathbf{y} by the same angle, then the new reference is given by $\mathbf{x}_{rot} = -\mathbf{z}$, $\mathbf{y}_{rot} = \mathbf{y}$ and $\mathbf{z}_{rot} = \mathbf{x}$. The original vector is then given by $\mathbf{v} = \mathbf{1x} = \mathbf{z}_{rot}$. Table 5.1 shows this difference. Therefore, in order to achieve an equivalence between these rotations, the angle employed must have its sign changed.

Table 5.1: Comparison of vector and reference rotation around \mathbf{y} by 90° .

Original vector	Rotated vector	Rotated reference
$\mathbf{v} = \mathbf{x}$	$\mathbf{v}_{\text{rot}} = -\mathbf{z}$	$\mathbf{v} = \mathbf{z}_{\text{rot}}$

So, in order to apply the Clarke transformation via quaternions, the angle of rotation employed must be the negative of the one found in (5.6). Therefore, the α and β components are

$$\mathbf{V}_{\alpha\beta 0} = \text{vec}^{-1} \left(\begin{bmatrix} 0 & V_\alpha & V_\beta & V_0 \end{bmatrix} \right) = \mathbf{R}_C \mathbf{V} \mathbf{R}_C^{-1}, \quad (5.12)$$

in which \mathbf{R}_C is name the quaternion Clarke rotational and is given by

$$\mathbf{R}_C = \mathbf{R}_{fC}^*. \quad (5.13)$$

Since there are two ways of computing this transformation, it is important to know which method is more computationally efficient. Both methods were implemented in Matlab and compared by the method applied for computing the QVL normal quaternion \mathbf{n} in section 3.1. For more details, reader is referred to the code used, which is attached in the Appendix II.

Figure 5.4 presents a box plot for the computational time demanded for each method. The red line shows the mean value. The lower and upper part of the body represents the 25th and 75th percentil limits, respectively. The whisker represent the maximum and minimum values. The outliers have been removed for a better visualization. The quaternion method demanded an average computational time approximately six times higher than the matrix implementation, $2,4 \cdot 10^{-5}$ s and $0,4 \cdot 10^{-5}$ s, respectively. Additionally, the former presented a higher body interval. Although the quaternion method performed poorly, in terms of computation time, it requires only three elements stored (two for the axis of rotation and one for the angle) instead of the 9 elements in the matrix implementation. Figure 5.5 shows that the cumulative average for the demanded computational time in the quaternion implementation approaches smoothly and stabilizes around the time value obtained. Therefore, the number of conditions simulated has been shown to be enough for trustworthy results. Due to the large amount of data, the abscissa has been plotted in a log scale for better visualization. This same analysis was repeated for its classical version and results were analogous.

The Park transformation, known as DQ0, is also very important for electrical machine analysis [57]. It is usual to think of it as a change from a stationary reference frame to a non-stationary one in the two dimensional space. The angular speed of the new coordinate system is considered equal to the synchronous speed of the machine under analysis. However, this can be interpreted in the three-dimensional space, likewise. It is observable that it can be achieved through two subsequent

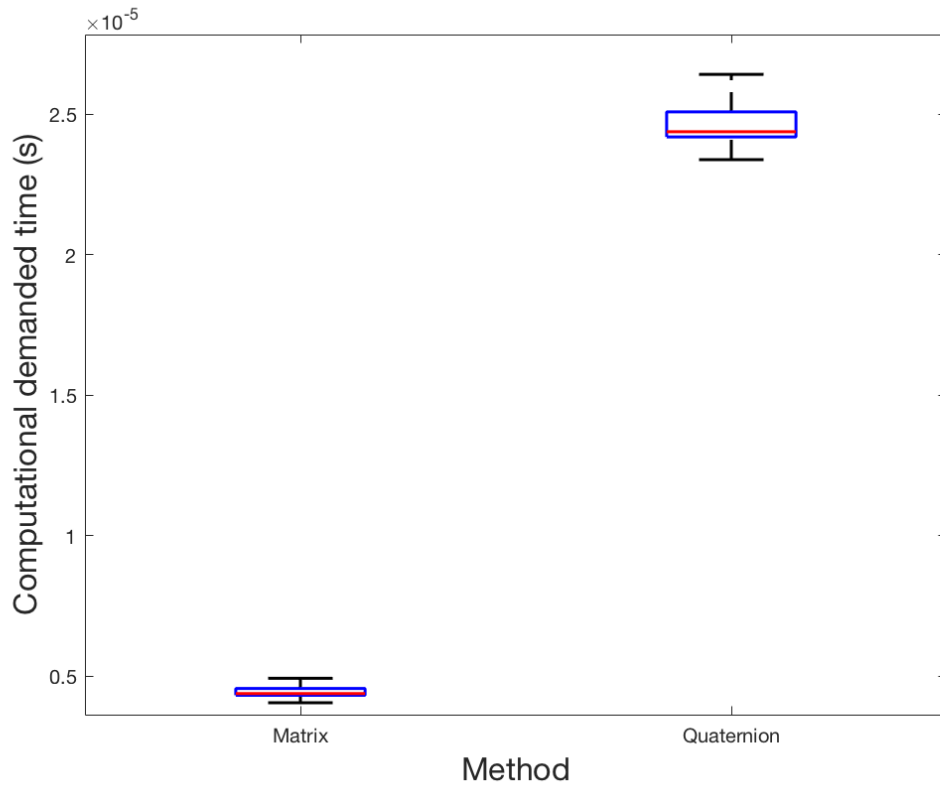


Figure 5.4: Comparison of the Clarke transformation implemented via matrix and via quaternions.

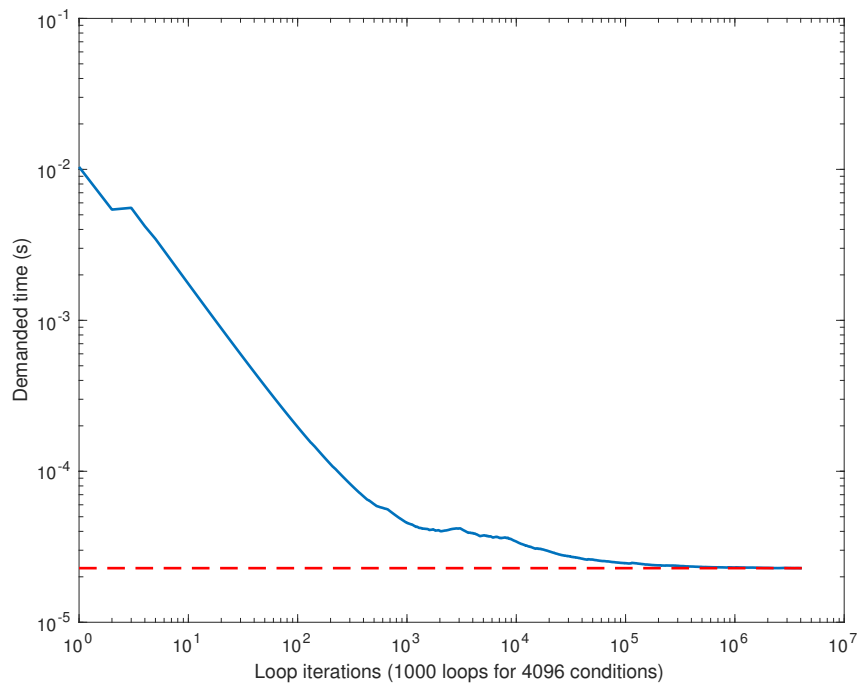


Figure 5.5: Cumulative average for the demanded computational time of the Clarke quaternion implementation. The red dashed line indicates the final average value obtained.

transformations given by

$$T_P = \underbrace{\begin{bmatrix} \cos(\theta) & \sin(\theta) & 0 \\ -\sin(\theta) & \cos(\theta) & 0 \\ 0 & 0 & 1 \end{bmatrix}}_{K_P} \underbrace{\sqrt{\frac{2}{3}} \begin{bmatrix} 1 & -\frac{1}{2} & -\frac{1}{2} \\ 0 & \frac{\sqrt{3}}{2} & -\frac{\sqrt{3}}{2} \\ \frac{1}{\sqrt{2}} & \frac{1}{\sqrt{2}} & \frac{1}{\sqrt{2}} \end{bmatrix}}_{T_C} \quad (5.14)$$

$$= \sqrt{\frac{2}{3}} \begin{bmatrix} \cos(\theta) & \cos(\theta - 120^\circ) & \cos(\theta + 120^\circ) \\ -\sin(\theta) & -\sin(\theta - 120^\circ) & -\sin(\theta + 120^\circ) \\ \frac{1}{\sqrt{2}} & \frac{1}{\sqrt{2}} & \frac{1}{\sqrt{2}} \end{bmatrix}, \quad (5.15)$$

in which T_P is the Park power invariant matrix. It is worth mentioning that K_P represents a rotation around the “z” axis, that is equivalent to the quaternion \mathbf{z} . Since it is performed after the Clark transformation, the rotation actually occurs around the vector orthogonal to the QVL balanced plane. In other words and using the quaternion notation, K_P is equivalent to

$$\mathbf{R}_{[K_P]} = e^{\mathbf{z}\frac{\theta}{2}}. \quad (5.16)$$

As previously mentioned, the angular speed used is equal to the synchronous. So, the angle θ is substituted by $\theta = wt$, in which w is the electrical angular frequency. Similarly to (5.12), the DQ0 transformation can be achieved via quaternions, regarding that the voltages are being rotated instead of the reference, *i.e.*

$$\mathbf{V}_{dq0} = \text{vec}^{-1} \left(\begin{bmatrix} 0 & V_d & V_q & V_0 \end{bmatrix} \right) = \mathbf{R}_{[K_P]}^{-1} \mathbf{R}_{fC}^{-1} \mathbf{V} \mathbf{R}_{fC} \mathbf{R}_{[K_P]}. \quad (5.17)$$

With some algebraic effort, it can be shown that the Park transformation axis and angle of rotation are time varying. So, although it is possible to achieve a more compact equation instead of (5.17), this will not be done for the sake of simplicity.

Both methods were implemented on Matlab, using the code in Appendix III, and the demanded computational time for each of them is compared, as shown in Figure 5.6. For this purpose, the Monte Carlo simulation previously discussed was run. It is noteworthy that the average demanded time via quaternion is approximately 4 times faster and its variance is 5,3 times lower. Moreover, this implementation requires storing 6 values (two for \mathbf{R}_{fC} axis, 1 for its angle, and likewise for $\mathbf{R}_{[K_P]}$) instead of the 9 required in (5.15). Figure 5.7 shows that the cumulative average for the demanded computational time in the quaternion implementation approaches smoothly and stabilizes around the time value obtained. Therefore, the number of conditions simulated has been shown to be enough for trustworthy results. Due to the large amount of data, the abscissa has been plotted in a log scale for better visualization. This same analysis was repeated for its classical version and results were analogous.

This chapter discussed the application of quaternions to perform Clarke and Park transformations, which are typical in the analysis of electrical machines. It has been shown that in both cases, the quaternion version is more efficient from the storage perspective because less variables are needed. For the Park transform, it performed approximately 3,6 times faster than the matrix version. Therefore, application of this novel implementation on control algorithms is suggested for future research.

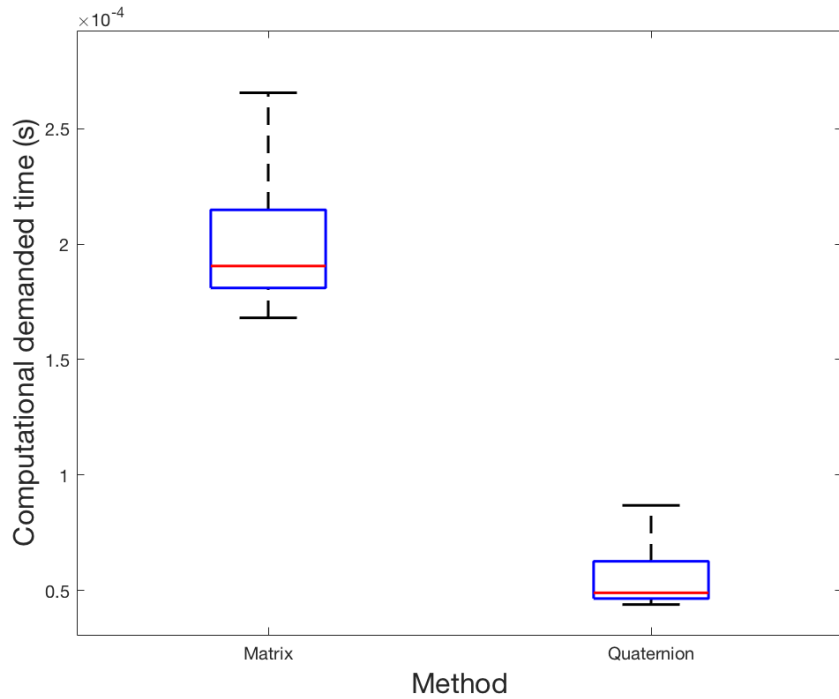


Figure 5.6: Comparison of the Park transformation implemented via matrix and via quaternions.

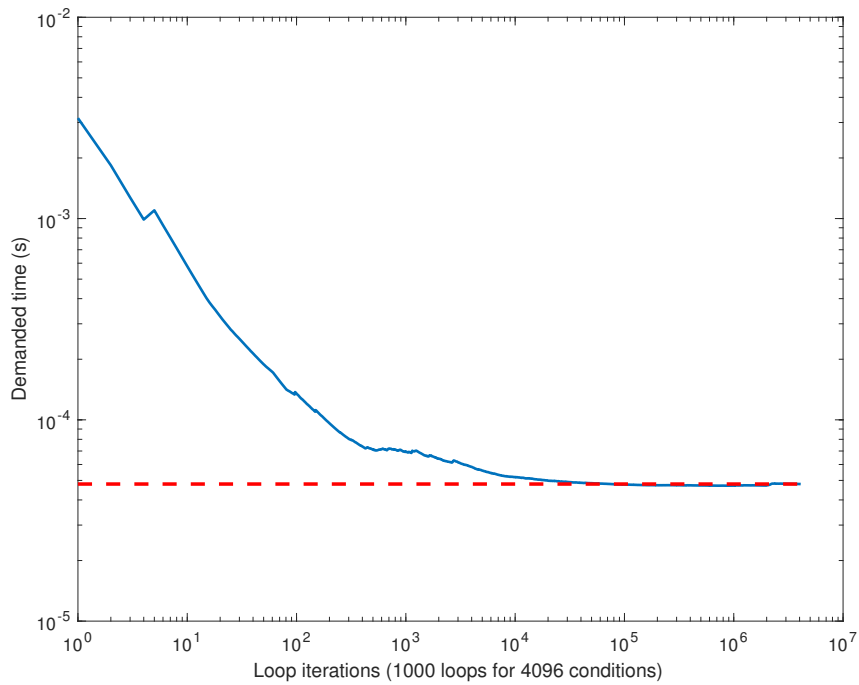


Figure 5.7: Cumulative average for the demanded computational time of the Park quaternion implementation. The red dashed line indicates the final average value obtained.

Chapter 6

Conclusions

This dissertation addressed the representation of a three-phase power system in the Hamilton number system \mathbb{H} instead of phasors. The objectives were to i) define voltage, current, passive elements and power as quaternions, ii) propose a novel symmetrical components theory, iii) provide a quaternion implementation of Clarke and Park transformations, and iv) indicate possible applications in up to date researching problems.

Definitions of voltage and current proposed in [36,38] were investigated with a geometrical point of view. It was observed that the quaternion voltage and current locus, QVL and QCL, respectively conveys steady state information about the system. This representation is not as compact as the phasorial one, because an additional real element is needed, which does not contribute with new information. Nonetheless, it offers a wide range of quantities that were shown to be related to the voltage unbalance. Therefore, they may be employed for quantifying this phenomenon. So, as a future research, it is suggested to investigate the relation of these quantities to the physical impacts on an induction motor and then compare it to the VUF. The methodology employed can also be repeated to characterize the geometrical aspects of the flux in usual electrical machines. Finally, it was shown that if the stator windings are disposed perpendicular to each other, then the total amount of rotating flux is higher because no components cancel out. So, a new type of electrical machine can be developed in the future.

Next, a novel quaternion symmetrical component decomposition was proposed. In contrast to Gou's definition [33], it was shown to be equivalent to Fortescue's theory. Additionally, it made possible to map derivatives and integrals into products, thus enabling a generalized three phase impedance definition. It is noteworthy that, in this new version, the components are represented in the time domain, rather than the frequency domain as in its traditional version. As a consequence, a linear state space model was achieved. Applying it to the dynamic estimation of the sequence components magnitudes and phases is suggested for future research. With these components, the phasors can be indirectly estimated. The usage of the model for harmonics quantification and for electrical frequency determination is also suggested for further research.

As discussed in the author's previous works [6,41], the quaternion theory allows to represent three phase quantities in one mathematical entity. Moreover, currents can be computed in the

time domain without solving differential equations. Exploring this characteristic for transient studies is also suggested for future investigation.

Afterwards, the instantaneous power as defined in [6,41] was investigated. It was shown that this definition allows to explain the reactive power direction. Hence, it is more appropriate than those based solely on three-dimensional temporal vector such as Peng's presented in [22]. An apparent power was proposed as the RMS value of the power norm. The differences between this quantity and the one resulting from Czarnecki's definition [13] were shown. A discussion on whether or not the former is more appropriate than the latter is suggested for future investigations. It was also shown that the unbalanced power is not decoupled, even for decoupled systems. This means that different components interact producing and/or absorbing power. For example, there are power terms originated from positive sequence voltage multiplying negative sequence current. With the phasorial theory, this phenomenon cannot be observed. Therefore, this is an advantage of quaternion representation. Additionally, active, reactive and unbalanced power are represented orthogonally.

In the last section of chapter 4, Clarke and Park transformations were investigated. A geometrical interpretation of both of them was presented based on [53]. Then, an equivalent quaternion implementation is proposed. It required only three and six variables, for Clarke and Park respectively, instead of the nine required in their classical matrix version. Although the quaternion required a longer computational time for the Clarke implementation, it was approximately 3,6 times faster in the case of the Park algorithm. Therefore, further investigations on this Park implementation, and its possible applications are suggested as research topics.

In summary, this dissertation consolidated the electrical circuit theory based on the hyper-complex non-commutative Hamilton algebra. The main contributions were the generalization of the quaternion impedance, the development of a novel symmetrical components theory and a new implementation of Clarke and Park transformations. As a consequence, estimation of electrical voltage and/or current parameters, such as frequency, magnitude and phase, are suggested for future research. Applications for the novel Park transform are also indicated as a feasible and required investigation.

Bibliography

- [1] IEEE. *IEEE Standard Definitions for the Measurement of Electric Power Quantities Under Sinusoidal, Nonsinusoidal, Balanced, or Unbalanced Conditions*. 2010. 1–50 p.
- [2] STEINMETZ, C. P.; KAISER, G. Does phase displacement occur in the current of electric arcs? (Translation by G. Kaiser). *ETZ*, v. 587, p. 1–3, 1892. Disponível em: <<http://arxiv.org/abs/1602.06868>>.
- [3] CZARNECKI, L. S. Energy flow and power phenomena in electrical circuits: Illusions and reality. *Electrical Engineering*, v. 82, n. 3, p. 119–126, 2000. ISSN 09487921.
- [4] EMANUEL, A. E. Apparent and reactive powers in three-phase systems: In search of a physical meaning and a better resolution. *European Transactions on Electrical Power*, Wiley-Blackwell, v. 3, n. 1, p. 7–14, sep 2007. ISSN 1430144X. Disponível em: <<http://doi.wiley.com/10.1002/etep.4450030103>>.
- [5] EMANUEL, A. E. On the definition of power factor and apparent power in unbalanced polyphase circuits with sinusoidal voltage and currents. *IEEE Transactions on Power Delivery*, v. 8, n. 3, p. 841–852, 1993. ISSN 19374208.
- [6] BRASIL, V. P. Undergraduate Conclusion Project, *AVALIAÇÃO DE GRANDEZAS ELÉTRICAS EM DIFERENTES REPRESENTAÇÕES*. 2017. 66 p.
- [7] USTARIZ, A. J.; CANO, E. A.; TACCA, H. E. Evaluación, Interpretación y Visualización de la Potencia Instantánea en Sistemas Eléctricos. In: *V Simposio Internacional sobre Calidad de la Energía Eléctrica*. [S.l.: s.n.], 2009. p. 7.
- [8] AKAGI, H.; KANAZAWA, Y.; NABAE, A. Instantaneous reactive power compensators comprising switching devices without energy storage components. *IEEE Transactions on industry applications*, IEEE, n. 3, p. 625–630, 1984.
- [9] AKAGI, H.; WATANABE, E. H.; AREDES, M. *Instantaneous Power Theory and Applications to Power Conditioning*. Hoboken, NJ, USA: John Wiley & Sons, Inc., 2007. 41–107 p. ISBN 9780470118931. Disponível em: <<http://doi.wiley.com/10.1002/9781119307181.ch2> <http://dx.doi.org/10.1002/9780470118931.ch3>>.
- [10] BUCHHOLZ, F. Die drehstrom-scheinleistung bei ungleichmassiger belastung der drei zweige. *Licht und Kraft*, v. 2, p. 9–11, 1922.

- [11] BUDEANU, C. I. Puissances réactives et fictives. Institut Romain de l'Energie. Bucharest. *Romania*, 1927.
- [12] CZARNECKI, L. S. Why the power theory has a limited contribution to studies on the supply and loading quality? In: *Proceedings of International Conference on Harmonics and Quality of Power, ICHQP*. [S.l.: s.n.], 2018. v. 2018-May, p. 1–6. ISBN 9781538605172. ISSN 21640610.
- [13] CZARNECKI, L. S. Orthogonal decomposition of the currents in a 3-phase nonlinear asymmetrical circuit with a nonsinusoidal voltage source. *IEEE Transactions on Instrumentation and Measurement*, IEEE, v. 37, n. 1, p. 30–34, 1988.
- [14] EMANUEL, A. E. The Buchholz-Goodhue apparent power definition: The practical approach for nonsinusoidal and unbalanced systems. *IEEE Transactions on Power Delivery*, v. 13, n. 2, p. 344–348, 1998. ISSN 08858977.
- [15] FRIZE, S. Active reactive and apparent power in circuits with nonsinusoidal voltage and current. *Elektrotechnische Zeitschrift*, v. 53, n. 25, p. 596–599, 1932.
- [16] JELTSEMA, D.; VOSS, T.; MALA, H. Physical vs economical power resolutions based on energy flow extrema. In: *Proceedings of International Conference on Harmonics and Quality of Power, ICHQP*. [S.l.: s.n.], 2018. v. 2018-May, p. 1–6. ISBN 9781538605172. ISSN 21640610.
- [17] MENTI, A.; ZACHARIAS, T.; MILIAS-ARGITIS, J. Geometric algebra: A powerful tool for representing power under nonsinusoidal conditions. *IEEE Transactions on Circuits and Systems I: Regular Papers*, v. 54, n. 3, p. 601–609, 2007. ISSN 10577122.
- [18] VLADIMIRTERZIJA, V.; LAZAREVIC, Z.; POPOV, M. Active and reactive power metering in non-sinusoidal conditions using newton type algorithm. *International Conference on ...*, v. 1, n. 1, p. 2–6, 1997. Disponible en: <<http://www.icrepq.com/full-paper-icrep/265-terzija.pdf>>.
- [19] DAI, X.; LIU, G.; GRETSCH, R. Generalized theory of instantaneous reactive quantity for multiphase power system. *IEEE Transactions on Power Delivery*, IEEE, v. 19, n. 3, p. 965–972, 2004. ISSN 08858977.
- [20] LEV-ARI, H.; STANKOVIĆ, A. M. Instantaneous power quantities in polyphase systems - A geometric algebra approach. *2009 IEEE Energy Conversion Congress and Exposition, ECCE 2009*, p. 592–596, 2009.
- [21] NOS, O. V.; DUDIN, A.; PETZOLDT, J. The Instantaneous Power Quaternion of The Three-Phase Electric Circuit With Linear Load. In: *17th INTERNATIONAL CONFERENCE ON MICRO/NANOTECHNOLOGIES AND ELECTRON DEVICES EDM 2016*. [S.l.: s.n.], 2016. ISBN 9781509007868.
- [22] PENG, F. Z.; LAI, J.-S. Generalized instantaneous reactive power theory for three-phase power systems. *IEEE transactions on instrumentation and measurement*, IEEE, v. 45, n. 1, p. 293–297, 1996.

- [23] PETROIANU, A. I. Mathematical representations of electrical power: Vector or complex number? Neither! *Proceedings - 2014 Electrical Power and Energy Conference, EPEC 2014*, p. 170–177, 2014.
- [24] SALMERÓN, P.; HERRERA, R. S. Instantaneous reactive power theory—A general approach to poly-phase systems. *Electric Power Systems Research*, Elsevier, v. 79, n. 9, p. 1263–1270, 2009.
- [25] WILLEMS, J. L. A new interpretation of the Akagi-Nabae power components for nonsinusoidal three-phase situations. *IEEE Transactions on Instrumentation and Measurement*, IEEE, v. 41, n. 4, p. 523–527, 1992.
- [26] CASTILLA, M. et al. Clifford theory: A geometrical interpretation of multivectorial apparent power. *IEEE Transactions on Circuits and Systems I: Regular Papers*, v. 55, n. 10, p. 3358–3367, 2008. ISSN 10577122.
- [27] CASTRO-NÚÑEZ, M.; CASTRO-PUCHE, R. Advantages of geometric algebra over complex numbers in the analysis of networks with nonsinusoidal sources and linear loads. *IEEE Transactions on Circuits and Systems I: Regular Papers*, v. 59, n. 9, p. 2056–2064, 2012. ISSN 15498328.
- [28] CASTRO-NÚÑEZ, M.; CASTRO-PUCHE, R. The IEEE standard 1459, the CPC power theory, and geometric algebra in circuits with nonsinusoidal sources and linear loads. *IEEE Transactions on Circuits and Systems I: Regular Papers*, v. 59, n. 12, p. 2980–2990, 2012. ISSN 15498328.
- [29] XIA, Y.; MANDIC, D. P. Augmented MVDR spectrum-based frequency estimation for unbalanced power systems. *IEEE Transactions on Instrumentation and Measurement*, v. 62, n. 7, p. 1917–1926, 2013. ISSN 00189456.
- [30] JEON, H. J.; CHANG, T. G. Iterative frequency estimation based on MVDR spectrum. *IEEE Transactions on Power Delivery*, v. 25, n. 2, p. 621–630, 2010. ISSN 08858977.
- [31] AKKE, M. Frequency estimation by demodulation of two complex signals. *IEEE Transactions on Power Delivery*, v. 12, n. 1, p. 157–163, 1997. ISSN 08858977.
- [32] DASH, P.; PRADHAN, A.; PANDA, G. Frequency estimation of distorted power system signals using a robust algorithm. *IEEE Transactions on Power Delivery*, v. 14, n. 3, p. 761–766, 1999. ISSN 08858977.
- [33] GOU, X. et al. Quaternion-valued single-phase model for three-phase power system. *Journal of Electrical Engineering*, v. 69, n. 2, p. 183–186, mar 2018. ISSN 1339-309X. Disponível em: <<http://content.sciendo.com/view/journals/jee/69/2/article-p183.xml>>.
- [34] NOS, O. V. Linear transformations in mathematical models of an induction motor by quaternions. *International Workshop and Tutorials on Electron Devices and Materials, EDM - Proceedings*, v. 1, p. 295–298, 2012. ISSN 18153712.

- [35] BARRY, N. Electrical circuit analysis using four dimensional complex numbers, in the form of quaternions. In: IEEE. *Power Engineering Conference (UPEC), 2013 48th International Universities'*. [S.l.], 2013. p. 1–4.
- [36] NOS, O. V. Control strategy of active power filter for ineffective instantaneous power compensation. In: *2014 15th International Conference of Young Specialists on Micro/Nanotechnologies and Electron Devices (EDM)*. [S.l.: s.n.], 2014.
- [37] MALYAVKO, E. Y.; NOS, O. V. Control strategy of inactive instantaneous power compensation in quaternion basis. In: *2014 15th International Conference of Young Specialists on Micro/Nanotechnologies and Electron Devices (EDM)*. [S.l.: s.n.], 2014.
- [38] TALEBI, S. P.; MANDIC, D. P. A quaternion frequency estimator for three-phase power systems. In: IEEE. *2015 IEEE International Conference on Acoustics, Speech and Signal Processing (ICASSP)*. [S.l.], 2015. p. 3956–3960.
- [39] NOS, O. V. Control strategy of shunt active power filter based on an algebraic approach. In: IEEE. *2015 16th International Conference of Young Specialists on Micro/Nanotechnologies and Electron Devices*. [S.l.], 2015. p. 459–463.
- [40] BARRY, N. The application of quaternions in electrical circuits. In: IEEE. *2016 27th Irish Signals and Systems Conference (ISSC)*. [S.l.], 2016. p. 1–9.
- [41] BRASIL, V. P.; ISHIHARA, J. Y.; LELES, A. Electrical Three Phase Circuit Analysis Using Quaternions. In: *International Conference on Harmonics and Quality of Power (ICHQP)*. [S.l.: s.n.], 2018. p. 1–6. ISBN 9781538605172.
- [42] MIRON, S.; Le Bihan, N.; MARS, J. I. Quaternion-MUSIC for vector-sensor array processing. *IEEE Transactions on Signal Processing*, v. 54, n. 4, p. 1218–1229, 2006. ISSN 1053587X.
- [43] MANDIC, D. P.; JAHANCHAHI, C.; TOOK, C. C. A quaternion gradient operator and its applications. *IEEE Signal Processing Letters*, v. 18, n. 1, p. 47–50, 2011. ISSN 10709908.
- [44] JAHANCHAHI, C.; MANDIC, D. P. A class of quaternion kalman filters. *IEEE Transactions on Neural Networks and Learning Systems*, v. 25, n. 3, p. 533–544, 2014. ISSN 21622388.
- [45] CHOUKROUN, D.; BAR-ITZHACK, I. Y.; OSHMAN, Y. Novel quaternion Kalman filter. *IEEE Transactions on Aerospace and Electronic Systems*, v. 42, n. 1, p. 174–190, 2006. ISSN 00189251.
- [46] HAMILTON, W. R. On Quaternions; or on a new System of Imaginaries in Algebra (letter to John T. Graves, dated October 17, 1843). *Philos. Magazine*, v. 25, p. 489–495, 1843.
- [47] MAXWELL, J. C. *A treatise on electricity and magnetism*. [S.l.]: Clarendon press, 1881.
- [48] GIBBS, J. W. *Elements of Vector Analysis: Arranged for the Use of Students in Physics*. 1. ed. [S.l.]: Tuttle, Morehouse & Taylor, 1884.

- [49] HEAVISIDE, O. On the Forces, Stresses, and Fluxes of Energy in the Electromagnetic Field. *Proceedings of the Royal Society of London*, The Royal Society, v. 50, n. 302-307, p. 126–129, 1891.
- [50] PERUMAL, L. Quaternion and Its Application in Rotation Using Sets of Regions. p. 35–52, 2011.
- [51] CRISTALDI, L.; FERRERO, A. Mathematical foundations of the instantaneous power concepts: An Algebraic Approach. *European Transactions on Electrical Power*, v. 6, n. 5, p. 305–309, 1996. ISSN 1430144X. Disponível em: <<http://doi.wiley.com/10.1002/etep.4450060503>>.
- [52] FORTESCUE, C. L. Method of Symmetrical Co-Ordinates Applied to the Solution of Polyphase Networks. *Transactions of the American Institute of Electrical Engineers*, XXXVII, n. 2, p. 1027–1140, 1918. ISSN 0096-3860. Disponível em: <<http://ieeexplore.ieee.org/document/4765570/>>.
- [53] WIKIPEDIA the free encyclopedia. *Direct-quadrature-zero transformation*. Disponível em: <https://en.wikipedia.org/wiki/Direct-quadrature-zero_transformation#The_Park_transform_derivation>.
- [54] The Math Works Inc. Natick, M. A. . s. a. licença estudantil. *MATLAB R2017a*. [S.l.].
- [55] CZARNECKI, L. S. On Some Misinterpretations of the Instantaneous Reactive Power p - q Theory. *IEEE TRANSACTIONS ON POWER ELECTRONICS*, v. 19, n. 3, p. 828–836, 2004.
- [56] ANDERSON, P. M.; FOUAD, A. A. *Power System Control and Stability*. 2nd editio. ed. [S.l.]: Wiley-IEEE Press, 2002. 672 p. ISBN 978-0-471-23862-1.
- [57] PARK, B. Y. R. H. Two Reaction Theory of Synchronous Machines Generalized Method of Analysis-Part I. *Transactions of the American Institute of Electrical Engineers*, v. 48, n. 3, p. 716–727, 1929.
- [58] GATARIC, S. Polyphase Cartesian Vector Approach To Control Of Polyphase AC. In: *Conference Record of the 2000 IEEE Industry Applications Conference. Thirty-Fifth IAS Annual Meeting and World Conference on Industrial Applications of Electrical Energy*. [S.l.: s.n.], 2000. p. 1648–1654. ISBN 0780364015.

APPENDIX

I. MATLAB CODE FOR COMPARISON OF THE QVL PLANE COMPUTATION METHOD.

```
1 %% This file is intended to compare the performance of the null space
2 % method for determining the quaternion n and the cross product method
3
4 addpath Functions/
5
6 %% Electrical parameters
7
8 f = 60;
9 w = 2*pi*f;
10 Nsamp = 64; % # of samples per cycle
11 Cycles = 1; % # of simulated cycles
12 t = (0:Nsamp*Cycles-1)/(Nsamp*f);
13
14 %% Unbalance parameters
15
16 Ncases = 15625; % # of unbalanced cases
17
18 V0 = linspace(0,.5, Ncases^(1/6));
19 V1 = linspace(.5,1.5, Ncases^(1/6));
20 V2 = linspace(0,.5, Ncases^(1/6));
21 theta.V0 = deg2rad(linspace(0,360, Ncases^(1/6)));
22 theta.V1 = deg2rad(linspace(0,360, Ncases^(1/6)));
23 theta.V2 = deg2rad(linspace(0,360, Ncases^(1/6)));
24
25 [V0, V1, V2, theta.V0, theta.V1, theta.V2] = ndgrid(V0, V1, V2, theta.
    V0, theta.V1, theta.V2);
26
27
28 %% Monte Carlo Simulation
29 t1 = []; t2 = []; t1_avg_behaviour = []; t2_avg_behaviour = [];
30
31 for cond = 1:Ncases
32
33     %% Mapping from Sequence to Phase variables
34     fasor.V012 = [V0(cond) * exp(1i*theta.V0(cond));
35                 V1(cond) * exp(1i*theta.V1(cond));
```

```

36         V2(cond) * exp(1i*theta.V2(cond))]);
37
38     fasor.Vabc = sym2abc(fasor.V012);
39
40     %% Mapping to the time domain
41
42     va = sqrt(2) * real(fasor.Vabc(1) .* exp(1i*w*t));
43     vb = sqrt(2) * real(fasor.Vabc(2) .* exp(1i*w*t));
44     vc = sqrt(2) * real(fasor.Vabc(3) .* exp(1i*w*t));
45
46     Vabc = [va;vb;vc];
47
48     for c = 1:1e3
49
50         tic;
51         A = [Vabc(:,1), Vabc(:,2)].';
52         n1 = null(A);
53         t1(end+1) = toc;
54
55         tic;
56         n2 = cross(Vabc(:,1), Vabc(:,2));
57         n2 = n2./norm(n2);
58         t2(end+1) = toc;
59
60         lt1 = length(t1_avg_behaviour);
61         if lt1 == 0
62             t1_avg_behaviour(end+1) = t1(end);
63             t2_avg_behaviour(end+1) = t2(end);
64         else
65             t1_avg_behaviour(end+1) = ( t1_avg_behaviour(end) * lt1 + t1(end)
66                 ) / (lt1 + 1);
67             t2_avg_behaviour(end+1) = ( t2_avg_behaviour(end) * lt1 + t2(end)
68                 ) / (lt1 + 1);
69         end
70         % t1_avg_behaviour(end+1) = mean(t1(t1>0));
71         % t2_avg_behaviour(end+1) = mean(t2(t1>0));
72         % t1_var_behaviour(c,cond) = var(t1(t1>0));
73         % t2_var_behaviour(c,cond) = var(t2(t1>0));
74     end
75 end

```

```
76
77 toc
78
79 t1_avg = mean(t1(:))
80 t2_avg = mean(t2(:))
81
82 t1_var = var(t1(:))
83 t2_var = var(t2(:))
84
85
86 %% Save .mat workspace
87
88 save('Cases/Results/Computing_n_Comparison.mat');
```


II. MATLAB CODE FOR COMPARISON OF MATRIX AND QUATERNION IMPLEMENTATION OF CLARKE TRANSFORM.

```
1 %% This file performs the Clarke transformation via matrix and via
2 % quaternion for several balanced and unbalanced conditions. Both
3 % implementations are compared.
4
5 close all;
6 clear;
7 clc;
8
9 addpath(genpath('Functions/'));
10
11 %% Electrical parameters
12
13 f = 60;
14 w = 2*pi*f;
15 Nsamp = 64; % # of samples per cycle
16 Cycles = 1; % # of simulated cycles
17 t = (0:Nsamp*Cycles-1)/(Nsamp*f);
18
19 %% Unbalance parameters
20
21 Ncases = 4096; % # of unbalanced cases
22
23 V0 = linspace(0,.5, round(Ncases^(1/6)));
24 V1 = linspace(.5,1.5, round(Ncases^(1/6)));
25 V2 = linspace(0,.5, round(Ncases^(1/6)));
26 theta.V0 = deg2rad(linspace(0,360, round(Ncases^(1/6))));
27 theta.V1 = deg2rad(linspace(0,360, round(Ncases^(1/6))));
28 theta.V2 = deg2rad(linspace(0,360, round(Ncases^(1/6))));
29
30 [V0, V1, V2, theta.V0, theta.V1, theta.V2] = ndgrid(V0, V1, V2, theta.
    V0, theta.V1, theta.V2);
31
32
33 %% Definition of Clarke Matrix Transformation and the equivalent
    quaternion
```

```

34
35 T = sqrt(2/3) * [1           -1/2           -1/2;
36                 0           sqrt(3)/2        -sqrt(3)/2;
37                 1/sqrt(2)   1/sqrt(2)        1/sqrt(2)];
38
39 % Axis of rotation
40 [eigVec, eigVal] = eig(T);
41 d = (eigVec(:, 1));
42 q.d = quaternion(d);
43 % Angle of rotation
44 theta_r = acos(( trace(T) - 1 ) / 2);
45
46 % Quaternion rotation
47 Rt = R(-[0;d], theta_r);
48 Rtin = Rinv(-[0;d], theta_r);
49 q.Rt = quaternion(Rt);
50 q.Rtin = quaternion(Rtin);
51
52
53 %% Monte Carlo Simulation
54 NrunMonteCarlo = 1e3;
55 t1 = []; t2 = []; t1_avg_behaviour = []; t2_avg_behaviour = [];
56 for cond = 1:Ncases
57
58     %% Mapping from Sequence to Phase variables
59     fasor.V012 = [V0(cond) * exp(1i*theta.V0(cond));
60                 V1(cond) * exp(1i*theta.V1(cond));
61                 V2(cond) * exp(1i*theta.V2(cond))];
62
63     fasor.Vabc = sym2abc(fasor.V012);
64
65     %% Mapping to the time domain
66
67     va = sqrt(2) * real(fasor.Vabc(1) .* exp(1i*w*t));
68     vb = sqrt(2) * real(fasor.Vabc(2) .* exp(1i*w*t));
69     vc = sqrt(2) * real(fasor.Vabc(3) .* exp(1i*w*t));
70
71     Vabc = [va;vb;vc];
72     q.Vabc = quaternion(Vabc);
73     Vabc_Quat = [zeros(1,Nsamp*Cycles); Vabc];
74
75 for c = 1:NrunMonteCarlo

```



```

76 % Via matrices
77 tic;
78 V_T = T * Vabc;
79 t1(end+1) = toc;
80
81 % Via quaternions
82 tic;
83 V_TQuat = qproduct(qproduct(Rt, Vabc_Quat), Rtin);
84 t2(end+1) = toc;
85
86 % Graphical investigation of the avg and var of the computational time
87 % regarding each Monte Carlo loop
88
89
90 lt1 = length(t1_avg_behaviour);
91 if lt1 == 0
92     t1_avg_behaviour(end+1) = t1(end);
93     t2_avg_behaviour(end+1) = t2(end);
94 else
95     t1_avg_behaviour(end+1) = ( t1_avg_behaviour(end) * lt1 + t1(end)
96         ) / (lt1 + 1);
97     t2_avg_behaviour(end+1) = ( t2_avg_behaviour(end) * lt1 + t2(end)
98         ) / (lt1 + 1);
99 end
100 % t1_avg_behaviour(c,cond) = mean(t1(t1>0));
101 % t2_avg_behaviour(c,cond) = mean(t2(t2>0));
102 % t1_var_behaviour(c,cond) = var(t1(t1>0));
103 % t2_var_behaviour(c,cond) = var(t2(t2>0));
104
105 % tic;
106 % V_teste = RotateVectorQ(q.Rt, Vabc);
107 % t3(c,cond) = toc;
108 %
109 %
110 % tic;
111 % q.V_TQuat = q.Rt * q.Vabc * q.Rtin;
112 % t4(c,cond) = toc;
113
114 end
115

```

```

116 t1_avg = mean(t1(:))
117 t2_avg = mean(t2(:))
118 % t3_avg = mean(t3(:))
119 % t4_avg = mean(t4(:))
120
121 t1_var = var(t1(:))
122 t2_var = var(t2(:))
123
124
125 %% Graphical Comparison
126
127 h = boxplot([t1(:),t2(:)], 'Labels', {'Matrix', 'Quaternion'}, 'Symbol
    ', '');
128 set(h,{'linewidth'}, {1.5});
129 ylabel('Computational demanded time (s)','fontsize', 16);
130 xlabel('Method','fontsize', 16);
131 % title('Comparison of Two different Clarke Implementations');
132
133
134 %% Save .mat workspace
135
136 save('Cases/Results/Clarke_Comparison.mat');

```

III. MATLAB CODE FOR COMPARISON OF MATRIX AND QUATERNION IMPLEMENTATION OF PARK TRANSFORM.

```
1 %% This file performs the Park transformation via matrix and via
2 % quaternion for several balanced and unbalanced conditions. Both
3 % implementations are compared.
4
5 close all;
6 clear;
7 clc;
8
9 addpath(genpath('Functions/'));
10
11 %% Electrical parameters
12
13 f = 60;
14 w = 2*pi*f;
15 Nsamp = 64; % # of samples per cycle
16 Ncycles = 1; % # of simulated cycles
17 t = (0:Nsamp*Ncycles-1)/(Nsamp*f);
18
19 %% Unbalance parameters
20
21 Ncases = 4096; % # of unbalanced cases
22
23 V0 = linspace(0,.5, round(Ncases^(1/6)));
24 V1 = linspace(.5,1.5, round(Ncases^(1/6)));
25 V2 = linspace(0,.5, round(Ncases^(1/6)));
26 theta.V0 = deg2rad(linspace(0,360, round(Ncases^(1/6))));
27 theta.V1 = deg2rad(linspace(0,360, round(Ncases^(1/6))));
28 theta.V2 = deg2rad(linspace(0,360, round(Ncases^(1/6))));
29
30 [V0, V1, V2, theta.V0, theta.V1, theta.V2] = ndgrid(V0, V1, V2, theta.
    V0, theta.V1, theta.V2);
31
32
33 %% Definition of Park Matrix Transformation and the equivalent
    quaternion
34 for c = 1:Nsamp * Ncycles
```

```

35 P{c} = sqrt(2/3) * [cos(w*t(c))      cos(w*t(c) - 2*pi/3)
                    cos(w*t(c) + 2*pi/3);
36 -sin(w*t(c))      -sin(w*t(c) - 2*pi/3)      -sin(w*t(c) + 2*pi
                    /3);
37 1/sqrt(2)          1/sqrt(2)          1/sqrt(2)];
38 end
39
40 % Clarke transformation
41 T = sqrt(2/3) * [1          -1/2          -1/2;
42                 0          sqrt(3)/2      -sqrt(3)/2;
43                 1/sqrt(2)  1/sqrt(2)      1/sqrt(2)];
44
45
46 % Axis of rotation for Clarke transformation
47 [eigVec, eigVal] = eig(T);
48 d = (eigVec(:, 1));
49 q.d = quaternion(d);
50 % Angle of rotation for Clarke transformation
51 theta_r = acos(( trace(T) - 1 ) / 2);
52
53 % The second part of the Park rotation is achieved via an z rotation
    of wt.
54
55 % Quaternion Clarke rotational
56 RC = R(-[0;d], theta_r);
57 RCinv = Rinv(-[0;d], theta_r);
58 q.RC = quaternion(RC);
59 q.RCinv = quaternion(RCinv);
60
61 % Park Kp rotational
62 Rp = R(-[0;0;0;1], w*t);
63 Rpinv = Rinv(-[0;0;0;1], w*t);
64 q.Rp = quaternion(Rp);
65 q.Rpinv = quaternion(Rpinv);
66
67
68 %% Monte Carlo Simulation
69 NrunMonteCarlo = 1e3;
70 t1 = []; t2 = []; t1_avg_behaviour = []; t2_avg_behaviour = [];
71 for cond = 1:Ncases
72
73     %% Mapping from Sequence to Phase variables

```

```

74     fador.V012 = [V0(cond) * exp(1i*theta.V0(cond));
75                  V1(cond) * exp(1i*theta.V1(cond));
76                  V2(cond) * exp(1i*theta.V2(cond))];
77
78     fador.Vabc = sym2abc(fador.V012);
79
80     %% Mapping to the time domain
81
82     va = sqrt(2) * real(fador.Vabc(1) .* exp(1i*w*t));
83     vb = sqrt(2) * real(fador.Vabc(2) .* exp(1i*w*t));
84     vc = sqrt(2) * real(fador.Vabc(3) .* exp(1i*w*t));
85
86     Vabc = [va;vb;vc];
87     q.Vabc = quaternion(Vabc);
88     Vabc_Quat = [zeros(1,Nsamp*Ncycles); Vabc];
89
90     for c = 1:1e3
91     % Via matrices
92     tic;
93     for l = 1:Nsamp * Ncycles
94         V_T(:,l) = P{1} * Vabc(:,l);
95     end
96     t1(end+1) = toc;
97
98     % Via quaternions
99     tic;
100    V_TQuat = qproduct(qproduct(Rp, qproduct(qproduct(RC, Vabc_Quat),
101        RCinv)), Rpinv);
102
103    t2(end+1) = toc;
104
105    %% Graphical investigation of the avg and var of the computational time
106    %% regarding each Monte Carlo loop
107
108    lt1 = length(t1_avg_behaviour);
109    if lt1 == 0
110        t1_avg_behaviour(end+1) = t1(end);
111        t2_avg_behaviour(end+1) = t2(end);
112    else
113        t1_avg_behaviour(end+1) = ( t1_avg_behaviour(end) * lt1 + t1(end)
114            ) / (lt1 + 1);
115        t2_avg_behaviour(end+1) = ( t2_avg_behaviour(end) * lt1 + t2(end)
116            ) / (lt1 + 1);

```

```

113 end
114 % t1_avg_behaviour(c,cond) = mean(t1(t1>0));
115 % t2_avg_behaviour(c,cond) = mean(t2(t2>0));
116 % t1_var_behaviour(c,cond) = var(t1(t1>0));
117 % t2_var_behaviour(c,cond) = var(t2(t2>0));
118
119 % tic;
120 % V_teste = RotateVectorQ(q.Rp, RotateVectorQ(q.RC, Vabc));
121 % t3(c,cond) = toc;
122 %
123 %
124 % tic;
125 % q.V_TQuat = q.Rp .* q.RC .* q.Vabc .* q.RCinv .* q.Rpinv;
126 % t4(c,cond) = toc;
127
128 end
129 end
130
131 %% Computation of avarage and variance values
132
133
134 t1_avg = mean(t1(:)) %#ok<*NOPTS>
135 t2_avg = mean(t2(:))
136 % t3_avg = mean(t3(:))
137 % t4_avg = mean(t4(:))
138
139 t1_var = var(t1(:))
140 t2_var = var(t2(:))
141 % t3_var = var(t3(:))
142 % t4_var = var(t4(:))
143
144 fprintf('\nComputation via quaternions was in avarage %.2f times
        faster than via matrices.\n', t1_avg/t2_avg);
145 fprintf('\nVariance of the quaternion method was %.2f lower than the
        matrix one.\n', t1_var/t2_var);
146
147
148
149 %% Graphical Comparison
150
151 h = boxplot([t1(:),t2(:)], 'Labels', {'Matrix', 'Quaternion'}, 'Symbol
        ', '');

```

```
152 set(h,{ 'linewidth' }, {1.5});
153 ylabel('Computational demanded time (s)', 'fontsize', 16);
154 xlabel('Method', 'fontsize', 16);
155 % title('Comparison of Two different Park Implementations');
156
157
158 %% Save .mat workspace
159
160 % save('Cases/Results/Park_Comparison.mat');
```